THE MIDAS POND GOLD PROSPECT, VICTORIA LAKE GROUP: GEOLOGY, ALTERATION AND MINERALIZATION

DAVID THOMAS WILLIAM EVANS

THE MIDAS POND GOLD PROSPECT, VICTORIA LAKE GROUP: GEOLOGY, ALTERATION AND MINERALIZATION

BY

DAVID THOMAS WILLIAM EVANS, B.Ed., B.Sc. (Hons), P. Geo.

A thesis submitted to the School of Graduate Studies
in partial fulfillment of the
requirements for the degree of
Master of Science

Department of Earth Sciences
Memorial University of Newfoundland

May, 1993

St. John's, Newfoundland

ISBN 0-315-86690-X

Frontispiece

'Da bys' at Tulks Hill, 1985. From left to right Morris West, Robert Lane and Baxter Kean.

ABSTRACT

The Midas Pond gold prospect, discovered by BP Canada Inc. in 1985, is located at the southwest end of the Cambro-Ordovician Tulks Hill volcanics, Victoria Lake Group. Host rocks include variably deformed, waterlain felsic and mafic pyroclastic rocks of island arc origin.

Alteration and mineralization are confined to a 200 m wide, brittle, ductile-shear zone. This shear zone formed in response to regional D_1 deformation and the shear zone fabric parallels the regional S_1 foliation. D_2 deformation resulted in broad Z-shaped flexuring of the shear zone.

Advanced argillic alteration and an extensive Fe-carbonate and pyrite halo surrounds the gold mineralization. Alteration assemblages include pyrophyllite, paragonite, quartz, plagioclase, chlorite, fluorite, Fe-carbonate and pyrite.

The gold, which is intimately associated with pyrite, occurs in three structurally-controlled vein sets. These veins are confined to the contact between a highly deformed breccia termed the Banded Mafic unit and the structurally overlying, altered felsic tuffaceous rocks. The vein sets include: V_1 boudinaged veins developed parallel to the shear zone fabric (C-shear veins), and V_2 and V_3 extensional fracture veins which are controlled by an

S_2 fracture cleavage. V_1 veins are the earliest vein set and contain the lowest concentrations of gold. V_2 and V_3 veins appear to be concentrated within the hinges of the D_2 flexures and selected assays from these veins include 7.9 g/t Au over 0.9 m and 14.74 g/t Au over 1.15 m.

The mineralizing fluids are interpreted to have been CO_3^{2-} and F^- rich, slightly acidic and with a temperature range of 250 to 300°C. These fluids are interpreted to have originated through metamorphic dehydration and decarbonation of mixed island arc and continental crustal rocks. Gold precipitation resulted from the reaction of these fluids with the Fe-rich Banded Mafic unit. Pre-existing and simultaneously crystallizing pyrite served as nuclei for gold precipitation.

ACKNOWLEDGEMENTS

I would like to acknowledge the following sources of valuable support that I received during the course of this study.

Most of my support and financial support came from the Newfoundland Department of Mines and Energy (NDME) and I would particularly like to thank Mr. Baxter Kean, whose regional metallogenic project provided the opportunity for this study. I would also like to thank Dr. Scott Swinden who provided much of the incentive for me to finish this work. Mr. Ken Byrne and the staff of the Cartographic Unit are kindly thanked for their skill in drafting most of the figures for this thesis. Major and selected trace element analyses were performed at the geochemical laboratory under the direction H. Wagenbaur. Logistical support was provided by Wayne Ryder, Sid Parsons and Ted Hall.

I would like to thank my supervisor Dr. Derek Wilton for providing valuable assistance and funding to undertake this study. I would also like to acknowledge the help of the following co-workers, industry personnel and fellow students: Joe Atkinson, Tom Al, Judy Banton, Dave Barbour, Frank Blackwood, Rod Churchill, Keith Green, John Hayes, Liz Hearn, Anne Hogan, Dave King, Brian O'Brien, Cyril O'Driscoll, Bruce Ryan, Peter Tallman, Geoff Thurlow and John Tuach. Rob Lane of Buchans provided excellent assistance and comic relief both in the field and in the Union Hall. Anne

Hogan, Baxter Kean and Scott Swinden are thanked for critically reviewing early drafts of this thesis.

BP Canada Inc. through its chief geologist Dr. Geoff Thurlow suggested the project and provided unlimited access to the prospect, diamond drill core and all relevant data.

Finally I would like to thank my wife Sandra for her unlimited support in my return to university and putting up with long lonely field seasons. Both of us would like to express our gratitude to our parents for supporting us in this endeavour.

TABLE OF CONTENTS

LIST OF FIGURES

LIST OF TABLES

LIST OF PLATES

CHAPTER 1

INTRODUCTION

1.1 RATIONALE

This study, initiated in 1986, was undertaken as part of the detailed metallogenic study of the Victoria Lake Group conducted by the Newfoundland Department of Mines and Energy under the Canada - Newfoundland Mineral Development Agreement (1984-1989). The aim of this particular project was to document the geology, alteration and geochemistry of the Midas Pond gold prospect.

1.2 LOCATION AND ACCESS

The Midas Pond prospect is located within the Victoria Lake Group, central Newfoundland (Figure 1.1) and lies within the Victoria Lake (N.T.S. 12A/6) map area. The study area is bounded by 48° 26'20" latitude, 57° 19'30" longitude and 48° 26'40" latitude, 57° 20' longitude. Access to the area is provided by privately owned gravel logging roads which originate at Millertown, a small community on the shores of Red Indian Lake approximately 70 km to the northeast. The prospect is reached by a 25 minute walk from the nearest road.

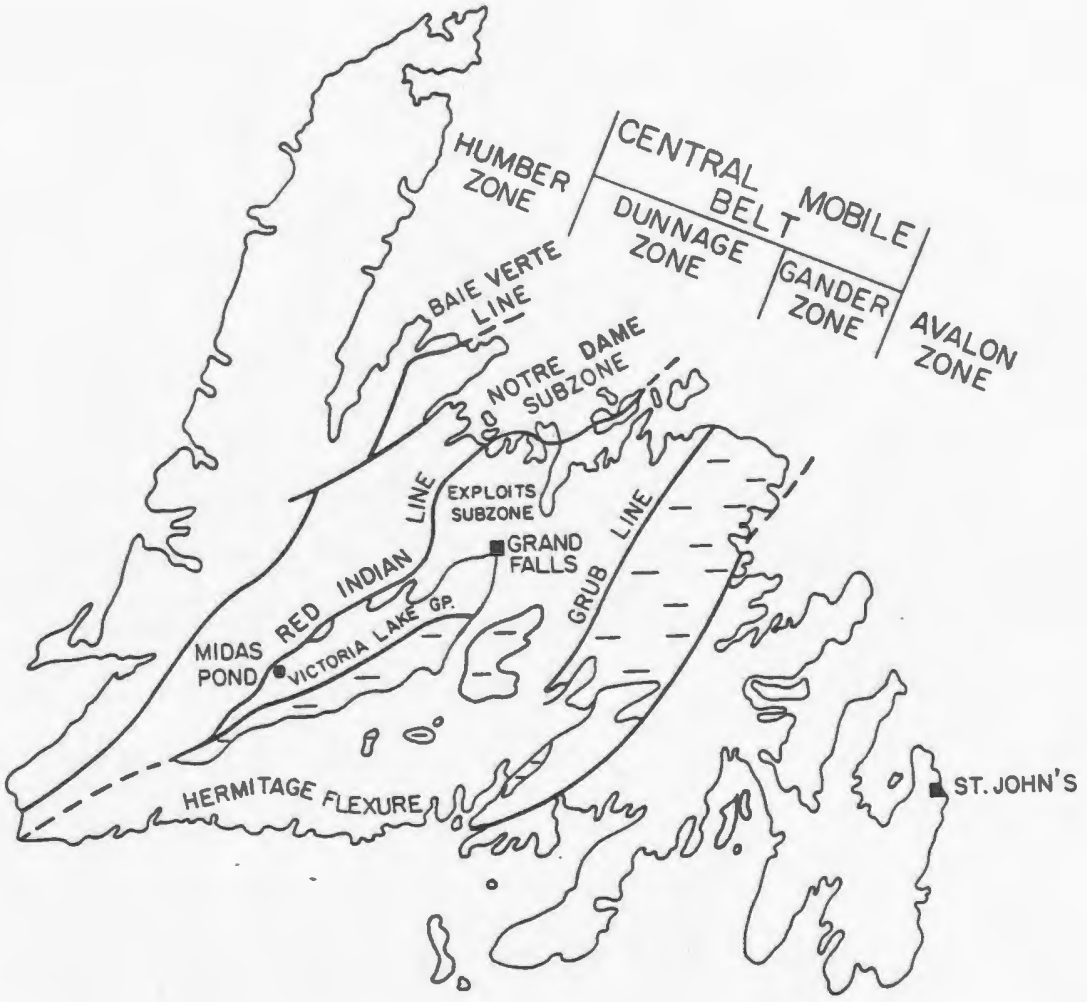

Figure 1.1. Tectonostratigraphic map of Newfoundland showing the location of Midas Pond and the Victoria Lake Group (modified after Williams et al., 1988; Swinden et al., 1988a).

1.3 PHYSIOGRAPHY AND GLACIATION

The study area is heavily forested (largely spruce and fir) with numerous intervening bogs and ponds. Topography is fairly rugged with elevations ranging between 300 and 400 m above sea level. The prospect is located near the crest of Tulks Hill which has a vertical relief of almost 160 m above Tulks Valley (Plate 1.1).

Extensive areas of glacial till result in generally poor bedrock exposure except along the linear, northeast-trending, locally barren ridges. The area was glaciated during the Wisconsin Glaciation (Twenhofel and MacClintock, 1940) and three directions of ice movement have been reported (B. Sparkes, personal communication, 1987) to have occurred southwest of Red Indian Lake. According to Sparkes, the earliest flow direction was southward directed from a centre northwest of Red Indian Lake; this was followed during the Late Wisconsin by a southwestward directed flow originating between Victoria Lake and Lake Ambrose and finally by southwestward directed flow from a centre to the northeast of Buchans.

1.4 PREVIOUS WORK

The earliest recorded geological work in the area was undertaken in 1871 by Alexander Murray for the Geological Survey of

Plate 1.1 Aerial view of the study area. Glitter Pond is in the foreground, Tulks Valley (Tulks Valley fault) in the distance. Midas Pond is the narrow pond located between the two bogs to the left of Glitter Pond.

Plate 1.2 Aerial view of Midas Pond (in foreground) and the northeast-trending shear zone which hosts the mineralization (view to the northwest). The quartz veining is developed along the west side of the small ridge immediately east of Midas Pond.

Newfoundland (Murray, 1872). He surveyed the Exploits River and reported the occurrence of sedimentary rocks along the river and of greenstones along Red Indian Lake. The next survey was undertaken by J.P Howley (Murray and Howley, 1881). Howley, accompanied by two Micmac guides, departed from Upper Sandy Point, Bay of Exploits on July 3, 1875 and ascended the Exploits, Lloyds and Victoria Rivers conducting geological mapping. The group proceeded cross-country to the telegraph station at Grandys Brook, on the south coast, where they arrived on October 27.

Logging was indirectly responsible for opening the area to mineral exploration. In 1905 the Newfoundland Government granted a 99 year lease to the Anglo Newfoundland Development Company (A.N.D.Co) for exclusive timber, water and mineral rights to a 3742 km^2 area surrounding Red Indian and Victoria Lakes, known as the Terra Nova Properties (Neary, 1981).

Prospecting surveys carried out the following summer resulted in the discovery of the Buchans Deposit by Matty Mitchell, a Micmac Indian prospector, trapper and guide. In 1907 William Scott, chief engineer with the A.N.D.Co., sent out prospecting parties to explore the areas surrounding Buchans (Neary, 1981; Martin, 1983). This work resulted in the staking of area known as the Victoria Mine. Captain Daniel McCuish was sent to the site with six miners and on November 1 they began to sink two of three exploratory shafts, however, the mine proved to be uneconomic and work was

halted.

In March 1926 an agreement was negotiated between the Terra Nova Properties Limited and the American Smelting and Refining Company (ASARCO) which gave ASARCO the right to explore for and develop any orebody within a 20 mile radius of Buchans (Neary, 1981). The agreement was renegotiated to include a 30 mile radius for a period of 50 years and resulted in an extensive exploration program by ASARCO.

Hans Lundberg Limited (Grimes-Graeme, 1934) conducted geological reconnaissance mapping and geophysical surveys, for the Terra Nova Properties Limited, of the area between Lloyds, Victoria and Long Lakes. Significant mineralized float, consisting of fragments of quartz veins containing 36.0 oz/t Ag, 1.02 oz/t Au, 12.6% Zn and 7.5% Pb, was discovered in the Pats Pond area. Float containing stibnite and arsenopyrite was also discovered in the same area.

Grimes-Graeme (1934, pages 14-15) described the quartz veining developed throughout the study area as follows.

> "Quartz veins are abundant in this area and often attain considerable widths although their linear extents do not appear to be very great. However there seems to be a marked tendency for the veins to extend for considerable distances in an "en echelon" arrangement. A number of the veins are mineralized, many of them containing pyrite and a little chalcopyrite. A few veins also contain fair amounts of galena in addition to

> pyrite, but the assays were disappointingly low in precious metal values. A characteristic of the veins is the presence of comb structures, ie., cavities lined with very perfect quartz crystals. This fact in conjunction with the physical form of the veins and their mineralogical association indicate that they originated at low temperatures and pressures at shallow depths in the earth's crust."

During the 1934 survey, reference was made to a concept that was to prove accurate almost sixty years latter with the discovery of a number of significant gold prospects associated with regional linear structures (Kean and Evans, 1988a; Evans et al., 1990). Grimes-Graeme (1934) alluded to the intersection of two east-west trending linears in the Long Lake area and indicated that such intersections were often favourable sites for ore deposition.

ASARCO, in following up an extensive gossan zone, originally discovered in 1930 by W.E. Moore (Cooper, 1967), conducted geochemical stream sampling along Tulks Brook in 1961. This work, along with further surveys (1961-1962) and an extensive diamond drilling program (1963-1966), resulted in the discovery of the Tulks Hill Deposit.

On March 17, 1976 the Terra Nova Properties reverted to Abitibi-Price Incorporated when the 1926 agreement between the A.N.D.Co. and ASARCO expired. Abitibi-Price continued exploration within the Victoria Lake Group and subsequently discovered the Tulks East deposit in 1977 and the Jacks Pond prospects in 1980

(Barbour and Thurlow, 1982).

BP Canada Incorporated (BP Resources Canada Limited) purchased the mineral rights to the Terra Nova Properties from Abitibi-Price in 1985. BP actively explored for gold and base metal mineralization and had encouraging results with major finds at Midas Pond, West Tulks, Valentine Lake and Daniels Pond. BP suspended exploration activities in 1991.

Noranda Exploration Company Limited initiated a program of extensive geological mapping and geophysical surveys in 1975 which lead to the discovery of the massive sulphide bodies at the Boundary deposit in 1981 and the Duck Pond deposit in 1986. The company has recently entered into an agreement with BP to purchase the mineral rights to the Terra Nova Properties.

The Millertown area was included in the Geological Survey of Canada regional mapping of the 1:250,000 Red Indian Lake (NTS 12A) sheet (Riley, 1957; Williams, 1970). Williams (1970) indicated that the volcanic and related sedimentary rocks outcropping to the south of Red Indian Lake were probably Ordovician.

Regional geological mapping of the area on a scale of 1:50,000 was begun by the Newfoundland Department of Mines and Energy in 1975 and continued until 1981. Geological maps and reports were completed for the following NTS areas: Victoria Lake 12A/6 (Kean,

1977); Star Lake 12A/11 east half (Kean, 1979a); Buchans 12A/15 (Kean, 1979b); Lake Ambrose 12A/10 (Kean and Jayasinghe, 1980); Noel Pauls Brook 12A/9 (Kean and Jayasinghe,1980); Grand Falls 2D/13 (Kean and Mercer, 1981); Badger 12A/16 (Kean and Jayasinghe, 1982); King George IV Lake 12A/4 (Kean, 1983). Kean (1977) formally proposed the name Victoria Lake Group for the sequence of pre-Caradocian volcanic and sedimentary rocks lying to the south of Red Indian Lake.

The Quaternary Geology Section of the Newfoundland Department of Mines and Energy initiated a program of surfical and glacial mapping of the Central Mineral Belt in 1978 (Sparkes, 1985).

The Victoria Lake Group was included in a regional lake sediment geochemical survey conducted by the Newfoundland Department of Mines and Energy. Results of this study included the definition of the distributions of Au and associated pathfinder elements, such as As and Sb (Davenport et al., 1990).

In 1984 the Newfoundland Department of Mines and Energy began a systematic study of the metallogeny of the Victoria Lake Group. The initial results of this work were covered in the following reports (Kean, 1985; Kean and Evans, 1986; Evans and Kean, 1986; Evans and Kean, 1987; Kean and Evans, 1988a; Swinden et al., 1989; Evans et al., 1990; Dunning et al., 1991; Evans, 1992; and Evans, 1993).

An airborne radiometric survey of the Tulks Hill volcanics was conducted by the Geological Survey of Canada (Ford, 1991). The objective of this survey was to identify possible areas of K alteration related to volcanogenic massive sulphide mineralization.

A number of theses, largely sponsored by ASARCO, have been undertaken on various aspects of the geology and mineral deposits of the Victoria Lake Group. A brief outline of these theses and other published works pertaining to specific aspects of the geology of the Victoria Lake Group is given in Table 1.1.

1.5 PRESENT INVESTIGATION

In the fall of 1985, a gold discovery was made at Midas Pond by personnel from BP Canada Inc. This find was significant for two main reasons: 1) it was the first major gold find within the Victoria Lake Group and, 2) it had an aluminous alteration zone that was unlike any previously known alteration zone associated with the volcanogenic massive sulphides. Because of these unique characteristics, the Newfoundland Department of Mines and Energy, as part of its regional metallogenic study of the Victoria Lake Group, decided to support an investigation of the prospect as part of an M.Sc. study.

During the 1986 field season detailed mapping (using 1:13,320

YEAR	AUTHOR(S)	SUBJECT
1940	Douglas et al.	Brief description of the geology of the Victoria Mine.
1952	Brown	M.Sc. study of the geology southeast of Victoria River.
1961	Mullins	M.Sc. study of the Lake Ambrose and Noel Pauls Brook areas.
1962	Hammond	B.Sc. study of the Long Lake Prospect.
1964	Collins	B.Sc. study of the Jacks Pond area.
1966	Coward	B.Sc. study of the Red Cross Lake, Long Lake and Glitter Pond areas.
1967	Cooper	M.Sc. study of the Tulks Hill Deposit.
1972	Besaw	B.Sc. study of the Halfway Pond area.
1971	Strickland	B.Sc. study of the Long Lake area.
1978	Thurlow	Brief description of the Victoria Mine.
1982	Barbour and Thurlow	Case history: discovery of the Jacks Pond Prospects and the Tulks East Deposit.
1984a	Jambor	Report on the mineralogy of the Tulks Hill Deposit.
1984b	Jambor	Report on the mineralogy of the Boundary Deposit.
1984	Moreton	M.Sc. study of the Tulks Hill Deposit.
1984	Swinden and Thorpe	Discussed lead isotope data from various deposits within the Victoria Lake
1985	Mihychuk	Drift prospecting in the Victoria Mine Tally Pond area.
1986	Dimmel	B.Sc. study of the Burnt Pond Prospect.
1986	Dunning	Discussed age dating of the Tally Pond volcanics.
1986	Dunning et al.	Discussed age dating of the Victoria Lake Group.

Table 1.1. Published works (excluding those mentioned in the text) and theses which deal with the Victoria Lake Group.

Table 1.1 continued.

1986	Evans	B.Sc. study of the Jacks Pond Prospect.
1986abcde	G.S.C.	Aeromagnetic vertical gradient and total field maps, central Newfoundland.
1986	Tod	VLF-EM studies of the Caradocian shales in Badger area.
1987	Colman-Sadd	Geology of the Snowshoe Pond Sheet 12A/7.
1987	Jambor and Barbour	Mineralogy and geology of the Tulks Hill Deposit.
1988a	Kean and Evans	Geology and mineral deposits of the Victoria Lake Group.
1988b	Kean and Evans	Geology and mineral deposits of the Victoria Lake Group.
1988	MacKenzie	Geology of the Boundary Deposit.
1988	MacKenzie et al.	Geology of the Duck Pond Deposit.
1989	Swinden et al.	Volcanic rock geochemistry as a guide for VMS mineralization.
1989	Wilton et al.	Geochemical and isotopic study of mineralized fault zones.
1990	Evans et al.	Geological studies of the Victoria Lake Group.
1990	Evans and Kean	Geology and mineral deposits of the Victoria Lake Group.
1990	Squires et al.	Geology and genesis of the Duck Pond VMS Deposit.
1990a	Desnoyers	The Victoria Mine prospect.
1990b	Desnoyers	The Bobby's Pond alteration zone.
1990	Evans	The Midas Pond gold prospect.
1990	Barbour	The Valentine Lake gold prospect.
1990	McKenzie et al.	VMS deposits of the Tulks Hill volcanics.
1991	Dunning et al.	Age dating and geochemistry of the Tally Pond volcanics.

scale aerial photographs) was conducted in an area approximately 1 x 2 km surrounding the Midas Pond prospect. A 100 m spaced grid was used in mapping bedrock exposures. Rock samples were collected for petrographic and geochemical analysis. The aluminous alteration zone associated with the mineralization is not exposed on surface and therefore could only be studied in drill core. Drill core from the prospect (stored in Buchans) was examined and sampled in detail (courtesy of B.P. Canada Inc). Approximately 6 weeks were spent mapping the area and examining the drill core. Visits were also made to most of the other known gold occurrences within the Victoria Lake Group. A limited amount of field work (< one week) was undertaken in the summer of 1987.

The field work was supplemented by petrographic analysis, geochemical analyses consisting of major, trace and REE determinations, and limited lead, carbon, oxygen and sulphur isotope analyses. These data, when combined with data collected during the regional metallogenic study are used to elucidate the parameters of gold mineralizing systems both at Midas Pond and elsewhere in the Victoria Lake Group.

1.6 REGIONAL SETTING

The island of Newfoundland forms the northern terminus of the Appalachian Orogen. Williams (1964) subdivided the orogen, based on stratigraphic and structural contrasts into three geological

zones which are termed the Western platform, the Central Paleozoic Mobile Belt and the Avalon platform. These zones are related to the formation and eventual destruction of the Late Precambrian-Early Paleozoic Iapetus Ocean. These divisions were later revised by Williams (1979) into five, broad, west to east zones; viz. Humber, Dunnage, Gander, Avalon and Meguma.

The Dunnage Zone is further subdivided into the Notre Dame and Exploits subzones on the basis of geochemical, metallogenic, geochronological, paleontological and geophysical parameters (Williams et al., 1988). These subzones are separated by an extensive fault system termed the Red Indian Line.

The geological evolution of the region (Figure 1.1) can be subdivided into two broad stages: 1) pre-accretionary, and 2) post-accretionary (Swinden, 1990). The first stage consists of pre-accretion volcanism and pre- and syn-accretion sedimentation recorded in a series of Cambrian to Middle Ordovician island arcs and back-arc basins. Cessation of volcanism coincided with the emplacement of the Taconic allochthons during the middle Ordovician (Kean and Strong, 1975; Swinden and Thorpe, 1984). Continued closure of Iapetus during the late Ordovician and early Silurian resulted in the deposition of flyschoid sequences in fault-bound basins in the central and eastern Dunnage Zone (Dean, 1978; Kean et al., 1981).

Second stage, post-accretion events are marked by the activation or re-activation of large strike-slip faults, the development of pull apart basins (Szybinski et al., 1990) and crustal melting resulting in epicontinental-style volcanism (Coyle and Strong, 1987) which led to the deposition of Silurian fluviatile sedimentary and terrestrial volcanic rocks.

Siluro-Devonian deformation (termed the Salinic Orogeny by Dunning et al., 1990) resulted in widespread crustal thickening, regional greenschist and amphibolite grade metamorphism, and caused the crustal melting that resulted in widespread plutonism (Dean, 1978; Strong, 1980; Colman-Sadd, 1980; Kean et al., 1981; Dallmeyer et al., 1983).

Carboniferous faulting, probably related to the Allegheny Orogeny, produced shallow pull apart basins in which continental and shallow water sediments were deposited (Dean, 1978; Kean et al., 1981).

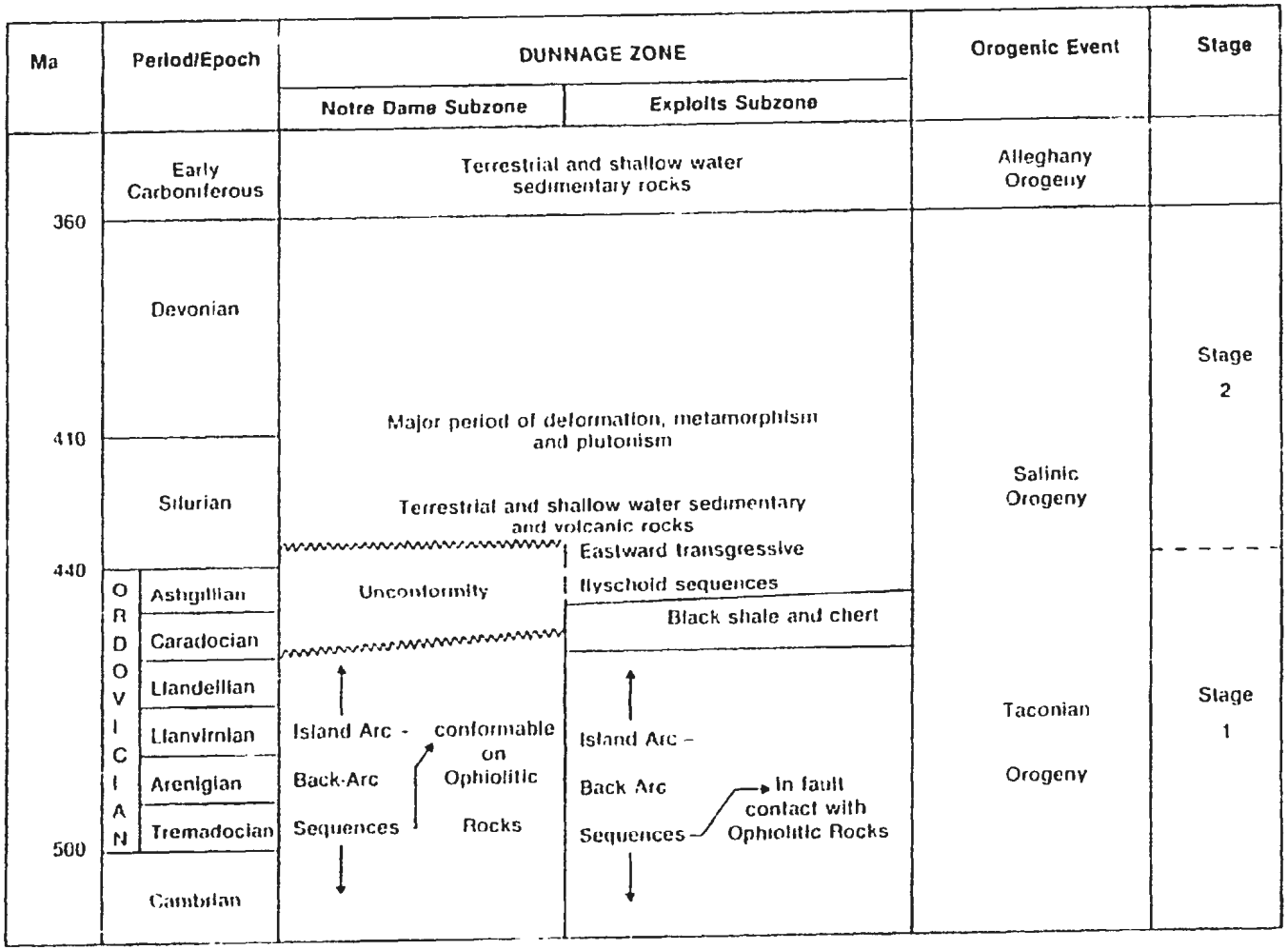

Figure 1.2. Simplified stratigraphic subdivisions of the Dunnage Zone (after Dean, 1978; Colman-Sadd and Swinden, 1984; Williams et al., 1988; and Swinden et al., 1988a). Geological time scale after Haq and Van Eysinge (1987).

CHAPTER 2

GEOLOGY AND METALLOGENY OF THE VICTORIA LAKE GROUP

2.1 REGIONAL SETTING OF THE VICTORIA LAKE GROUP

The Victoria Lake Group lies within the Exploits Subzone of the Dunnage Zone immediately south of the Red Indian Line. The group extends southwestwards from Grand Falls to King George IV Lake, and southwards from Red Indian Lake to Noel Pauls Brook (Figure 2.1).

To the northwest the Victoria Lake Group is in fault contact with the Southwest Brook Complex and the Buchans Group along the Lloyds River-Red Indian Lake Fault. Along its northern margin, south of Red Indian Lake, the group is conformably overlain by siltstone and tuffaceous sandstone of the Harbour Round Formation. To the northeast, Caradocian black shales and cherts conformably overlie the Victoria Lake Group and in turn are overlain by Middle Ordovician to Early Silurian flysch, argillite and conglomerate (Kean and Jayasinghe, 1980; 1982).

The group is unconformably overlain along its southern margin by the Silurian (?) Rogerson Lake Conglomerate. This conglomerate extends 160 km southwestward from Diversion Lake to King George IV Lake, and is interpreted to represent a molasse-like fault scarp deposit (Kean and Evans, 1988a). The conglomerate, along its

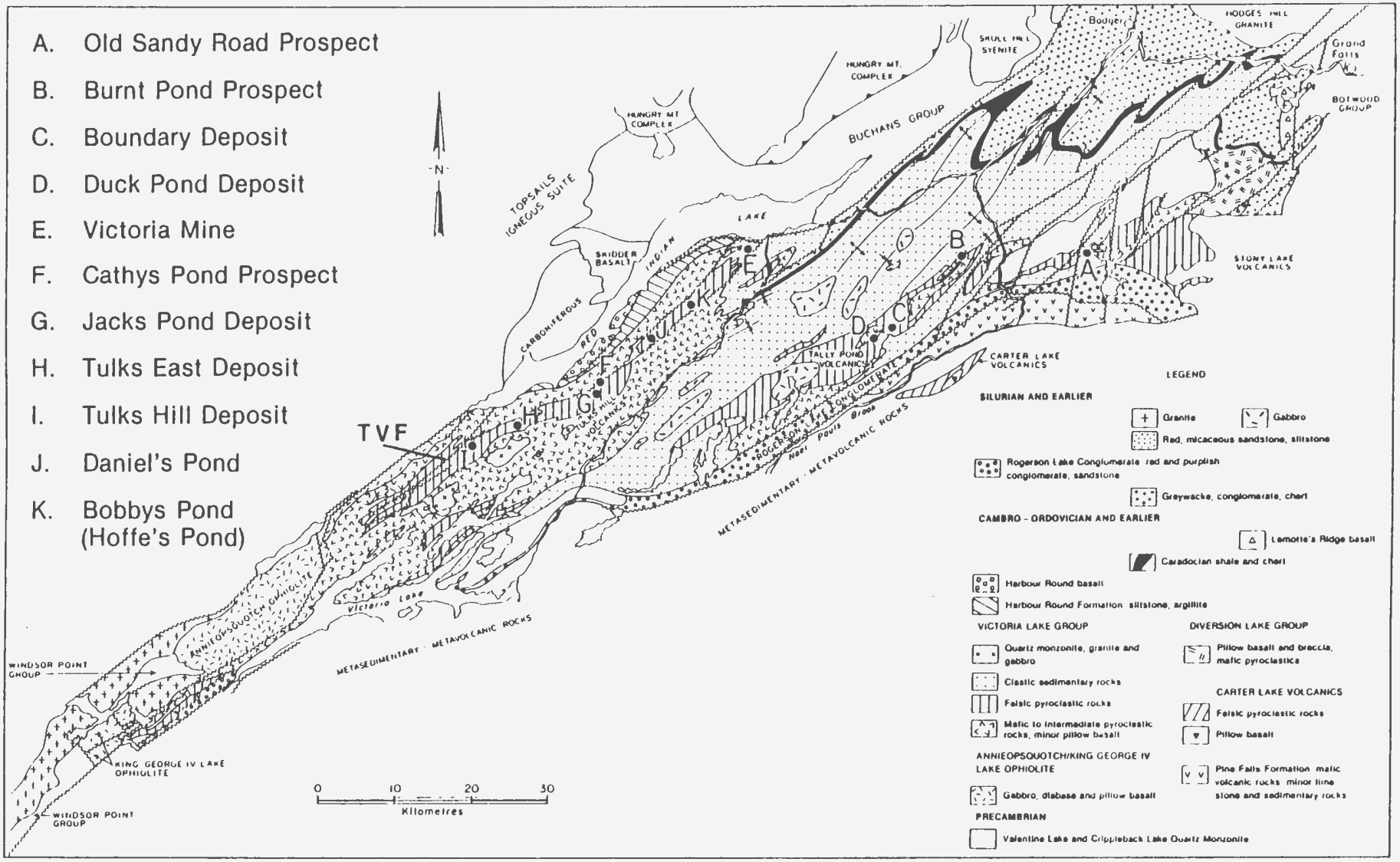

Figure 2.1. Regional geology of the Victoria Lake Group (after Kean and Evans, 1988a). Also shown are the locations of the major volcanogenic massive sulphide showings and deposits: A) Old Sandy Road, B) Burnt Pond, C) Boundary, D) Duck Pond, E) Victoria Mine, F) Cathys Pond, G) Jacks Pond, H) Tulks East, I) Tulks Hill, J) Daniel's Pond and K) Hoffe's Pond (Bobby's Pond). TVF-Tulks Valley Fault.

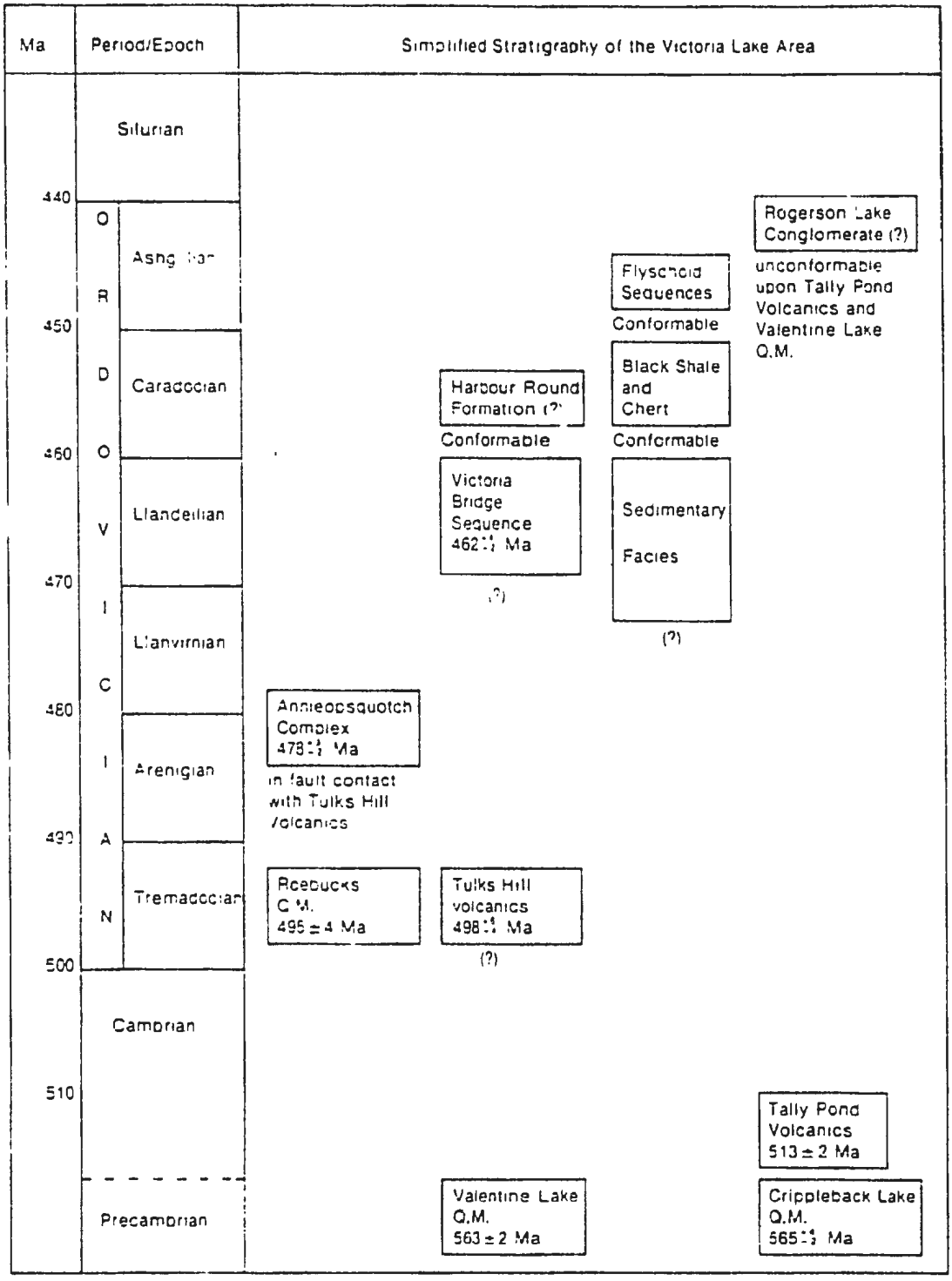

Figure 2.2. Simplified stratigraphy of the Victoria Lake area (after Kean and Jayasinghe, 1980; Dunning and Krogh, 1985; Dunning, 1986; Dunning et al., 1987). Geologic time scale after Haq and Van Eysinge (1987).

southern margin, is faulted against mafic volcanic rocks of the Pine Falls Formation and unnamed and undated volcanic and sedimentary rocks south of Noel Pauls Brook (Kean and Jayasinghe, 1980).

2.2 GEOLOGY OF THE VICTORIA LAKE GROUP

The Victoria Lake Group, as originally proposed by Kean (1977), includes all the pre-Caradocian sedimentary and volcanic rocks lying southeast of Red Indian Lake and to the north of the Rogerson Lake Conglomerate. The group was initially considered to be Middle Ordovician and older based on conodonts collected near the stratigraphic top of the group (Kean and Jayasinghe, 1980). However, recent U/Pb zircon age dating (Dunning, 1986; Dunning et al., 1987) indicates that elements of the group are Cambrian (this will be discussed further in a later section).

Regionally the Victoria Lake Group can be subdivided into two major lithofacies (Kean and Jayasinghe, 1980; 1982; Kean, 1985): 1) a sequence of mafic and felsic volcanic rocks represented by the linear Tulks Hill volcanics in the southwest and the Tally Pond volcanics in the east which combined account for approximately 60 percent of the group; and 2) a sedimentary facies in the central and northeastern portion of the group, interpreted to have been deposited in an extensive basin marginal to the adjoining volcanic sequences. The Tally Pond and Tulks Hill volcanics are informal

units of formational rank within the Victoria Lake Group.

The Victoria Lake Group occupies a regional northeast-trending structure termed the Victoria Anticlinorium (Kean, 1985). Regionally, the group dips steeply and faces northwesterly on the north limb and dips gently and faces southerly on the southern limb. Poor exposure and complicated structural relations (ie. first and second order folds result in variable facing directions) inhibit a detailed structural interpretation.

An inhomogeneously developed, regional penetrative foliation, subparallel to bedding and axial planar to tight to isoclinal folds, is developed throughout the Victoria Lake Group (Kean, 1985). The intensity of this deformation increases to the southwest. Lower greenschist facies metamorphism is prevalent throughout the group, however, middle greenschist to amphibolite grade metamorphism is locally developed along the southern margin (Kean, 1985).

2.2.1 TALLY POND VOLCANICS

Kean and Jayasinghe (1980) defined the Tally Pond volcanics as a linear belt of intercalated mafic and felsic volcanic rocks that occur along the southeastern margin of the Victoria Lake Group. The mafic volcanic rocks consist of pillowed flows and breccias. Felsic volcanic rocks consist of tuff, lapilli tuff, breccia and

locally flow-banded and brecciated rhyolite.

U/Pb zircon dating of the felsic volcanic rocks from the Tally Pond volcanics has defined an age of 517 +/-5 Ma (Dunning, 1986). This date is significantly older than the Middle Ordovician and older age previously assigned the group (Kean and Jayasinghe, 1980) and is older than any of the known ophiolitic rocks in central Newfoundland (Dunning and Krogh, 1985).

2.2.2 TULKS HILL VOLCANICS

The Tulks Hill volcanics (Kean and Jayasinghe, 1980) extend from the mouth of Victoria River 65 km southwestward to Pats Pond. The volcanic rocks form a linear belt of felsic pyroclastic and minor mafic volcanic rocks and intercalated bedded mafic to siliceous volcaniclastic and epiclastic sedimentary rocks

The felsic volcanic rocks, which consist of felsic tuff, quartz crystal tuff, breccia, locally flow banded rhyolite and minor subvolcanic porphyries, are typically dacitic to rhyolitic in composition (Kean and Jayasinghe, 1980).

Mafic volcanic rocks are typically pyroclastic, consisting of mafic to intermediate aquagene tuff, lapilli tuff, agglomerate and breccia. Pillow lavas are locally developed. Geochemical studies (Kean and Evans, 1988a) of these mafic volcanic rocks indicate that

the late Cambrian-early Ordovician sequences are island-arc tholeites.

Trace element and REE studies of mafic volcanic rocks from Tulks Hill volcanics (Kean and Evans, 1988a) suggest that the mafic volcanic rocks record a transition from island arc volcanism to a rifted arc setting and then to a non-arc setting. Within the Tulks Hill volcanics this transition conforms with the general northwest-facing stratigraphic succession (Evans et al., 1990). There appears to be a close spatial association between the rifted-arc volcanic rocks (which are depleted in incompatible elements) and the volcanogenic massive sulphide deposits suggesting that the rifted-arc environment was integral to the formation of these mineral occurrences.

Geochronological, lead isotope and geochemical studies of the Tulks Hill volcanics suggest a structural or stratigraphic break within the belt (Kean and Evans, 1988a). U/Pb zircon dating studies from the southern end of the Tulks Hill volcanics indicate a late Cambrian-early Ordovician age of 498 +6/-5 Ma (Evans et al., 1990). This concurs with the evidence from a single conodont, identified as Tremadocian in age, collected from limestone near the mid-point of the belt (Kean and Evans, 1988a).

Conodonts collected from the northern end of the belt, at the mouth of Victoria River (Kean and Jayasinghe, 1980), give a

Llanvirn-Llandeilo age. A porphyry near this fossil locality gave a U/Pb zircon age of 462 +/-2 Ma (Dunning et al., 1987) which concurs with the fossil age. Mafic volcanic rocks associated with this sequence are typically calc-alkaline (Kean and Evans, 1988a).

Recent work by BP geologists (Desnoyers, 1990a; McKenzie et al., 1990) indicates that the Llanvirn-Llandeilo age rocks, located at the northern end of the belt, are actually in fault contact with rocks of the Tulks Hill volcanics near the old Victoria Mine. These younger rocks, tentatively termed the Victoria Bridge sequence, may not in fact form part of the Victoria Lake Group and therefore rocks to the southeast of this fault originally interpreted to be Middle Ordovician may actually be Cambro-Ordovician in age as well. This sequence is tentatively correlated with the Harbour Round Formation and as such is included within this formation in Figure 2.1.

2.2.3 SEDIMENTARY LITHOFACIES

The sedimentary facies of the Victoria Lake Group consist of greywacke with interbedded siltstone, shale, argillite, conglomerate and minor limestone. The rocks exhibit cyclic bedding with ABCD, ABE, and locally CE, Bouma divisions (Kean and Jayasinghe, 1982). The rocks are typically volcaniclastic and both the coarseness and abundance of clasts increase towards the

volcanic sequences, suggesting that the sedimentary rocks were derived from the volcanic sequences, and deposited in a marginal basin or basins.

2.2.4 INTRUSIVE ROCKS

Small felsic porphyries, extensive quartz monzonitic and minor granitic and granodioritic intrusions are common, particularly within the Tulks Hill volcanics. These rocks are interpreted to have been comagmatic with the volcanism (Kean and Jayasinghe, 1980; 1982) and U/Pb zircon dating of a small quartz monzonitic body confirmed this interpretation (Evans et al., 1990). The intrusion located near Roebucks Pond was dated at 495 +/-4 Ma. These granitic bodies commonly contain blue quartz phenocrysts and quartz crystals within the felsic tuffaceous rocks of the Tulks Hill volcanics are typically blue implying a possible genetic link.

Gabbroic rocks occur locally as small intrusions within the volcanic belts. More extensive mafic intrusions appear to be restricted to the sedimentary facies.

2.3 METALLOGENY OF THE VICTORIA LAKE GROUP

Mineralization within the Victoria Lake Group was divided into two main groups by Evans and Kean (1987): 1) volcanogenic massive sulphides and associated hydrothermal alteration hosted by felsic

and depleted mafic volcanic rocks; and, 2) epigenetic gold mineralization. The epigenetic gold mineralization can be further subdivided into five styles or classes (Evans, 1992).

2.3.1 VOLCANOGENIC MASSIVE SULPHIDES

The Victoria Lake Group is host to a significant number of volcanogenic massive sulphide occurrences, five of which are of deposit status (Table 2.1). The occurrences are generally small, and comprise pyritic polymetallic (Zn-Pb-Cu) sulphides that form both stratiform-exhalative and stockwork mineralization associated with laterally extensive sheets of felsic pyroclastic rocks (Kean et al., 1981). Massive sulphide lenses within the Tulks Hill volcanics are variably deformed, and generally exhibit lensoidal shapes which typically parallel the inhomogeneously developed regional schistosity. Deposits within the Tally Pond volcanics appear to be less deformed. Specific information on size, grade and alteration is contained in Table 2.1.

DEPOSIT	DEPOSIT DESCRIPTION (SEE FIGURE 2.1)
TALLY POND VOLCANICS	
OLD SANDY ROAD	Massive and disseminated pyrite and minor chalcopyrite hosted by mafic volcanic rocks.
BURNT POND PROSPECT	Stockwork (?) and massive, banded sulphides hosted by felsic pyroclastic rocks. Assays up to 0.94% Cu, 1.05% Pb, 5.64% Zn, 0.82 oz/t Ag and trace Au (Dimmel, 1986). Alteration consists of quartz-chlorite-talc and sericite.
BOUNDARY DEPOSIT	Three massive sulphide lenses with a combined tonnage of 500,000 tonnes grading 3.5% Cu and 4.0% Zn (MacKenzie, 1988). Pervasive alteration, consisting of chlorite, pyrite, sericite and silica is extensively developed in the footwall. Bedded and brecciated sulphides are present (Kean, 1985).
DUCK POND DEPOSIT	Two massive sulphide lens, the largest has an average thickness of 18 metres, and contains published reserves of 4,033,000 tonnes grading 3.53% Cu, 1.05% Pb, 6.62% Zn, 67.39 oz/t Ag and 1.02 g/t Au. The deposit is hosted by chloritic and sericitized rhyolite and tuffaceous rocks (MacKenzie et al., 1988).
TULKS HILL VOLCANICS	
VICTORIA MINE	The prospect consists of four, small, fault bound massive sulphide lenses which contain up to 10% Cu and < 3% combined lead-zinc (Kean and Thurlow, 1975; Thurlow, 1978; Desnoyers, 1990a). Host rocks to the prospect are either strongly chloritized or quartz-carbonate altered felsic pyroclastics. Pyrite and chalcopyrite are associated with the chloritic alteration, whereas pyrite and sphalerite (+/- galena) are associated with the quartz-carbonate.

Table 2.1. Significant volcanogenic massive sulphide occurrences located within the Victoria Lake Group.

Table 2.1. continued.

JACKS POND	The prospect consists of four pyritic massive sulphide lenses which range in size from 200,000 to 900,000 tonnes and contain low base metal values (Barbour and Thurlow, 1982). Disseminated and stringer sulphides hosted within a chlorite-quartz gangue are the dominant style of mineralization, however, - exhalative sulphides are locally developed in one lens (Kean and Evans, 1986). The alteration mineralogy consists primarily of chlorite, sericite, pyrite, and silica. The alteration zone is enriched in K2O relative to felsic rocks outside the zone (Evans, 1986). Microprobe analysis of chlorite from the within the zone indicates the chlorite is Mg-rich.
TULKS EAST DEPOSIT	The deposit contains three stratiform pyritic, massive sulphide lenses, with low base metal values, and a combined tonnage of approximately 5,600,000 tonnes (Barbour and Thurlow, 1982). Banding is locally developed. Host rocks to the mineralization are felsic pyroclastics and these exhibit sericite, pyrite and silica alteration (Thurlow and Barbour, 1982; Kean and Evans, 1986).
TULKS HILL DEPOSIT	The deposit contains four pyritic, locally banded, massive sulphide lenses that have a combined tonnage of approximately 750,000 tonnes grading 5-6% Zn, 2% Pb, 1.3% Cu, 41 g/t Ag and 0.4 g/t Au (Kean and Thurlow, 1976; Jambor and Barbour, 1987). Sulphide layering is well developed, however, this may be a tectonic fabric. Host rocks to the mineralization are felsic pyroclastics. Subvolcanic felsic porphyries and aphanitic rhyolite are present. Alteration consists of silica, sericite, pyrite and locally chlorite. Chlorite from the mineralized zones are enriched in Mg relative to chlorite from less mineralized zones (Moreton, 1984).

Table 2.1. continued.

DANIEL'S POND	Lensoid, Ag-rich, Zn-Pb mineralization which is confined to a narrow, north-south-trending high strain zone. Host rocks to the mineralization are variably deformed felsic pyroclastic rocks (McKenzie et al., 1990). Published grades from the diamond drilling include 5.5 m of 1.12 % Cu, 18.82 % Zn, 10.92 % Pb, 399.5 g/t Ag and 1.1 g/t Au (BP Canada, 1990).
HOFFE'S POND	Massive sulphide mineralization (BOBBY'S POND) associated with extensively altered felsic volcanic rocks.

2.3.2 EPIGENETIC GOLD MINERALIZATION, VICTORIA LAKE GROUP

Five styles of gold-enriched mineralization or possible gold-related alteration are present within the Victoria Lake area (Evans, 1992): 1) base metal sulphide-rich quartz veins; 2) pyritiferous quartz veins; 3) disseminated gold; 4) barite veins; and 5) epithermal-stye high alumina alteration.

2.3.2.1 PYRITIFEROUS QUARTZ VEINS

The most economically significant gold mineralization within Victoria Lake area comprises pyritiferous quartz veins. These veins contain pyrite (with which the gold is often associated), tourmaline, sericite, local paragonite, minor base metals, traces of scheelite, tungstite, pyrrhotite, arsenopyrite, bornite and locally free gold. Three significant showings exhibit this style of mineralization; Midas Pond, Valentine Lake and Long Lake (Figure

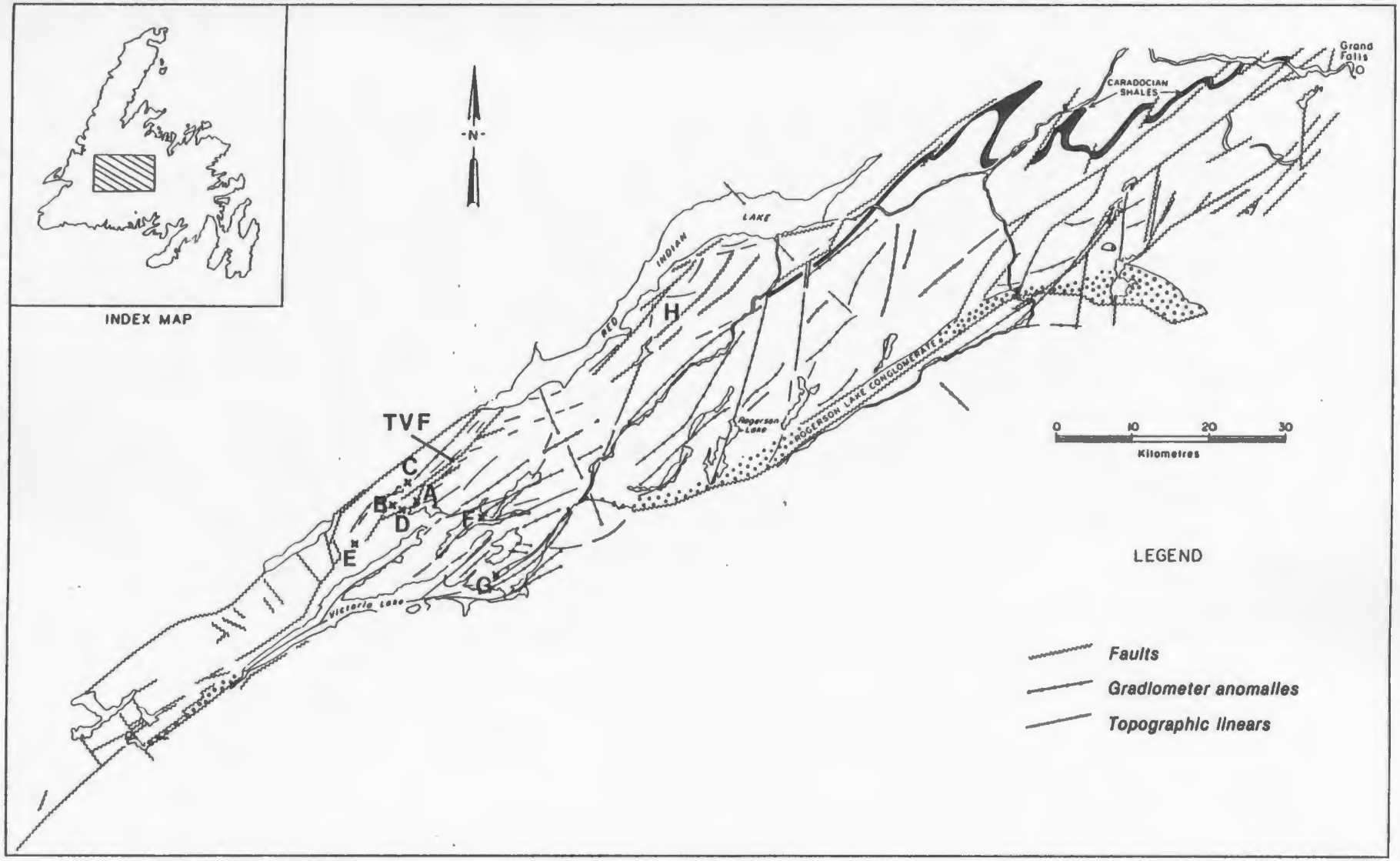

Figure 2.3 Epigenetic gold occurrences and structural, topographic and gradiometer anomaly (aeromagnetic vertical gradient) linears developed within the Victoria Lake Group (after Kean and Evans, 1988a; Tuach et al., 1988). A) Midas Pond, B) Road Showing, C) West Tulks, D) Glitter Pond, E) Pats Pond, F) Long Lake, G) Valentine Lake, and H) Bobbys Pond. TVF-Tulks Valley Fault.

2.3).

2.3.2.2 BASE METAL SULPHIDE-RICH QUARTZ VEINS

Base metal sulphide-rich veins are typically small, less than 5 cm thick and discontinuous. These veins are dominantly extensional and exhibit comb structures, open-space filling textures and little evidence of shearing along vein margins. Silver contents can be quite variable, ranging from nil to greater than 100 g/t for mineralized float from Pats Pond (Thurlow and Barbour, 1982), and appear to be directly related to the relative abundance of galena. This style of mineralization is present at the Pats Pond prospect, the Road showings and along strike from the West Tulks showing (Figure 2.3). This style of mineralization appears to be largely confined to small brittle structures and based on current knowledge offer little hope of being economic.

2.3.2.3 BARITE VEINS

The Glitter Pond prospect (Figure 2.3; Kean and Evans, 1988a; Howse, 1992) is the only auriferous barite vein system reported from the Dunnage Zone. The prospect, hosted by sericitic felsic tuff of the Tulks Hill volcanics, is located approximately 3.5 km southwest of Midas Pond. It can be traced along a northeast-southwest-trending ridge for a distance of approximately 20 m and is partially exposed by trenching.

The mineralization comprises a mixture of white and greyish-white barite, quartz and small clots and bands of pyrite (Howse, 1992). A grab sample from the prospect assayed 2.55 g/t gold and 14.0 g/t silver (Thurlow and Barbour, 1985; Thurlow et al., 1987). Diamond drilling intersected a zone which assayed 0.22 g/t gold over 7.6 m. The prospect was determined to be uneconomic.

2.3.2.4 DISSEMINATED GOLD

Disseminated gold mineralization occurs within intensely siliceous banded rocks at the West Tulks showing (approximately 2 g/t from a grab sample; Thurlow et al. 1987). The rocks are described as either mylonitic felsic volcanic rocks, cherty sediments or a silica precipitate (Kean and Evans, 1988a). They are fine-grained, strongly banded, grey to white with minor hematite staining. No sulphide minerals are visible and the nature of the gold mineralization is unknown. Auriferous base metal veins are also present but occur along strike to the northeast.

2.3.2.5 EPITHERMAL-STYLE ALTERATION

Epithermal-style high alumina alteration is developed at Bobbys Pond (Figure 2.3) within sheared felsic pyroclastic rocks of the Tulks Hill volcanics. The alteration zone was located following the discovery, in the fall of 1985, of boulders containing silica, sericite, pyrophyllite, alunite, native sulphur,

orpiment and minor pyrite.

The alteration zone forms a northeast-trending linear belt which has been traced for approximately three km. Exposure is sparse but isolated outcrops comprise sheared, highly siliceous rocks (Desnoyers, 1990b). Abundant disseminated and massive pods of pyrite are locally developed particularly in areas of strong argillic alteration. A thin halo of chloritic alteration mantles the alteration zone (Desnoyers, 1990b). To date economic concentrations of gold have eluded exploration activities in the area.

$^{40}Ar/^{39}Ar$ dating of sericite from one of the altered boulders at Bobbys Pond produced a plateau age of 392 +/-4 Ma (Kean and Evans, 1988a). This would be a minimum age for the alteration and is interpreted to represent the age of peak regional metamorphism. Flow-banded (?) rhyolites (Kean and Jayasinghe, 1980), located to the northeast of the Bobbys Pond alteration zone, may either represent a change from subaqueous to a subaerial volcanism within the Tulks Hill volcanics or are the product of Silurian volcanism. Such volcanic activity would favour the formation of epithermal systems.

The style of alteration at Bobbys Pond is somewhat akin to the acid-sulphate type of epithermal deposit described by Heald et al. (1987). The acid-sulfate style is characterized by intense

silicification, acid leaching producing argillic alteration, and the presence of sulphur minerals. It is best developed in rhyodacitic rocks of caldera complexes where localized extensional tectonics produce well-developed fracture systems. The alteration and mineralization is produced during the waning stages of volcanism as gases such as H_2S and CO_2 are evolved.

2.4 SUMMARY

The Victoria Lake Group is a structurally complex assemblage of Cambro-Ordovician island-arc volcanic, volcaniclastic and epiclastic rocks. Geochemical studies indicate that the mafic volcanic rocks record a transition from island-arc to back-arc environments.

Mineralization within the Victoria Lake Group comprises: 1) volcanogenic massive sulphide mineralization, believed to have formed during arc-rifting process (Swinden et al., 1989; Evans et al., 1990); and, 2) epigenetic, structurally controlled gold mineralization. The gold mineralization can be subdivided into five classes or styles, based on alteration, mode of occurrence and/or mineralogy. These classes are; 1) pyritiferous quartz veins; 2) base metal sulphide-rich quartz veins; 3) barite veins; 4) disseminated gold; and, 5) epithermal style alteration.

CHAPTER 3

GENERAL GEOLOGY

3.1 INTRODUCTION

This chapter examines the general geology and petrology of the Midas Pond prospect. Lithologies within the study area are typical of the Tulks Hill volcanics, Victoria Lake Group, and can be subdivided locally into 4 units on the basis of rock type, composition and degree of deformation (Figure 3.1). These subdivisions do not necessarily represent stratigraphic units. A geology map is located in Appendix 5.

Intense hydrothermal alteration overprints much of the felsic volcanic rock, particularly within the shear zone which hosts the gold mineralization. The alteration and mineralization will be discussed in Chapter 5.

3.2 TULKS HILL VOLCANICS (UNITS 1-4)

Volcanic rocks in the Midas Pond area are comprised of approximately 60 percent felsic, crystal tuff, lapilli tuff and breccia and 40 percent coarse mafic breccia and mafic, feldspar crystal tuff.

A 7 m intersection of graphitic shale was observed in diamond

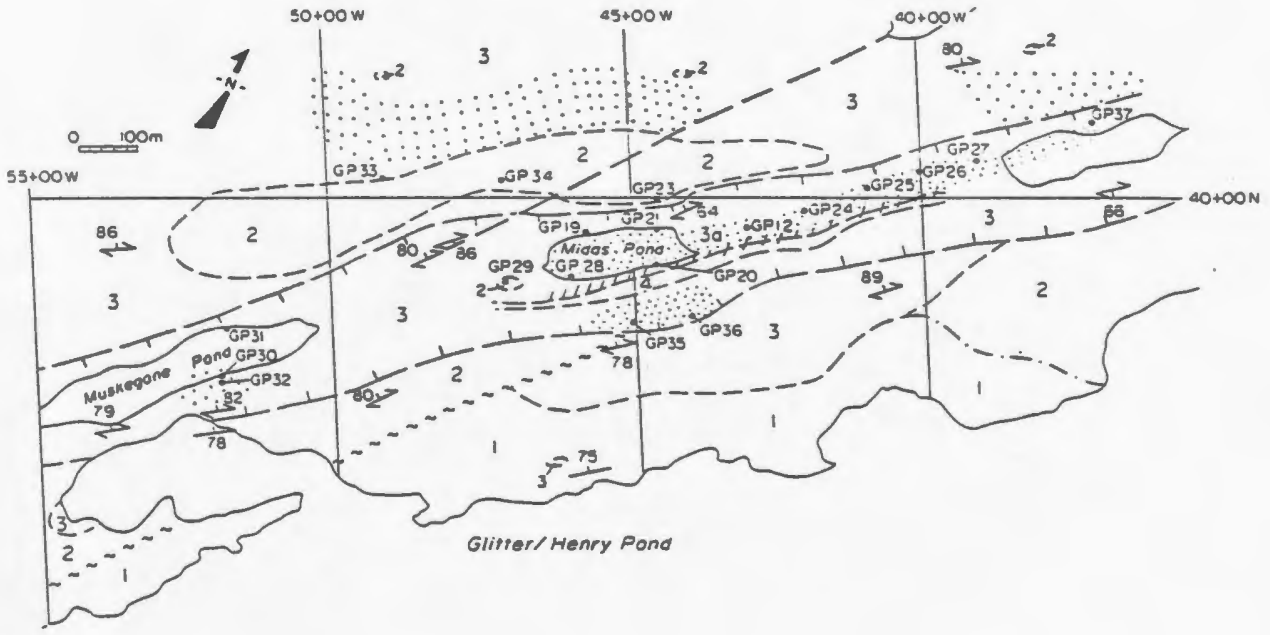

LEGEND

4	Banded mafic unit
3	Felsic crystal tuff, lapilli tuff and minor mafic crystal tuff
2	Mafic, feldspar crystal tuff and minor breccia
1	Mafic breccia and minor feldspar crystal tuff
////	Zone of gold enrichment
:::::	Zone of alumina alteration
: : : :	Zone of silicification

SYMBOLS

	geological contact (defined, approximate, gradational)
~ ~ ~	fault (approximate)
	shear zone
	air-photo lineament
•GP	diamond drill hole
	bedding tops known (inclined)
	cleavage (inclined)

Figure 3.1. Geology of the Midas Pond area.

drill hole GP-34 (for location see Figure 3.1) which was drilled at an angle of 45° south. The shale occurs within the shear zone, in a sequence of deformed felsic to intermediate tuffaceous rocks of Unit 3. The contact between the shale and the structurally overlying tuff is not preserved in the drill core. However, the contact between the shale and the structurally underlying felsic tuff appears to be gradational. This shale is not exposed at surface and has an unknown lateral extent, but it is similar to black graphitic shales observed outside the study area in Tulks Valley and at the southwestern extremity of Tulks Hill. The regional significance, if any, of these graphitic shale horizons is not known.

Plutonic rocks are absent within the immediate study area. However, a number of small, medium-grained gabbroic plugs outcrop on islands within Glitter Pond and to the north of Midas Pond. Mafic dikes appear to be absent although rocks of possible dike origin have been reported from drill core. The rocks in question are fine-grained, schistose and have either poorly preserved or veined contacts and are indistinguishable from the deformed mafic tuffs.

The metamorphic grade of the rocks within the study area is lower greenschist facies with quartz, feldspar, sericite, chlorite and epidote as widely developed metamorphic minerals.

An inhomogeneous, northeast-trending, northwest steeply-dipping, foliation is developed within the Midas Pond area. This foliation parallels bedding and is consistent with the regional foliation trend of the Tulks Hill volcanics (Kean and Jayasinghe, 1980).

A northeast-trending, 200 m wide, inhomogeneously developed shear zone transects the Midas Pond area and parallels the regional schistosity. The trace of this structure is outlined by Muskegone and Midas ponds, and an unnamed pond to the northeast (Figure 3.1).

Deformation has largely obliterated primary textures resulting in a paucity of facing directions. However, facing directions obtained from graded bedding at two localities, within Units 1 and 2, indicate the sequence faces northwest which is consistent with observations elsewhere in the Tulks Hill volcanics (Kean, 1985; Kean and Evans, 1986). At the Tulks Hill Deposit, 12 km along strike to northeast, Moreton (1984) identified an isoclinal folding event within the Tulks Hill volcanics. He suggested that this folding episode was responsible for the spatial distribution of two of the massive sulphide lenses. No evidence of such folding was observed within the Midas Pond area. It is therefore postulated that the rocks form a conformable sequence which has been subjected to inhomogeneous deformation, and shearing.

3.2.1 UNIT 1 MAFIC BRECCIA

Unit 1 is comprised of coarse, angular, locally flattened breccia and minor feldsparphyric tuff (Plate 3.1). The unit outcrops and is best exposed along the shore of Glitter Pond. It has a mappable thickness of between 150 and 200 m and a strike length of greater than 1.5 km. The unit passes gradationally into Unit 2. South of Muskegone and Midas ponds the contact between the two units is faulted. To the north, Unit 1 is overlain by felsic crystal tuff of Unit 3, the nature of the contact is unknown as it is not exposed.

Primary structures are typically obscured by the deformation, particularly northwards through the unit where the breccia becomes quite flattened. Graded bedding, which was observed at one outcrop (86-87), indicates that the unit youngs to the NW. Foliation trends and dips vary between 46°/80° NW and 54°/70° NW and appear to more or less parallel bedding.

The matrix to the breccia is fine-grained, dark green, typically feldsparphyric and is generally compositionally indistinguishable from the mafic feldspar crystal tuffs of Unit 2. Locally the matrix is highly epidotized and cut by abundant calcite and minor epidote veinlets. Calcite also forms coatings on fracture surfaces. Small 1-2 mm pyrite cubes are locally developed.

The breccia blocks are generally quite angular and have a maximum observed size of 1 m x 15 cm. Flattened clasts up to 45 cm x 15 cm were observed close to the northern contact of the unit. The clasts are generally more siliceous than the matrix; however, mafic, feldsparphyric, locally vesicular and epidotized clasts are also present in particular in the eastern part of the unit. The siliceous clasts are fine-grained, light grey-green and weather cream to light greenish-grey in colour.

In thin section the matrix of these breccias is comprised of aggregated clumps of plagioclase phenocrysts in a quartzo-feldspathic groundmass. The plagioclase phenocrysts exhibit both albite and Carlsbad twinning and are variably altered and veined by carbonate, sericite and locally epidote. The quartzo-feldspathic groundmass is comprised of fine-grained, variably deformed and altered quartz crystals, plagioclase microlites and minor disseminated pyrite. The feldspars are locally epidotized and altered to blue chlorite, sericite and carbonate as a result of greenschist metamorphism. Sericitic-rich zones or bands take up most of the deformation and form narrow anastomosing flattened veinlets which generally parallel the regional foliation.

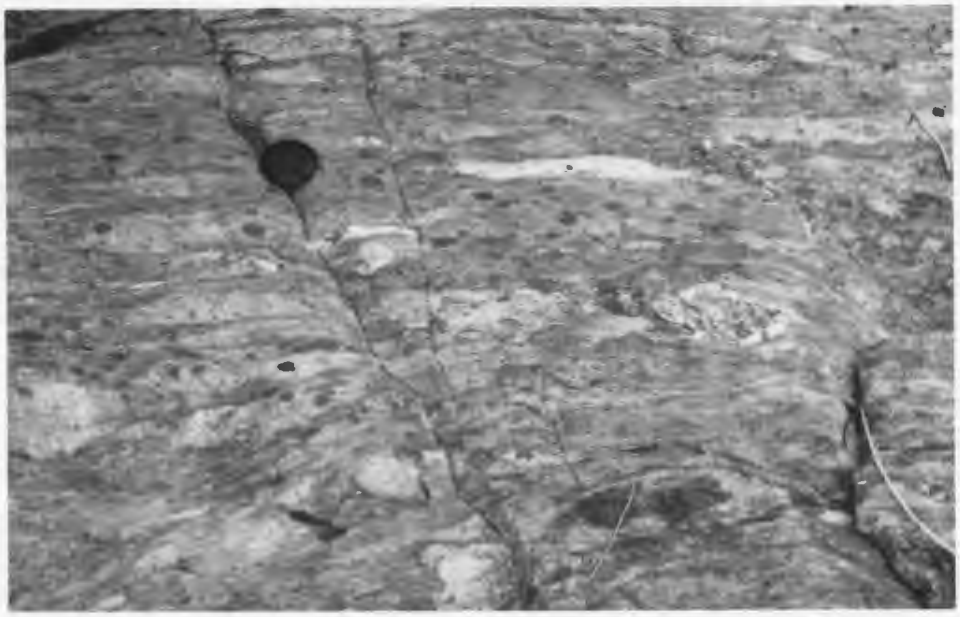

Plate 3.1 Deformed breccia of Unit 1, located east of Midas Pond. Felsic blocks comprise the majority of the breccia fragments.

Plate 3.2 Olive green, mafic feldspar crystal tuff (Unit 2) west of Midas Pond.

3.2.2 UNIT 2 MAFIC FELDSPARPHYRIC TUFF

This unit is comprised of dark-green, fine-grained, intermediate to mafic, feldsparphyric tuff (Plate 3.2) and minor breccia. It is exposed in three areas: along the shore of Glitter Pond to the east of Unit 1, south of Muskegone and Midas ponds to the north of Unit 1 and as a long linear belt to the north of Muskegone and Midas ponds. The thickest part (approximately 300 m) of this unit occurs to the east of Unit 1. The northernmost portion of this unit (north of Muskegone and Midas ponds) has an exposed strike length of approximately 1.1 km. Contacts with the surrounding felsic volcanic rocks of Unit 3 are generally not exposed and are interpreted to be fault-modified conformable contacts. This interpretation is based on a single exposure which is located in a trench (L 52+00) south of Muskegone Pond. At that locality the mafic tuff of Unit 2, exhibiting graded bedding striking and dipping 57°/82° NW and facing NW, is conformably overlain by felsic crystal tuff of Unit 3. Pyritiferous quartz veining, barren of gold, is developed along this contact.

The mafic, feldsparphyric tuffs exhibit an inhomogeneously developed penetrative foliation which parallels the regional northeast trend. The rocks vary from undeformed, ie. exhibiting graded bedding, to highly schistose, particularly along a fault which runs from Henry Pond northeastwards to Midas Pond. The tuffs also become more deformed as the contact with the shear zone

hosting the gold mineralization is approached. The intensity of the foliation increases and breccia fragments become flattened.

The mafic, feldsparphyric tuffs are fine-grained, dark to olive-green in colour, chloritic and are locally epidotized. Feldspar phenocrysts weather white and range in size from 1-3 mm. Calcite is a common constituent occurring as patches, veinlets and fracture coatings. Quartz-carbonate veins with locally developed coarse patches of fine-grained chlorite or epidote are common.

Mafic breccias are a minor component of Unit 2 and these breccias are similar to those of Unit 1 but are not as coarse-grained. The matrix is fine-grained, dark green to olive green and feldsparphyric. Both mafic and felsic blocks are present in the breccia.

The mafic feldsparphyric tuffs, as seen in thin section, are comprised of plagioclase phenocrysts in a randomly oriented groundmass of plagioclase microlites. The phenocrysts range up to 3-4 mm in size and are typically andesine in composition. They exhibit both albite and Carlsbad twinning and locally exhibit weak zoning. The phenocrysts are weakly saussuritized and epidotized. In more deformed rocks the feldspar phenocrysts are rotated and chlorite is developed in pressure shadows (Plate 3.3).

Locally quartz phenocrysts form a significant, although

restricted, component of these mafic rocks, particularly south of Muskegone Pond (outcrop 162 on large map). The quartz occurs as single phenocrysts, locally exhibiting embayed margins, and as aggregates of phenocrysts up to 3 mm in diameter.

The groundmass of these mafic tuffs is comprised of randomly oriented microlites of plagioclase which exhibit both twinned and untwinned crystals. The feldspars are locally altered to epidote and minor brown, green and locally purple chlorite as part of the regional metamorphism (Plate 3.3)

The chlorite in the pressure shadows is dominantly purplish-brown. Brownish-green and green chlorites are locally developed throughout the groundmass. All of these chlorites, based on electron microprobe analyses (Table 3.1), are Fe-rich and are typical of chlorite from mafic volcanic rocks throughout the Tulks Hill volcanics (see Figure 7.1). The chlorites plot in the ripidolite-pycnochlorite fields of Hey's (1954) nomenclature diagram (Figure 3.2).

With an increase in the intensity of deformation these plagioclase microlites become rotated into alignment and are cut by anastomosing, locally flattened veinlets of sericite and chlorite. These high strain zones form bands which range from millimetres in thickness to zones enveloping whole outcrops reflecting the inhomogeneity of the regional deformation. Opaques comprise 1-2

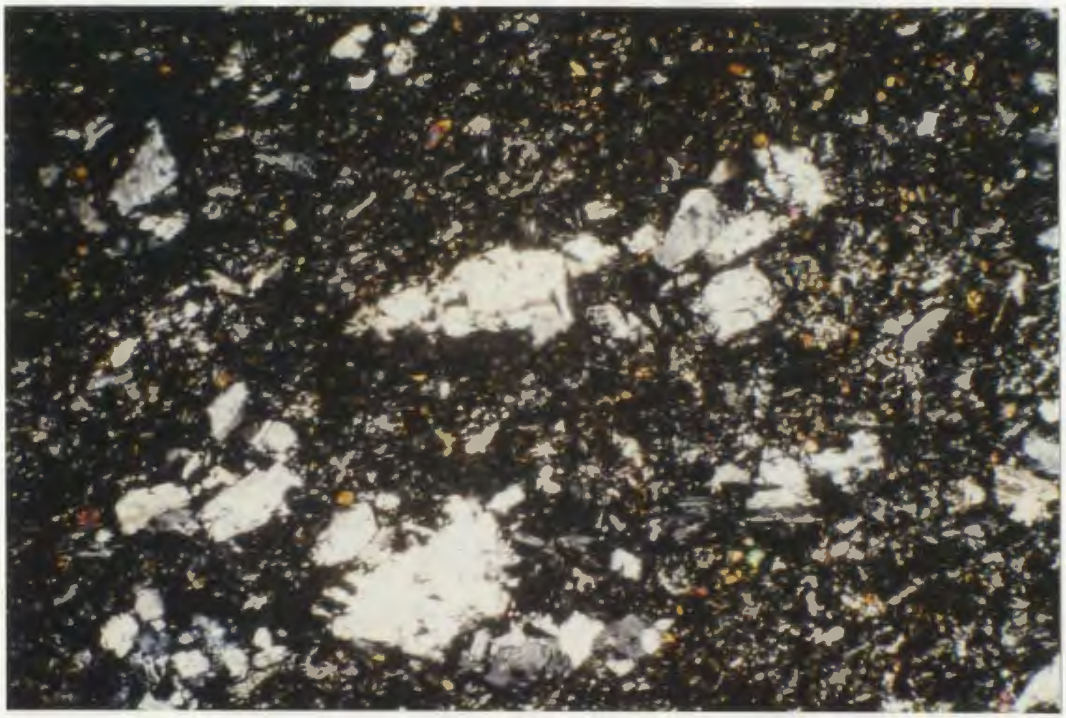

Plate 3.3 Photomicrograph of mafic feldsparphyric tuff (Unit 2). Broken plagioclase phenocrysts in a groundmass of feldspar microlites. Both phenocrysts and groundmass exhibit alteration to epidote and chlorite. Field of view is approximately 3.25 by 5 mm.

Sample	86-70	86-70-1	86-83-1	86-83-2	86-114A	86-135-1	86-135-2	86-135-3	86-149A	86-222
	2	1	3	2	3	1	2	2	4	1
Na_2O	.08	.02	.01	.05	.04	.05	.02	.00	.01	.12
MgO	15.85	15.35	11.81	12.24	13.63	14.36	15.49	14.68	12.29	13.23
Al_2O_3	19.66	18.97	22.08	21.71	20.89	21.28	21.86	21.78	22.15	21.18
SiO_2	26.79	26.52	24.45	25.49	26.46	25.71	25.65	26.09	25.06	23.34
K_2O	.02	.00	.01	.01	.00	.00	.00	.01	.01	.00
CaO	.00	.00	.00	.02	.02	.02	.00	.02	.01	.00
TiO_2	.06	.04	.05	.05	.03	.05	.03	.04	.03	.04
Cr_2O_3	.03	.03	.01	.02	.02	.03	.00	.01	.015	.03
MnO	.27	.40	.11	.09	.05	.20	.05	.03	.065	.04
FeO*	24.72	24.79	30.48	30.41	26.17	24.75	25.82	27.12	30.41	23.38
NiO	.02	.07	.01	.01	.01	.06	.03	.05	.01	.00
Total	87.51	86.17	89.02	90.09	87.32	86.49	88.96	89.82	90.08	81.36
Na	.031	.006	.000	.018	.012	.019	.006	.000	.003	.053
Mg	4.966	4.899	3.753	3.830	4.301	4.553	4.794	4.518	3.847	4.468
Al	4.867	4.792	5.548	5.378	5.214	5.333	5.356	5.300	5.487	5.652
Si	5.632	5.679	5.210	5.353	5.600	5.471	5.332	5.391	5.272	5.286
K	.006	.000	.000	.000	.000	.000	.000	.000	.000	.000
Ca	.00	.000	.000	.000	.000	.000	.000	.000	.000	.000
Ti	.006	.000	.006	.006	.000	.006	.000	.006	.000	.000
Cr	.00	.000	.000	.000	.000	.000	.000	.000	.000	.000
Mn	.043	.069	.019	.012	.066	.031	.006	.000	.023	.006
Fe	4.343	4.440	5.430	5.341	4.630	4.403	4.483	4.688	5.345	4.428
Ni	.000	.006	.000	.000	.000	.006	.000	.006	.001	.000
Total	19.893	19.891	19.966	19.938	19.763	19.821	19.978	19.909	19.964	19.894

Table 3.1 Chlorite microprobe analyses, computed cation proportions are based on 28 oxygen atoms. Each analysis is an average, the number of analyses per grain is given immediately below the sample number; mafic tuff (86-70 and 86-83) and Banded Mafic unit (86-114A, 86-135, 86-149A and 86-222). Analytical techniques and parameters are listed in Appendix 1.

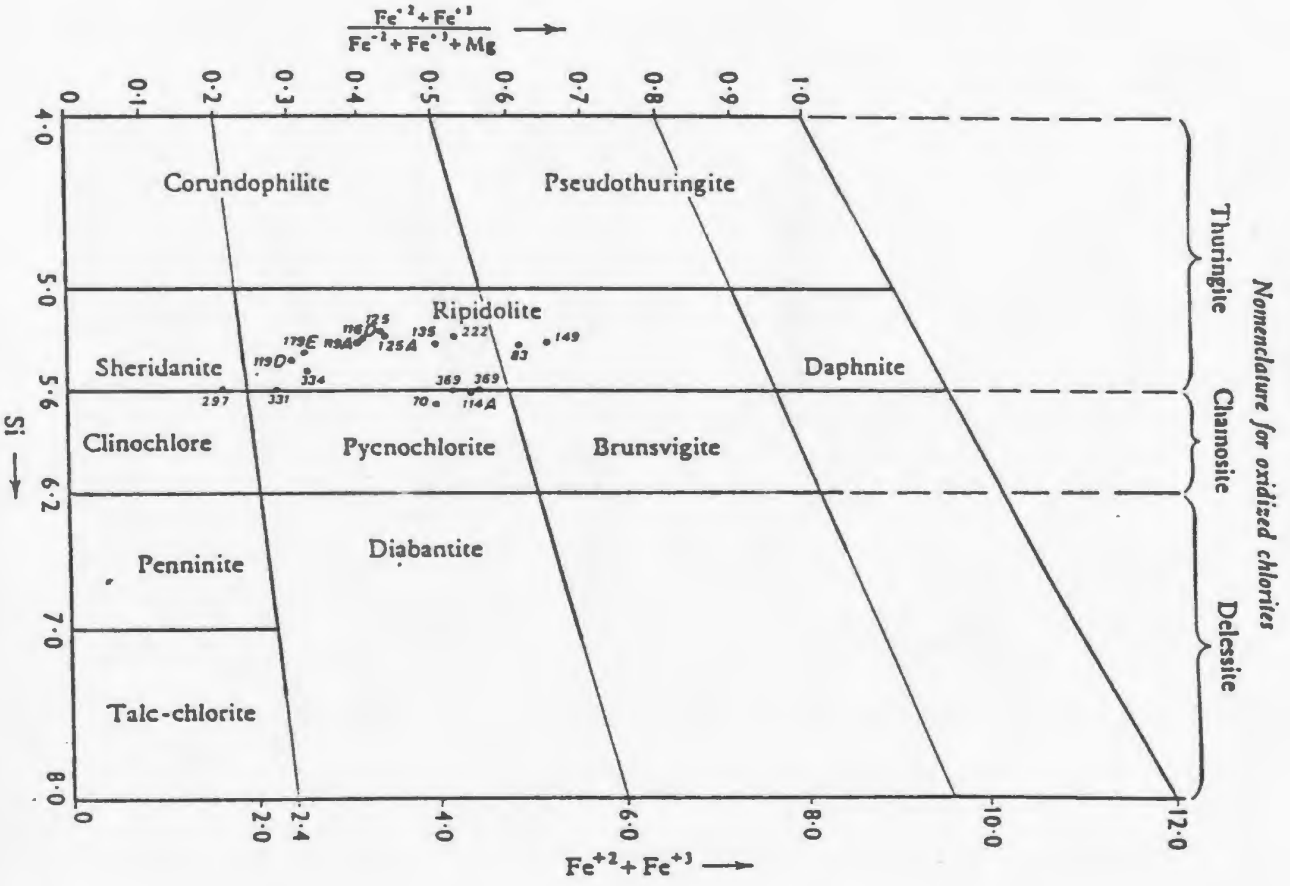

Figure 3.2 Chlorite nomenclature diagram (after Hey, 1954) illustrating the compositional range for Midas Pond chlorites. Samples 70 and 83 are from Unit 2 and samples 114a, 135, 149 and 222 are from the banded mafic rocks of Unit 4. Data for Jacks Pond are taken from Evans (1986); samples 297, 331 and 334 (chloritic alteration); and samples 369 (mafic tuffs). The remaining Midas Pond samples (116d, 119A, 119D, 125, 125A and 179E) are discussed in Section 7.2.3.

percent disseminated, often oxidized, pyrite which is typical for the Tulks Hill volcanics.

3.2.3 UNIT 3 FELSIC CRYSTAL TUFF

Unit 3 is comprised of felsic, quatrz-feldspar crystal tuff with minor lapilli tuff and breccia. The unit is the most extensive within the study area and hosts both the shear zone and most of the alteration associated with the gold mineralization. The regional extent of this unit is unknown.

Unit 3 is variably deformed, ranging from massive crystal tuff (Plate 3.4) to sericitic schist. Foliation trends and dips vary from 45°/65° SE to 56°/88° NW and largely reflect the wrapping of the foliation around more competent lozenges of siliceous tuff. The shear zone is discussed in Chapter 4.

The felsic crystal tuffs weather cream to white and are light green on fresh surfaces. The matrix is typically fine-grained and siliceous. Quartz phenocrysts (eyes) range from 1 to 4 mm across and are either glassy to milky white. Feldspar phenocrysts are white and range from 1 to 3 mm across. Wispy, fine-grained sericite or paragonite is abundant and largely define the foliation. Locally, the tuffs are deformed to mica schists, especially within the shear zone, with quartz phenocrysts being the only primary feature preserved. Lapilli and breccia clasts are of

the same composition as the host lithology.

Minor disseminated pyrite is common and often causes the tuffs to weather a rusty colour. Quartz and quartz-carbonate veins are widely developed.

In thin section the felsic crystal tuffs are comprised of phenocrysts of quartz and plagioclase and lesser K-feldspar in a quartzo-feldspathic groundmass (Plate 3.5). The quartz phenocrysts are typically crystal fragments exhibiting embayed margins and wavy extinction. Patches of recrystallized quartz up to 2 mm in diameter are common.

Plagioclase phenocrysts exhibit both albite and Carlsbad twinning and are typically andesine. Saussuritization of the phenocrysts is variable from a very fine dusting to intense almost total replacement of the crystal. Sericite locally mantles the phenocrysts and occurs as fine veinlets which cut both the phenocrysts and the groundmass.

K-feldspar, possibly orthoclase, is present as variably sericitized crystal fragments which exhibit Carlsbad twinning. The K-feldspar, which is more prone to sericitization than the plagioclase, has been completely destroyed in the more altered felsic pyroclastic rocks.

Within Unit 3 there is a zone of siliceous felsic volcanic rock which is exposed along the crest of Tulks Hill to the north of Midas Pond. These siliceous rocks have a mappable thickness of approximately 100 m and appear to form a discontinuous zone extending across the study area for a distance of 1.4 km.

The siliceous felsic rocks are comprised of either narrow, siliceous bands separated by zones of sericite or a ubiquitous blue-grey, massive, aphanitic rock with abundant, fine-grained, disseminated pyrite. The rocks vary in colour from white or beige in the least altered (?) portions to a washed out blue-grey in the most siliceous areas (outcrops DE-86-63 and 66). These rocks appear to pass gradationally into less siliceous-looking felsic volcanic rocks.

Thin sections indicate that these siliceous rocks have a groundmass comprised of tiny, randomly oriented feldspar laths and recrystallized fine-grained quartz. The feldspar laths are locally altered to purplish-blue and green chlorite, carbonate and minor epidote. Fine veinlets of sericite and pyrite cross-cut the matrix, and small euhedral pyrite cubes are scattered throughout the groundmass. Feldspar phenocrysts are largely unaltered but are locally mantled by carbonate and exhibit minor sericitization. In deformed areas, the feldspar microlites and fine-grained sericite are developed parallel to the foliation. No pyrophyllite was observed in these rocks.

Plate 3.4 Typical Tulks Hill felsic quartz crystal tuff.

Plate 3.5 Photomicrograph of a weakly deformed felsic crystal tuff from Unit 3 (field of view is approximately 3.25 by 5 mm). Quartz and feldspar phenocrysts are developed in a quartzo-feldspathic matrix. The quartz phenocrysts exhibit undulatory extinction and the feldspar phenocrysts show typical albite twinning. Small wispy patches of sericite define the cleavage.

Accessory minerals consist of 1-2 percent pyrite which occurs as disseminated, rounded to subhedral crystals, and minor patches of fine-grained, amorphous sphene which appears to be altered to leucoxene.

3.2.4 UNIT 4 BANDED MAFIC UNIT

A large lens, referred to as the Banded Mafic unit, occupies the central portion of the shear zone immediately south of Midas Pond. These rocks have a strike length of approximately 700 m and a maximum thickness of approximately 30 m. Rocks of the Banded Mafic unit are distinctive in that they are comprised of alternating narrow, dark green, fine-grained chloritic, locally feldsparphyric, bands and discontinuous, sugary-textured siliceous, locally rusty-weathering, bands (Plate 3.6). These siliceous bands range from 1 to 2 mm up to 2 cm in width and from 1 to 30 cm in length. The protolith to this banded unit is interpreted to have been a coarse mafic breccia with felsic clasts similar to the breccias of Unit 1 (Plate 3.7). Clasts have been transposed into the plane of flattening to give a banded characteristic to the rock.

In thin section these rocks are comprised of alternating fine-grained quartz-rich and chlorite-rich bands (Plate 3.8). Remnant feldspar phenocrysts, exhibiting albite twinning and altered to quartz, carbonate, minor brown chlorite and sericite,

are present in the chloritic bands. These phenocrysts often have very ragged edges. The chlorite is similar in compositions to those from the mafic tuffs (Table 3-1, Figures 3.2 and 7.1) Locally, quartz phenocrysts are preserved in the siliceous bands. The rocks are cut by fine stringers and veinlets of sericite.

The rocks of the banded mafic unit become rusty and siliceous-looking proximal to the auriferous quartz veins. The importance of this unit with respect to the gold mineralization is addressed in later chapters.

3.4 SUMMARY

Rocks of the Midas Pond area, outside the zone of intensive hydrothermal alteration associated with the gold mineralization, are fairly typical of the Tulks Hill volcanics. Both mafic and felsic rocks comprise waterlain pyroclastic lithologies from which most of the primary textures have been obliterated by regional deformation. The lithologies have all been variably affected by metasomatism related to both regional metamorphism and hydrothermal alteration related to mineralizing processes. Mineralogically the rocks contain minerals typical of greenschist facies metamorphism; chlorite, epidote, sericite, albite, carbonate and quartz.

Plate 3.6 Typical banded mafic rocks of Unit 4. Bands are comprise alternating chlorite- and quartz-rich layers.

Plate 3.7 Pyroclastic breccia developed within Unit 4 (Trench 40+00). Breccia fragments are felsic and are similar to those observed in the breccia of Unit 1.

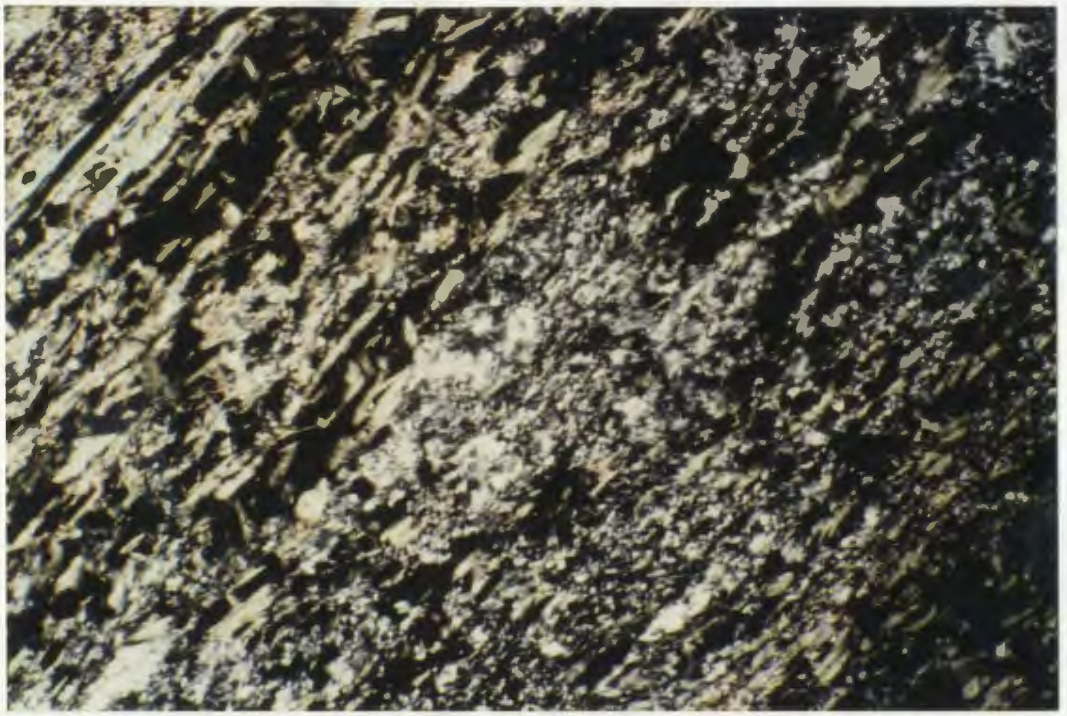

Plate 3.8 Photomicrograph which exhibits the alternating chlorite- and quartz-rich bands observed in Unit 4 (field of view is approximately 3.25 by 5 mm). The chlorite-rich bands are comprised of olive green chlorite, euhedral pyrite and locally carbonate. The quartz-rich bands are comprised of fine-grained recrystallized quartz, pyrite, sericite and locally fine-grained feldspar. The banding parallels the shear zone fabric.

CHAPTER 4

STRUCTURAL GEOLOGY

4.1 INTRODUCTION

The Midas Pond prospect occurs within a northeast-trending, northwest-dipping shear zone which extends indefinitely in both directions beyond the study area (Figure 3.1; Plate 1.2). The shear zone has a width of approximately 200 m and has gradational contacts with less deformed felsic and mafic volcanic rocks. The shear zone consists of a system of smaller, ductile, anastomosing shears which wrap around more competent, less deformed, lozenge-shaped structures.

Two episodes of deformation, termed D_1 and D_2, are apparent within the study area. The earliest deformation (D_1) produced a regional penetrative foliation (S_1). The foliation within the Midas Pond shear zone is parallel to S_1 and is interpreted to have also formed during D_1 deformation.

The second phase of deformation (D_2) was part of the regionally extensive Dunnage Zone flexuring (Blackwood, 1985 and O'Brien et al., 1986). At Midas Pond this deformation produced small Z-shaped flexures of the shear zone and resulted in the development of a fine crenulation cleavage, kink bands and a fracture cleavage. This brittle phase of deformation enhanced the

development of the mineralized quartz veins along the contact between the Banded Mafic unit and the structurally overlying altered felsic volcanic rocks.

4.2 SHEAR ZONES - A BRIEF REVIEW

A complete review of shear zones and kinematic indicators is beyond the scope of this study. The reader is referred to comprehensive reviews of shear zones and kinematic indicators by Bursnall (1989) and Hanmer and Passchier (1991) and shear zone-hosted mineralization (vein systems) by Roberts (1988) and Hodgson (1989).

4.2.1 SHEAR ZONE DEFINED

A shear zone is defined as a narrow generally planar zone across which there has been significant parallel displacement (Bursnall, 1989). Shear zones can be subdivided, based upon the rheological behaviour of the rocks being deformed, into three types (Figure 4.1) (Ramsay, 1980): 1) brittle shears which exhibit discontinuity of features across the structure; 2) brittle-ductile shears (discussed below), and 3) ductile shears which exhibit continuity of features across the structure.

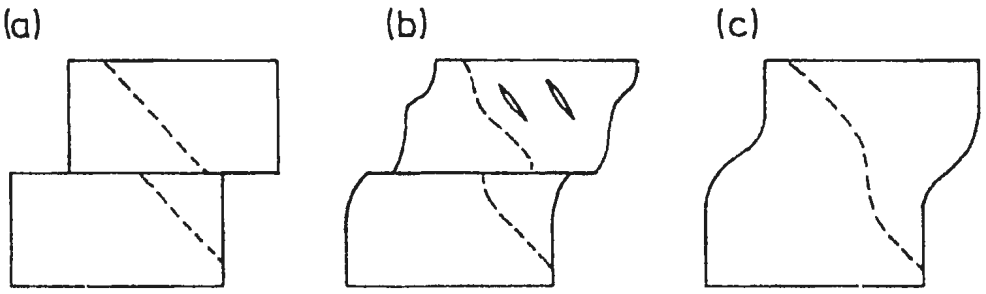

Figure 4.1 Types of shear zones: (a) brittle; (b) brittle-ductile and, (c) ductile (after Bursnall, 1989).

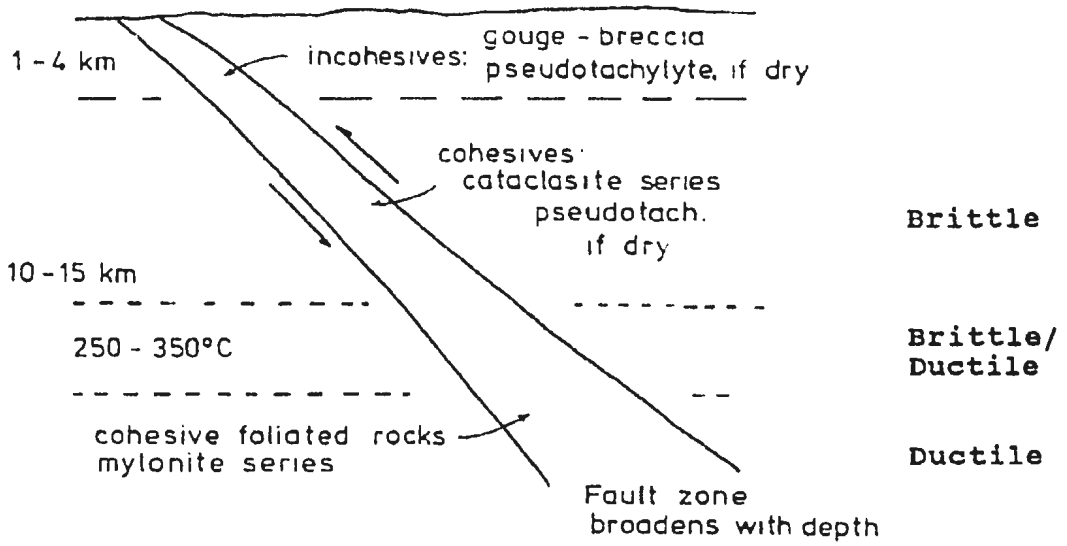

Figure 4.2 Variation in the style of shear zone deformation with depth. Brittle-ductile deformation would occur in the area between the broken lines (after Bursnall, 1989).

Brittle-ductile shear zones exhibit a complex history of both brittle and ductile deformation styles. Typically such zones are comprised of schistose or mylonitic rock across which there has been both continuous and discontinuous offset of external markers (Hodgson, 1989). Brittle-ductile deformation is thought to occur in the transition zone between brittle and ductile behaviour (Sibson, 1977; 1989) at depths of 10-15 km and within a temperature range of 250 to 300°C (Figure 4.2).

Strain history within brittle-ductile shear zones is complex with simple shear (rotational strain), as opposed to pure shear (nonrotational strain), forming the main distortional response to the deformation (Ramsay, 1980). To illustrate the strain history of a deformed rock a distorted sphere, called the strain ellipsoid, (Ramsay, 1967) is used (Figure 4.3). This ellipsoid has a fixed set of axes (X, Y and Z) called the principal axes. The X-axis is parallel to the principal direction of extension and the Z-axis is parallel to the principal direction of shortening within the shear zone. These axes only model finite strain and provide no information on incremental strain within the shear zone.

4.2.2 KINEMATIC INDICATORS

Kinematic indicators such as C-S fabrics, asymmetrical extensional shear bands, and rotated phenocrysts with pressure shadows are important shear zone elements which provide information

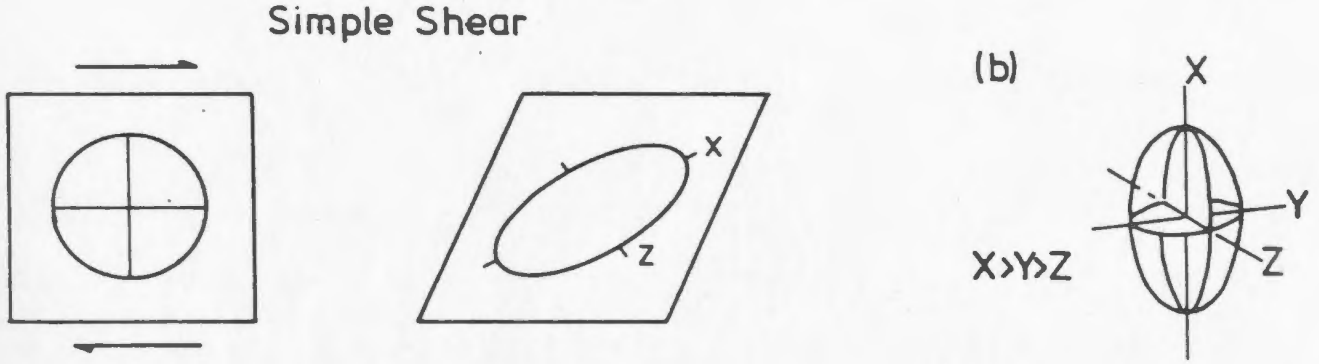

Figure 4.3 Simple (rotational or noncoaxial) shear and the strain ellipsoid with principal axes x,y and z (from Bursnall, 1989).

on the directional sense of shear (cf. Hanmer and Passchier, 1991). C-S fabrics are planar structural elements which develop in ductile shear zones (Figure 4.4). The C fabric or C shear (C from the French word cisaillement meaning shear) are small slip (discontinuity) surfaces (zones of mineral alignment or reduced mineral grain size) which develop parallel to the shear zone boundaries (Berthe et al., 1979).

The S fabric or S plane is the dominant foliation developed within a shear zone (Ramsay and Graham, 1970). It forms, by pressure solution, recrystallization or rotation of mineral grains, parallel to the plane of flattening within the shear zone. At the shear zone margins the S fabric is inclined about 45° to the shear zone boundary. Towards the central portions of the shear zone (higher strain levels) the S fabric rotates towards parallelism with the C fabric. The acute angle formed by the intersection of the C-S fabric points in the direction of movement within the shear zone. In zones of high strain it becomes impossible to distinguish between the C and S planes.

Where C-S planes are well developed the S plane exhibits a typical crenulated cleavage resulting in a sigmoidal S-plane shape (Figure 4.4). An S-shaped asymmetrical crenulation of the S plane indicates a dextral sense of displacement on the shear zone. A Z-shaped asymmetrical crenulation of the S plane indicates a sinistral sense of displacement.

Asymmetrical extensional shear bands (Hanmer and Passchier, 1991) are small scale shear zones which develop at angles less than 45° to the C plane (Figure 4.4). Such bands may be sporadically developed or they may form a penetrative foliation or crenulation cleavage. They may occur singularly or as a conjugate set. Movement on these small-scale shears gives the same sense of shear as in the main zone.

Kink bands are comprised of small asymmetrical folds with sharp angular hinges, the short limb defines the band (Hobbs et al., 1976). These can occur either microscopically within crystals or megascopically within foliated rocks. The folding or rotatation of the short limb is driven by slippage on the rotating segment. The sense of rotation of the short limb is antithetic to the overall sense of shear within the shear zone (Hanmer and Passchier, 1991). Kink bands are unreliable sense of shear indicators because even moderate values of shear strain may reverse the sense of asymmetry of the kink band (Hanmer and Passchier, 1991).

Pressure shadows are typically formed by the precipitation from solution (pressure solution) of minerals such as quartz or calcite at the contact between a stiff inclusion (a quartz phenocryst or a pyrite cube) and the less competent matrix (Figure 4.5) (Hanmer and Passchier, 1991). Progressive deformation produces a rotation of the stiff inclusion. As the inclusion begins to rotate the softer matrix begins to flow away from the

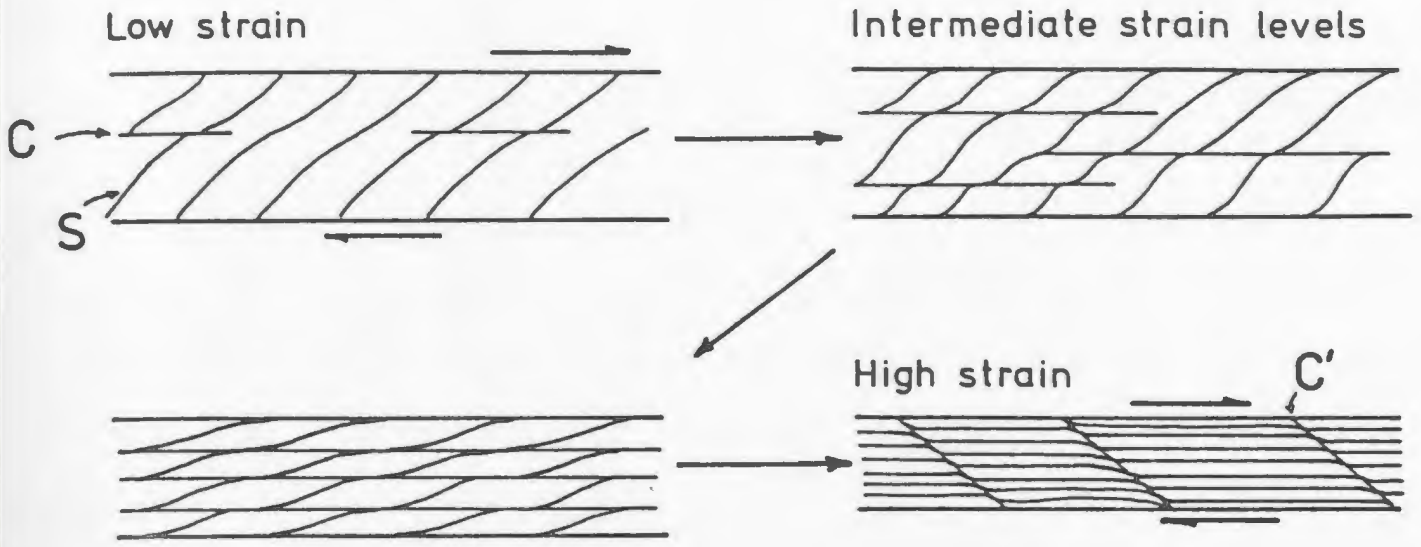

Figure 4.4 Variation in planer fabrics within ductile shear zones with increasing strain levels (from Bursnall, 1989). At intermediate strain levels the S fabric becomes sigmoidal (S-shaped in dextral shears and Z-shaped in sinistral shears). Within high strain zones S rotates into parallelism with C and shear bands C' form.

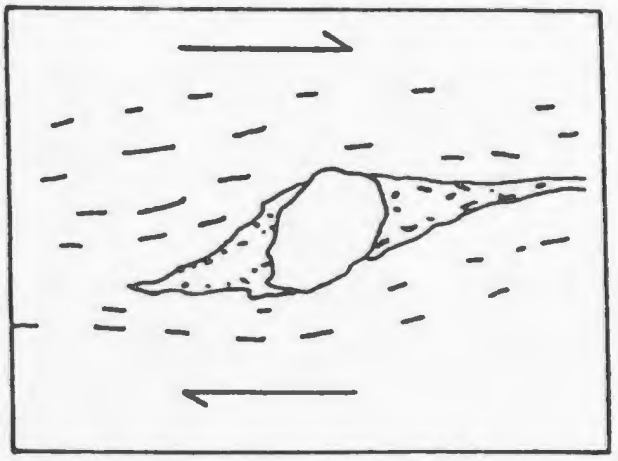

Figure 4.5 The formation of a pressure shadow due to the rotation of a stiff inclusion within a dextral shear zone (modified after Hanmer and Passchier, 1991). The shadow forms in zones of extension where the softer matrix is pulled away from the inclusion.

inclined margins of the inclusion creating a zone of low pressure into which fluid can migrate.

4.2.3 SHEAR ZONE VEIN SYSTEMS

Brittle-ductile shear zones can exhibit a sequential system of fractures and small-scale shears which develop in response to deformation within the zone (Figure 4.6) (Roberts, 1988). These shears and fractures provide the dilatencies into which fluids can migrate and form veins. Extensional fractures (T, tension gashes) (Figure 4.6b) maybe the first structure to form, however, they can also form at any instant of strain within the shear zone (Roberts, 1988). Such dilational features develop perpendicular to the plane of flattening within the shear zone (45° to the shear zone boundary) and often form en echelon structures. With progressive deformation these fractures rotate so that they are no longer oriented at 45°. However, the tips of the fractures continue to propagate at 45° giving a sigmoidal shape to the fracture. This propagation continues until the fracture rotates beyond a certain point and a new fracture forms perpendicular to the plane of flattening. Continued deformation and multiple vein generations can result in "Centipede veins" (Hodgson, 1989).

The first shear fractures to form are low angle (R) and high angle (R') Riedel shears (Figure 4.6b). These fractures develop at approximately 30° to the plane of extension within the shear zone

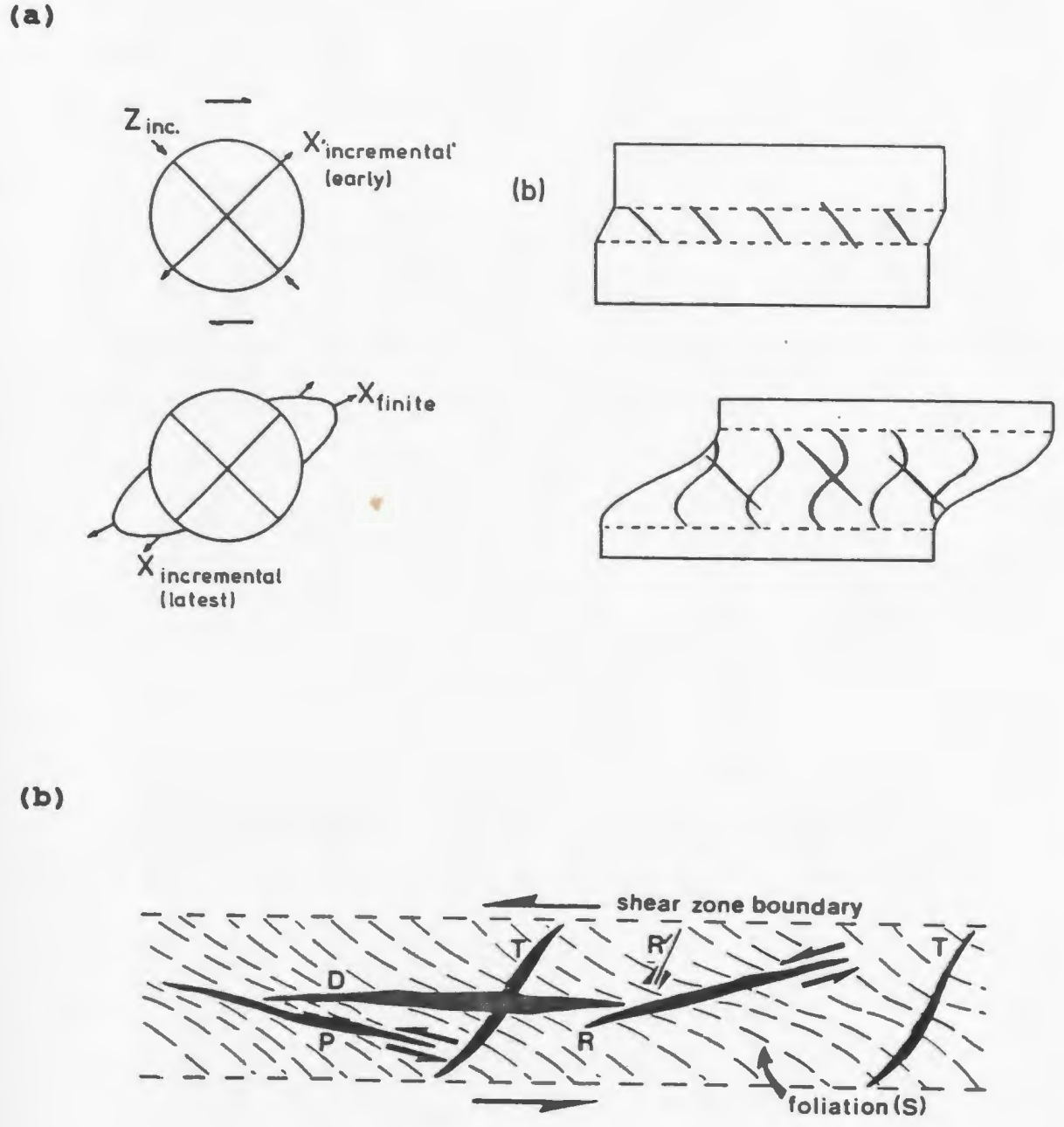

Figure 4.6 (a) The progressive development of en echelon extension fractures within a brittle-ductile shear zone. (b) The orientation of extension fractures (T) and shear fractures (R, R′, P and D) which develop during brittle-ductile deformation. R, low angle Riedel shears; R′ high angle Riedel shear; P, pressure shears, and D, central shears.

and are generally inclined at about 15° and 75° to the shear zone trend. R shears are oriented at a low angle to the shear zone fabric and exhibit the same sense of offset as the main shear zone. R′ shears develop at a high angle to the shear zone fabric and exhibit a sense of offset opposite to that of the main zone.

Pressure shears (P) (Figure 4.6b) develop next and these are oriented approximately 15° to the shear zone (Hodgson, 1989). P shear development is followed by D or C shears. These are central shear veins which are oriented parallel to the shear zone trend. Both P and C shears have the same sense of offset as is exhibited by the main shear zone.

Shear fracture veins typically form the best exploration targets because they are larger and more economically significant than the extension fracture veins (Roberts, 1988). The development of the various types of shears and fractures is synchronous with progressive deformation. This can result in a complex system of vein overprinting.

4.3 REGIONAL DEFORMATION D_1 VICTORIA LAKE GROUP

The D_1 deformation produced a regional S_1 foliation which is defined as an east-northeast striking, moderate to steeply dipping, bedding subparallel cleavage which is axial planar to tight to isoclinal folds within the Victoria lake Group (Kean and

Jayasinghe, 1980; Evans et al., 1990). Regionally the fabric is inhomogeneously developed, however, the intensity of this foliation increases to the southwest. In the Midas Pond area this foliation trends 52°/85° NW (Figure 4.1) and is defined by chlorite, mica, flattened crystal augen and pyroclastic fragments.

Kean and Jayasinghe (1980) interpreted this east-northeast-trending foliation to be in part related to major regional faults. This interpretation is based on the fact that the intensity of the foliation increases towards the fault zones. They also indicate that these structures may be related to eastward directed thrusting that occurred during the Silurian. In the Dunnage Zone this regional deformation was traditionally viewed as being related to the Acadian Orogeny, however, a distinct Silurian orogeny termed the Salinic has now been proposed (Dunning et al., 1990).

Within the southern Tulks Hill volcanics, particularly in the Midas Pond area, this regional deformation has produced a number of northeast-trending linears and cross structures which, upon examination, are large ductile shear zones (Figure 2.3). Many of these are interpreted to be secondary and tertiary structures related to larger and deeper ductile shear zones such as the Tulks Valley fault. The Midas Pond shear zone is probably a secondary structure off the Tulks Valley fault which is located approximately 1.5 km to the north (see Figure 2.3; Plate 1.1). These shear zones may have been reactivated a number of times during regional

deformation processes.

$^{40}Ar/^{39}Ar$ age dating of sericite (Kean and Evans, 1988a) from the Tulks Hill and Jacks Pond massive sulphide deposits and from epithermal style alteration at Bobbys Pond produced ages of 391 +/- 4 Ma, 395 +/-8 Ma and 392 +/-4 Ma respectively. These dates are interpreted to reflect the age of the last metamorphic event and possibly date the last significant deformation of the Victoria Lake Group.

Carboniferous rocks (Horton age, Newhouse, 1931; Belt, 1969) exposed on the shores of Red Indian Lake show no evidence of deformation and lack the east-northeast-trending fabric. These rocks provide an upper age limit for the regional deformation (Kean and Jayasinghe, 1980).

4.3.1 THE MIDAS POND SHEAR ZONE

The shear zone at Midas Pond is developed parallel to the regional, northeast-trending, penetrative fabric S_1. Trends within the shear zone vary between 64°/74°NW and 48°/80°NW. Slight variations in these trends are due to a combination of the wrapping of the shear zone fabric around large competent lozenges of rock preserved within the shear zone and regional-scale flexuring (Blackwood, 1982; O'Brien et al., 1986; and Evans et al., 1990).

The shear zone grades outwards into variably deformed felsic and mafic volcanic rocks making it difficult to pinpoint the shear zone boundaries. The shear zone itself is a braided network of anastomosing ductile shears of various sizes from millimetre scale upwards.

Locally, the shear zone fabric has a shallow dip as is exposed in the trench on L 47+00. At this location the cleavage in the felsic rocks dip southwards at 42° degrees. Such variations from the steep northwest dip of the shear zone is attributed to a later cross fault. The trace of this assumed fault is marked by a topographic linear developed just to the north of Midas Pond. A similar fault is developed to the south of the shear zone. The fault strikes approximately north-northeast and merges with the main shear zone south of Midas Pond and is defined by highly cleaved mafic tuffaceous rocks and a narrow linear valley.

4.3.1.1 BRITTLE-DUCTILE DEFORMATION

Deformation within the Midas Pond shear zone is inhomogeneous. Locally, primary features such as undeformed quartz and feldspar phenocrysts are preserved within low strain zones and the less deformed, more competent lozenges (discussed below). Within high strain zones quartz phenocrysts and aggregates exhibit undulatory extinction and are locally fractured indicating brittle deformation.

More competent rocks within the shear zone are preserved as lozenges around which the anastomosing high strain zones wrap (Plate 4.1). These rocks are generally more siliceous and contain a widely spaced, anastomosing cleavage defined by wisps of mica and pyrophyllite. In thin section these rocks consist largely of recrystallized quartz grains that decrease in size towards the high strain zones. This 'lozenging process' is developed on a wide range of scales from millimetres to huge silicified and albitized blocks 20 to 40 m thick. Hodgson (1989) described similar features, common to most shear zone-hosted gold occurrences, as "...anastomosing domains of higher deformation separating rhomboid domains of lower deformation...".

High strain zones (ductile deformation), usually areas of intense alteration, are preserved as pyrophyllitic and micaceous schists (Plate 4.1). These phyllosilicate minerals form curvilinear zones that localized and enhanced deformation. Since deformation and alteration appear to have been contemporaneous, the preferred orientation for the development of these minerals should be parallel to the shear zone fabric.

4.3.1.2 SENSE OF SHEAR

Kinematic indicators within and adjacent to the Midas Pond shear zone are poorly preserved and contradictory. Definitive C-S fabrics were not observed. Structures that could be shear bands

(Plate 4.2) as exposed in trench 48+73 and rotation of broken phenocrysts suggest a possible dextral sense of movement on the shear zone but this is inconclusive. This is indicative of: 1) the high shear strain developed within the altered rocks; and 2) the fine-grained nature of the majority of lithologies within the shear zone. The sense of shear during regional deformation is, however, inconsequential to the main episode of auriferous quartz veining as this veining is related to D_2 deformation.

4.4 D_2 DEFORMATION

Large flexures, such as the Hermitage and Baie Verte flexures and similar flexures eleswhere in the Central Mobile Belt, have been interpreted to result from sinistral movement along the major fault zones (Cape Ray-Long Range-Cabot faults and the Hermitage Bay-Dover faults) bordering the Central Mobile Belt (Blackwood, 1985; O'Brien et al., 1986)(Figure 4.7). This sinistral movement would result in a anticlockwise rotation of the structural elements within the Central Mobile Belt resulting in the flexured pattern. Such flexuring is observed on a variety of scales throughout the Victoria Lake Group as is illustrated by the orientation of both the geological units and the larger lakes, rivers and brooks (see Figure 2.1).

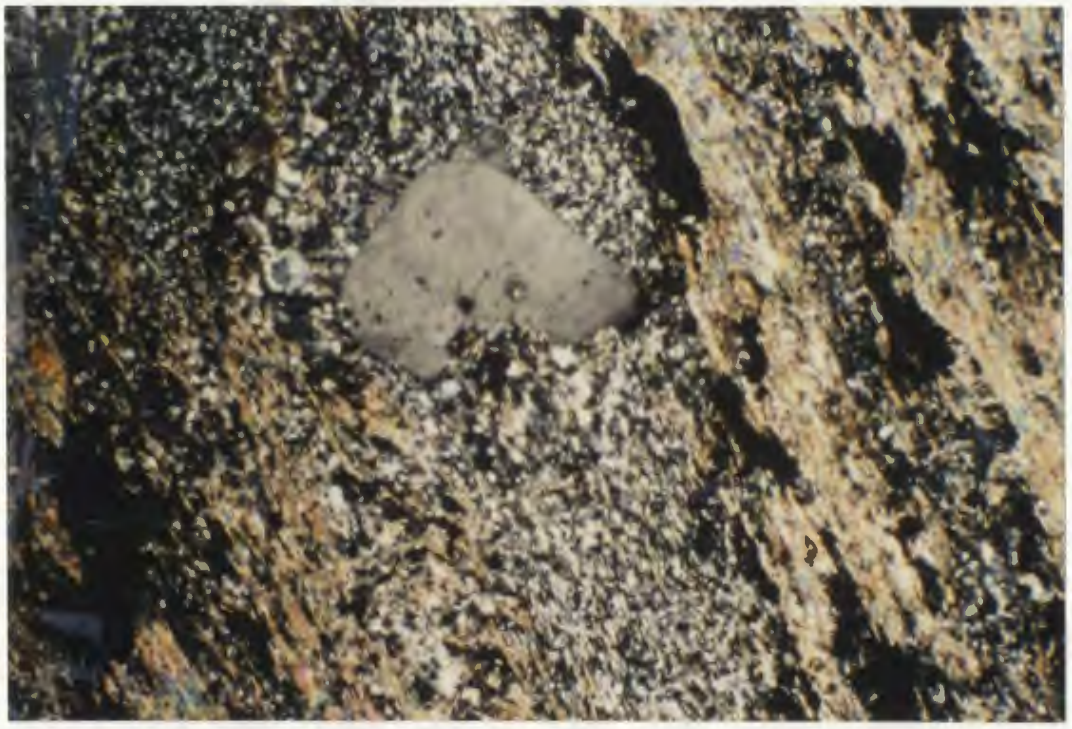

Plate 4.1 Photomicrograph exhibiting pyrophyllite-rich bands and lozenge-shaped quartz-rich band or lens. Preserved within the quartz-rich band is an embayed quartz phenocryst. Field of view is approximately 3.25 by 5 mm.

Plate 4.2 Shear bands (?) developed within sheared felsic volcanic rocks at Midas Pond. Stretching lineations associatiated with these features were not observed. Sense of shear is dextral.

4.4.1 MIDAS POND FLEXURING

At Midas Pond deformation related to this flexuring is referred to as D_2. Structures related to this deformation are: 1) broad, asymmetrical Z-shaped flexures of the shear zone (see Figure 3.1 and map at back), defined by variations in the shear zone foliation; 2) a fine crenulation cleavage; 3) conjugate kink bands, and 4) a prominent fracture cleavage. The largest of the Z-shaped flexures extends from approximately line 44+00 to line 48+00. Along this flexure variations in the shear zone foliation are as follows: line 44+00, outcrop DE-86-53 43°/64°NW; line 45+15, 70°/52°N; and, line 48+00, 45°/60°NW. A smaller flexure is located between lines 42+00 and 43+00.

A fine crenulation cleavage dipping 40° towards 273° is preserved within the schistose felsic rocks exposed in trench 45+15. This trench is located immediately north of Midas Pond near the shear zone margin. In thin section this cleavage defines the intersection of the S_1 foliation with a sigmoidal-shaped fabric which is defined by wispy pyrophyllite and mica (Plate 4.3). This cleavage appears to be restricted to the flexured portions of the shear zone and adjacent country rocks and is therefore considered to be a D_2 fabric.

Both S- and Z-shaped kink bands (locally conjugate sets) are preserved within the Midas Pond shear zone (Plate 4.4). These

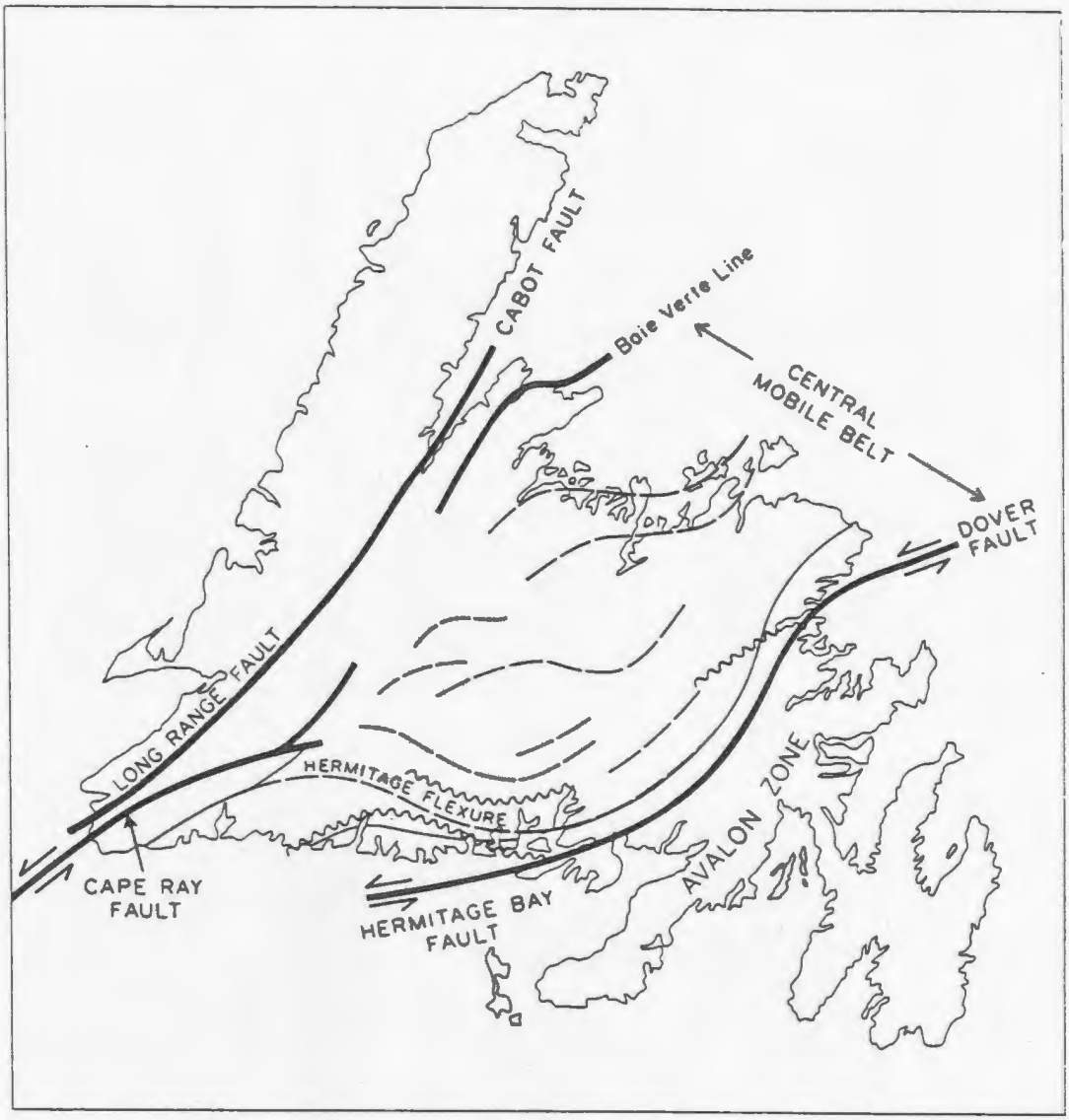

Figure 4.7 Flexuring of the Central Mobile Belt due to sinistral movement along the major bounding wrench faults (Dover-Hermitage Bay Fault and the Cape Ray Fault). This sinistral movement produced clockwise rotation of the Central Mobile Belt resulting in the Hermitage and Baie Verte Flexures (after Blackwood,1985).

structures fold or kink the shear zone fabric with little apparent brittle offset. The kink bands are locally tightly folded which may indicate that they were affected by later ductile deformation. Both sinistral and dextral offsets are exhibited by these kink bands. The kink bands have the same orientation as a prominent, conjugate fracture cleavage which is developed throughout the shear zone (Plate 4.5). The average orientation of this fracture cleavage is: S_2, 144°/79°SE, and S_2', 64°/79°SE.

4.5 MINERALIZED D_1 and D_2 STRUCTURES

Within the shear zone at Midas Pond auriferous quartz veining is developed over a strike length of 800 m. Over much of this distance the veining is relatively narrow, however, there are locally thicker concentrations of veins (7 m wide in trench 45+00) which carry significant but sporadic gold values. These thicker zones of quartz veining coincide with the flexures.

Minor dilational structures containing quartz veins occur along the entire length of the shear zone but the auriferous quartz veins are only developed near the contact between the Banded Mafic unit and the structurally overlying altered felsic volcanic rocks. Along this contact there appears to have been sufficient competency contrast to allow dilatencies to develop. Such rheological properties together with the flexuring and increased fluid pressure related to the migration of the hydrothermal fluids would promote

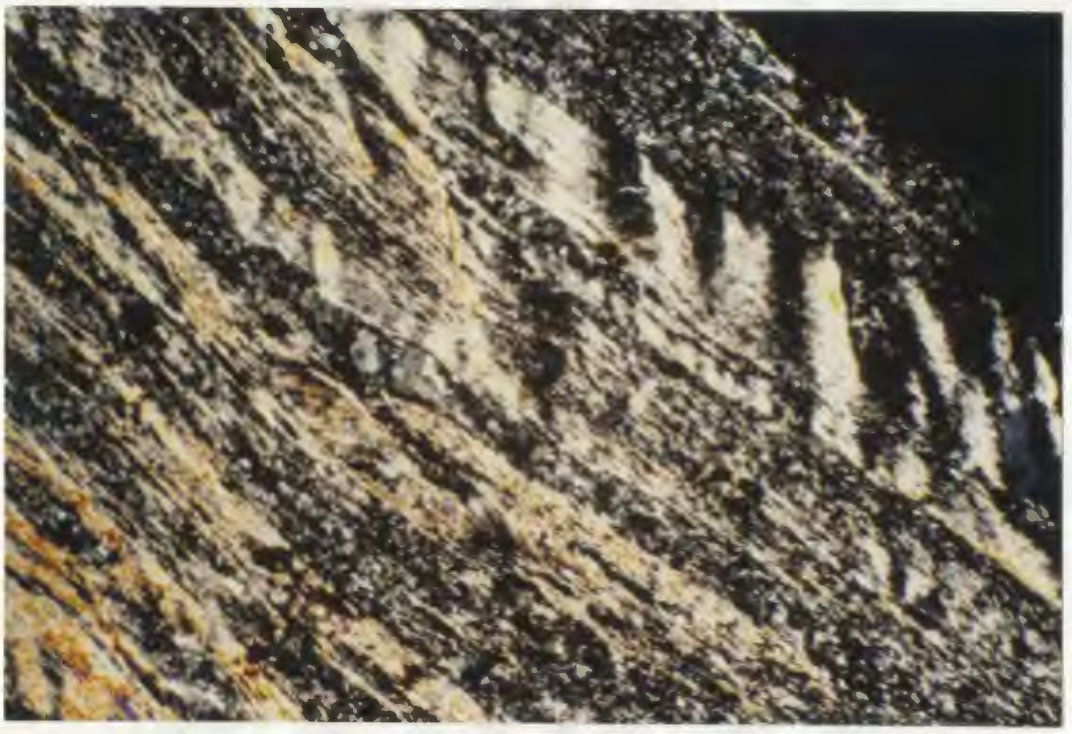

Plate 4.3 Photomicrograph illustrating crenulation cleavage developed in pyrophyllite-mica schist. The crenulation, defined by wavy extinction, folds the shear zone fabric (field of view approximately 3.25 by 5 mm).

Plate 4.4 Kink bands, developed in felsic tuffaceous rocks, fold the shear zone fabric.

the formation of dilatencies and quartz veining.

Three sets of auriferous quartz veins related to brittle-ductile deformation are recognized within the shear zone. The earliest veins (V_1) are considered to be related to D_1 structures. Veins 2 and 3 (V_{2-3}) occupy later crosscutting D_2 structures. Vein 1 is the oldest set of veins. These are central shear veins (after Hodgson, 1989) which parallel the shear zone fabric (Plate 4.6). The relationship between V_1 and S_1 can be seen on an equal area stereographic projection (Figure 4.8). The average trend of these veins is 55°/81°NW, the average trend for the shear zone fabric is 52°/85°NW. These veins are boudinaged and have anomalous gold concentrations. They are much more deformed than Veins 2 and 3, the other auriferous quartz veins, so they are considered to be older, however, cross-cutting relationships were not observed. Their formation is related to dilation of C shears (Hodgson, 1989) which parallel the shear zone boundaries. The formation of these veins indicate that there were auriferous fluids migrating through the shear zone prior to regional flexuring.

The latest veins are a set of extensional fracture veins (Plate 4.7), which have average orientations of 54°/76°S (Vein 2) and 124°/71°S (Vein 3) respectively. Vein set 2 is developed approximately parallel to the weakly developed fracture cleavage S_2' which has an average orientation of 64°/79°SW. Vein set 3 is developed approximately parallel to the prominent fracture cleavage

Plate 4.5 Widely spaced fracture cleavage developed in felsic tuffaceous rocks.

S_2 which trends 144°/73°SW. The relationship between these vein sets and the fracture cleavages is shown on the equal area stereographic projection (Figure 4.8). These veins contain locally developed comb structures and vuggy quartz-lined cavities which suggests that the veins were dilational in origin and formed late in the shear zone development in a relatively strain-free environment.

Figure 4.9 is a schematic diagram which illustrates the orientation of the of the S_1 foliation and S_2 fractures and their relationships to the auriferous quartz veins V_1, V_2 and V_3. The location of the veining is primarily controlled by the intersection of these D_1 and D_2 structures with the Banded Mafic unit.

Slightly thickened sections of veining (V_2 and V_3) appear to coincide with the flexures. Therefore, the hinges of these flexures may form the best target for gold exploration.

4.3 SUMMARY

The Midas Pond gold prospect is developed within a 200 m wide anastomosing brittle-ductile shear zone which is related to regional D_1 deformation. Kinematic indicators are poorly preserved within the shear zone and are contradictory. The shear zone is developed parallel to, and considered to be a secondary structure of, the larger, ductile, Tulks Valley fault.

Plate 4.6 Boudinaged, V_1 quartz veining developed parallel to the shear zone fabric. These veins have anomalous gold concentrations.

Plate 4.7 Vein network formed by V_2 and V_3 quartz veins, Trench 46+00. From left to right the author, Baxter Kean, Dave Barbour and Geoff Thurlow.

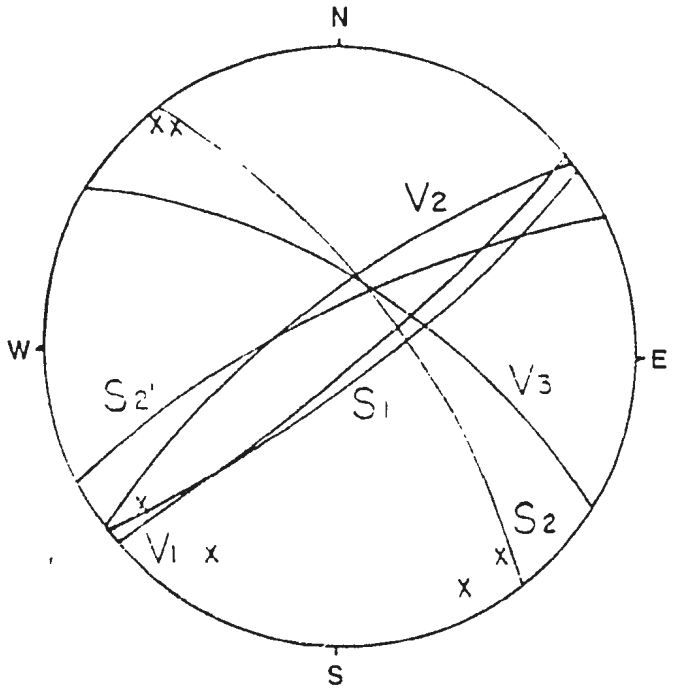

Figure 4.8 Equal area stereographic great circle projections of the average orientation of: a) the shear zone fabric, S_1 (87 measurements); b) the fracture cleavage, S_2 and S_2' (18 measurements); c) shear central veins, V_1 (4 measurements), and d) extensional fracture veins, V_2 and V_3 (12 measurements).

Brittle-ductile deformation related to both regional deformation (D_1) and flexuring (D_2), was focused along the contact between the Banded Mafic unit and the structurally overlying altered felsic volcanic rocks. The deformation resulted in the formation of three auriferous quartz vein sets: Vein 1) shear central veins, hosted by D_1 structures, and Veins 2 and 3) extensional fracture veins, hosted by D_2 structures. Veins 2 and 3, the most economically significant veins, are related to flexuring of the shear zone and the Banded Mafic unit. The thickest sections of quartz veining appear to coincide with the hinges of these flexures. If this is the case then the hinges of these flexures may prove to form auriferous shootes. Temporal relationships between D_1 and D_2 have not been resolved, therefore the time span between V_1 and V_{2-3} is not known.

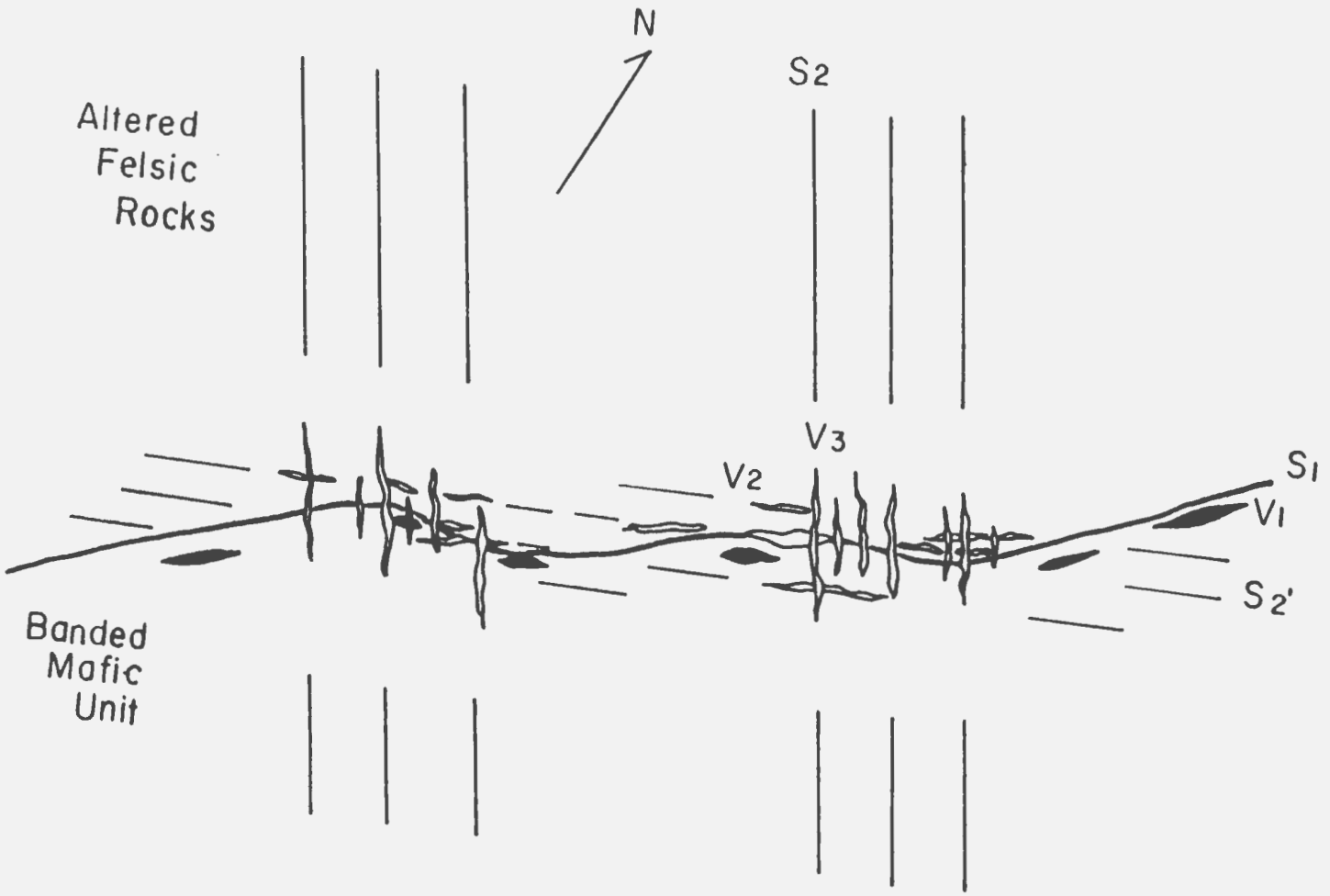

Figure 4.9 Schematic diagram which illustrates the relationships between: S_1 and V_1, and S_2-S_2' and V_2-V_3.

CHAPTER 5

ALTERATION AND MINERALIZATION

5.1 INTRODUCTION

Aluminous alteration and silicification is widely developed within the Midas Pond shear zone. This alteration appears to be most intense in the immediate structural hangingwall to the auriferous quartz veins. The alteration was a progressive, syn-to late syn- D_1 deformation phenomenon with its distribution controlled by the shear zone. Progressive ductile deformation aligned many of the alteration minerals parallel to the S_1 foliation.

5.2 ALTERATION ZONATION

Alteration in the structural hangingwall, above the auriferous quartz veins, exhibits a zonation from weakly altered mafic tuffs at the northern shear zone margin to highly altered felsic tuffaceous rocks proximal to the veins. Three styles of alteration are present within this zone, these are: 1) advanced argillic, which overprints and largely obliterates earlier argillic alteration; 2) pyritization; and 3) carbonatization (Figure 5.1). Advanced argillic alteration was accompanied by remobilization of silica and albitization. Similar alteration, though lacking the intense Fe-carbonate and pyrite, occurs throughout the shear zone.

Alteration assemblages associated with the three alteration styles are shown in Table 5.1.

5.2.1 ADVANCED ARGILLIC ALTERATION

Advanced argillic alteration, which consists of pyrophyllitization, based on microprobe and petrographic analyses, and "paragonitization", is the most prevalent and widely developed style at Midas Pond. It is intensely developed in the structural hangingwall to the mineralization, but also occurs throughout the shear zone particularly beneath Muskegone Pond. Alteration associated with the auriferous quartz veins underlies Midas Pond and has an estimated strike length of approximately 800 m and a width of approximately 70 m. Since this style of alteration produces a soft easily eroded rock type, exposures are limited and as a result the alteration can only be studied in drill core.

The altered rocks are buff to grey, fine-grained and are generally strongly foliated (see Plate 5.1). Abundant quartz and feldspar phenocrysts occur throughout the zone. The quartz phenocrysts are generally clear to milky white and range from 1 to 3 mm in diameter. Protoliths to these altered rocks are interpreted to have been felsic, crystal-lithic and lapilli tuffs based on their mineralogy and chemistry (see Chapters 3 and 6 for discussion).

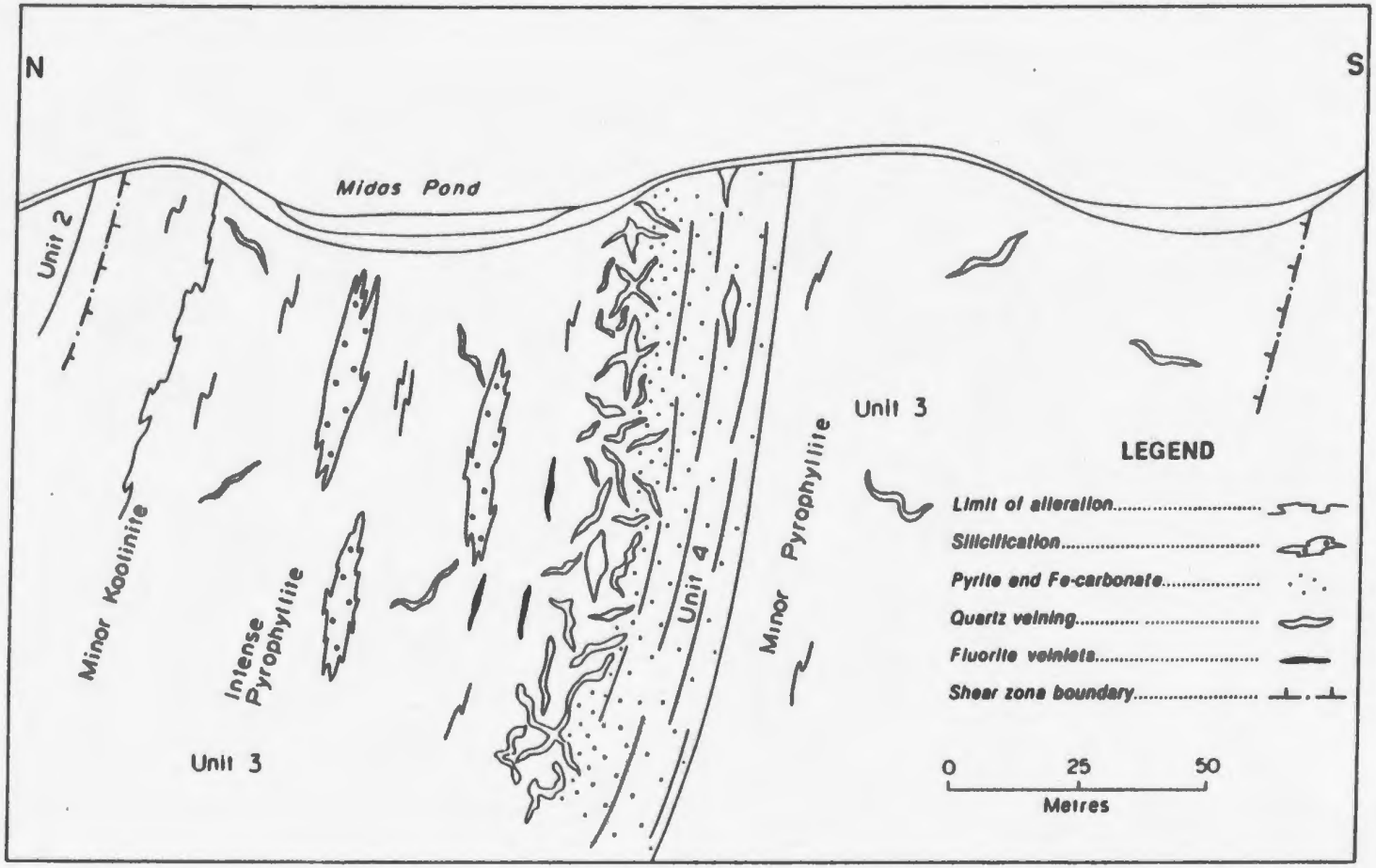

Figure 5.1 Schematic cross-section showing the distribution of the main alteration assemblages at Midas Pond.

ALTERATION MINERALS	DEFORMATION	
	EARLY-SYN	LATE-SYN
ADVANCED ARGILLIC ALTERATION		
Quartz	----------	----------
Albite	----------	----------
Chlorite	? ----------	----------
Pyrophyllite	----------	----------
Paragonite/Sericite	----------	----------
Fluorite	? ----------	
Sphene\Leucoxene	? ----------	
ARGILLIC ALTERATION		
Kaolinite	--------	
SULPHIDATION		
Pyrite	? ----------	----------
CARBONITIZATION		
Fe-Carbonate		----------
GOLD		
V_1 Veins		---------?
V_2 Veins		?----------

Table 5.1 Paragenetic sequence of alteration assemblages in relation to deformation, Midas Pond.

The alteration in these rocks appears to increase in intensity towards the mineralized zone. The pyrophyllite, which is waxy and green to orange brown, occurs as thin seams in the outer portion of the alteration zone and as the intensity of the alteration increases, these seams become wider and more common. In zones of intense alteration, pyrophyllite comprises up to 95 percent of the rock.

Abundant, non-auriferous quartz-dolomite veins with local concentrations of pyrite, chlorite and paragonite are common throughout the alteration zone. Approximately 1 to 2 percent pyrite, with local concentrations of coarse-grained pyrite up to 5 percent, is developed throughout the alteration zone. Thin 1 to 2 mm wide purple fluorite veinlets are developed parallel to the shear zone fabric (Plate 5.1). These veinlets occur throughout the hangingwall alteration zone but appear to be more common proximal to the auriferous quartz veins.

In thin section these rocks are either strongly foliated or banded. The foliation is defined by pyrophyllite and sericite/paragonite (Plate 4.1). The banding, which is also developed parallel to the foliation is comprised of alternating quartz-rich bands and pyrophyllite and sericite/paragonite-rich bands

The pyrophyllite is generally fine-grained and highly

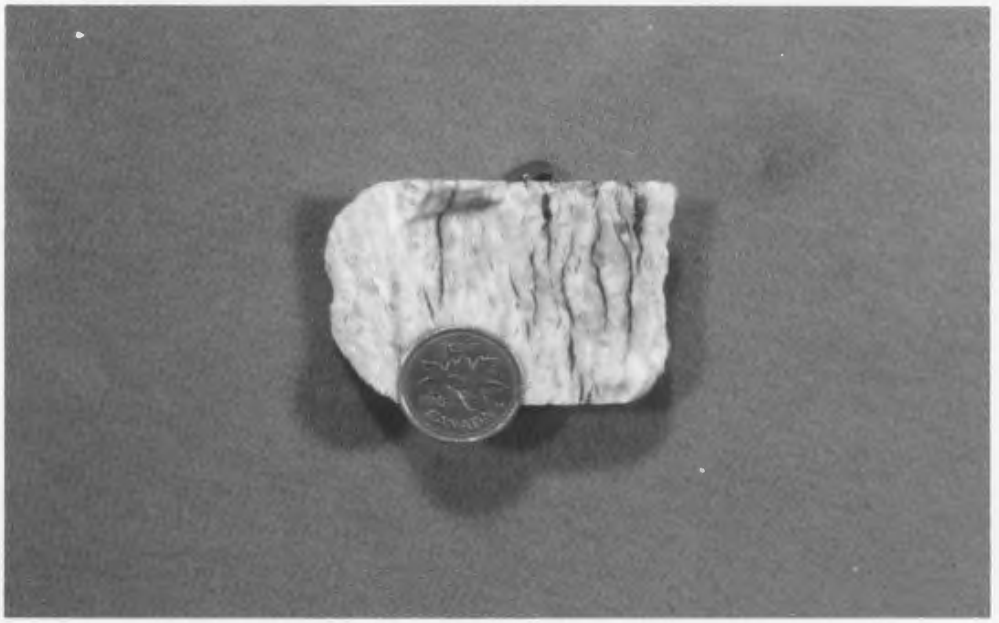

Plate 5.1 Fine, wispy, foliation parallel, purple fluorite veinlets developed within pyrophyllite schist. Small 1-2 mm quartz phenocrysts are preserved.

birefringent. Locally, in less deformed portions of the alteration zone, the pyrophyllite forms coarse crystals. Randomly oriented pyrophyllite also occurs within the quartz-rich bands. The pyrophyllite and the sericite/paragonite form anastomosing stringers which enclose small quartz-rich lozenges of varying dimensions (Plate 4.1).

Sericite and paragonite cannot be readily distinguished in thin section. They are generally fine-grained and are almost indistinguishable from, and occur in, the same manner as pyrophyllite. The rocks containing these minerals are typically enriched in Na relative to K and electron microprobe analyses indicate that much of the mica is indeed paragonite (Table 5.2). K-rich zones do, however, occur sporadically throughout the shear zone and it is therefore impossible to visually distinguish between the micas.

The quartz-rich bands are comprised of recrystallized quartz minor feldspar, chlorite, sericite/paragonite, pyrophyllite and carbonate. Stringers of pyrophyllite and mica commonly crosscut the quartz-rich bands. Patches of recrystallized quartz are common. Quartz and pale green chlorite are developed in pressure shadows surrounding deformed pyrite grains.

Fluorite forms narrow, discontinuous, irregularly shaped, locally coalescing veinlets which parallel the foliation. The

fluorite is typically colourless to pale purple.

The paragenetic sequence of mineral assemblages related to advanced argillic alteration is shown in Table 5.1. Quartz, albite and paragonite/sericite developed at all stages of alteration-deformation from early-syn to late syn. Chlorite and pyrophyllite appear to have developed later and extended into the late-syn deformation and alteration. Fluorite and leucoxene have a more limited range and appear to be restricted to the mid-syn deformation and alteration.

5.2.1.1 OVERPRINTING OF EARLIER ALTERATION

Possible remnants of argillic alteration (kaolinite) are preserved within this portion of the alteration zone. Small rectangular porphyroblasts (?), 2 to 3 mm long, composed of a waxy brown material with white powdery rims are preserved within in this portion of the alteration zone (Plate 5.2). In thin section this waxy brown substance forms an extremely fine-grained grey, amorphous mass, with no birefringence. A crude banding is defined by the alignment of these masses (Plate 5.3). Locally, small patches of recrystallized quartz and rare twinned feldspar are preserved in the interiors of these patches. Electron microprobe analyses (Table 5.2) indicate that the amorphous material is probably kaolinite. Surrounding the kaolinite are narrow rims of fine-grained pyrophyllite marked by higher birefringence (see Table

5.2). Outside of this rim larger crystals of pyrophyllite and paragonite are ubiquitously developed. These masses either represent porpyroblasts of kaolinite which developed parallel to the shear zone foliation or kaolinitized feldspar phenocrysts. The kaolinite is interpreted to have developed during early-syn alteration and deformation (Table 5.2)

5.2.1.2 SILICA REMOBILIZATION/ALBITIZATION

This alteration style is associated with the advanced argillic alteration stage so the discussion of silica remobilization and albitization is included in the discussion of advanced argillic alteration. The silica remobilization/albitization is best preserved within large lozenge-shaped bodies of unknown lateral extent with thicknesses generally up to 20 m, but locally up to 40 m (Figure 5.1). The rocks are fine-grained, textureless and have a mottled grey colour (Plate 5.4). Zones with mottled breccia-like textures are locally developed and are probably related to brittle fracturing. A moderately developed anastomosing cleavage, defined by fine-grained mica and/or pyrophyllite, affects all of these rocks.

In thin section it can be seen that these rocks consist of a fine matrix of recrystallized quartz and plagioclase microlites with minor fine-grained mica, disseminated subhedral and ragged pyrite (Plate 5.5) and altered patches of sphene (leucoxene).

Plate 5.2 Rectangular brown patches of kaolinite with white powdery rims of pyrophyllite developed in pyrophyllite-paragonite schist (felsic volcanic rocks) from the structural hangingwall. Section is from diamond drill hole GP-21.

Plate 5.3 Photomicrograph showing the patches of fine-grained kaolinite encased by fine-grained, birefringent pyrophyllite and quartz. The pyrophyllite gives way to coarser-grained pyrophyllite and paragonite. Small patches of quartz are preserved within the cores of the kaolinite. The kaolinite patches define a weak banding (field of view approximately 3.25 by 5 mm).

	86-223-1	86-223-2	86-215	86-223-3	86-119A	86-200	86-218A	86-220	86-223
	(2)	(2)	(2)	(2)	(1)	(1)	(1)	(1)	(1)
Na_2O	0.11	0.3	0.02	0.06	6.29	3.03	6	6.75	4.84
MgO	0.04	0.07	0.05	0.01	0.13	0.48	0.18	0.14	0.07
Al_2O_3	38.24	27.91	59.76	29.27	37.18	36.49	34.41	38.32	36.01
SiO_2	48.55	64.25	37.57	56.43	48.66	51.37	43.41	50.58	49.76
K_2O	0.07	0.14	0.01	0.01	0.99	5.72	2.17	0.48	2.18
CaO	0.09	0.06	0	0.02	0.04	0.04	0.04	0.06	0.13
TiO_2	0.02	0.1	0.02	0.02	0.09	0.09	12.41	0.03	0.05
Cr_2O_3	0	0	0	0.03	0.02	0.01	0.01	0.02	0.04
MnO	0	0	0	0	0.03	0.01	0	0	0
FeO*	0.27	0.08	0.04	0.11	0.79	0.31	0.19	0.07	0.22
NiO	0.01	0.02	0.02	0	0	0	0	0	0.04
Total	87.39	92.94	97.48	85.96	94.21	97.53	98.8	96.46	93.34
Na	0.022	0.059	0.002	0.009	1.568	0.738	2.137	1.634	0.986
Mg	0.003	0.009	0.005	0	0.022	0.088	0.043	0.02	0.009
Al	4.896	3.306	6.989	3.765	5.643	5.407	7.458	5.64	4.472
Si	5.272	6.458	3.728	6.161	6.266	6.458	7.981	6.318	5.245
K	0.006	0.018	0	0	0.162	0.915	0.507	0.073	0.291
Ca	0.009	0.006	0	0	0.003	0.003	0.005	0.007	0.012
Ti	0	0.006	0	0	0.007	0.007	1.716	0	0.003
Cr	0	0	0	0	0	0	0	0	0.003
Mn	0	0	0	0	0	0	0	0	0
Fe	0.022	0.006	0.002	0.009	0.083	0.029	0.027	0.007	0.019
Ni	0.003	0.003	0.002	0	0	0	0	0	0.009
Total	10.233	9.869	10.729	9.944	13.755	13.646	19.873	13.706	11.049

Table 5.2 Electron microprobe analyses of kaolinite (86-223-1), pyrophyllite rim (86-223-2), pyrophyllite bladed crystal (86-215 and 86-223-3) and mica (sericite and paragonite) (86-119A, 86-200, 86-218A, 86-220 and 86-223) from the alteration zone at Midas Pond. Each analysis is an average value, the number of analyses per grain is given immediately below the sample number.

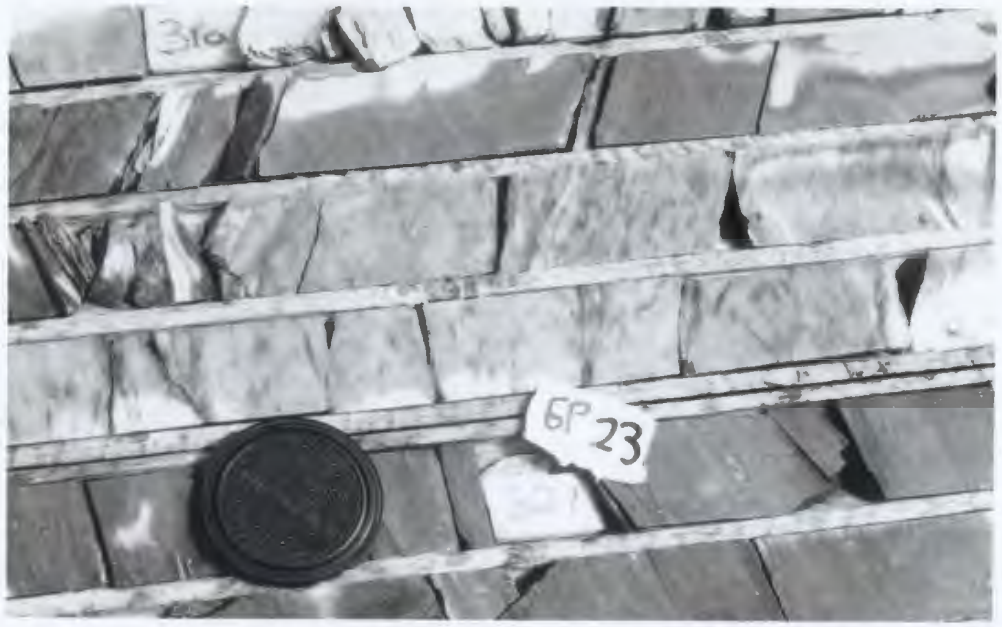

Plate 5.4 Mottled, fine-grained, grey silicification developed within the structural hangingwall. Section is from diamond drill hole GP-23.

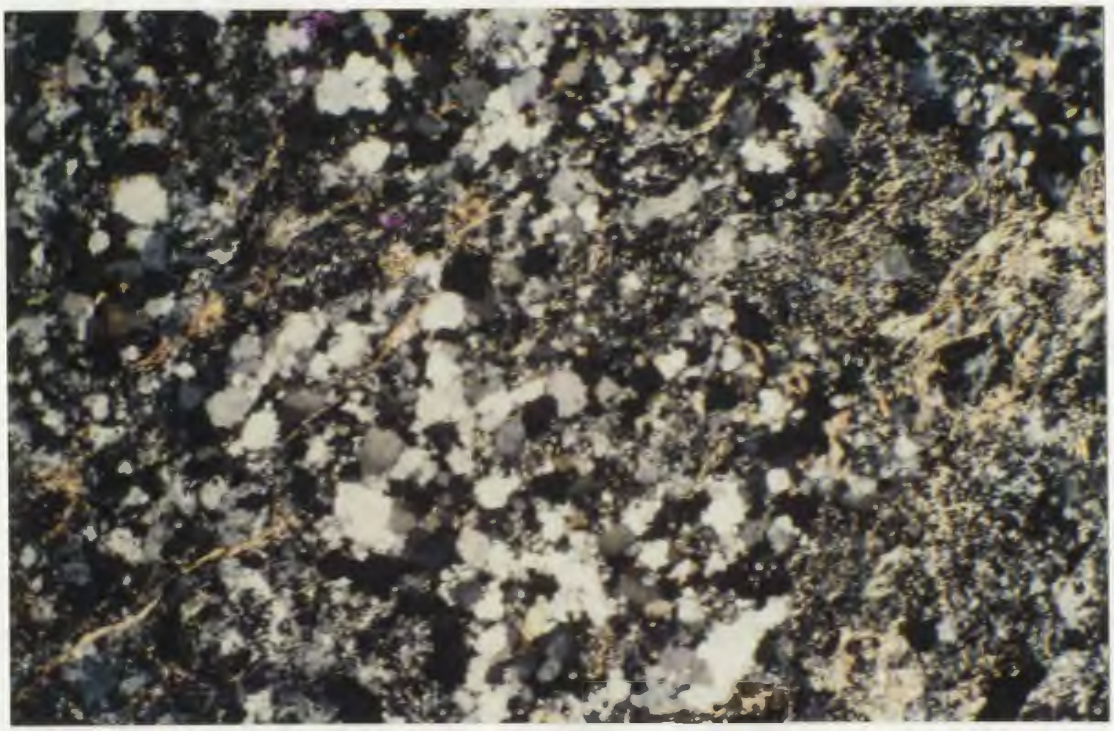

Plate 5.5 Photomicrograph of intense silicification. Coarse patches of recrystallized quartz are developed within a fine-grained quartzo-feldspathic matrix. Ragged pyrite is evenly distributed throughout the section. Fine anastomosing stringers of mica are developed in the finer-grained portions of the section. Field of view is approximately 3.25 by 5 mm.

Phenocrysts up to 1 to 2 mm are preserved and consist of quartz and plagioclase (andesine). The feldspar phenocrysts exhibit local intense alteration to carbonate and minor pale grey-green chlorite. As the alteration is increasingly more intense the rock becomes dominated by fine-grained quartz and feldspar. Coarser patches of quartz up to 2 mm in diameter, and randomly oriented feldspar phenocrysts increase in abundance. Patches of carbonate and perfectly preserved carbonate rhombs are widely developed particularly in the more altered sections; this is discussed further in Section 5.2.2. Slightly flattened subhedral pyrite grains up to 2 x 1 mm, with quartz and carbonate-filled pressure shadows, are also common in these areas. The pyrite is present in concentrations up to 3 percent.

Anastomosing stringers and veinlets of mica and pyrophyllite are profuse, particularly towards the margins of the siliceous zones. Here bands of fine-grained quartz and feldspar intercalated with bands of sericite or paragonite and pyrophyllite give way to ubiquitous pyrophyllite and paragonite.

5.2.1.3 SILICA REMOBILIZATION AND THE BANDED MAFIC UNIT

Silica remobilization and minor albitization are also developed in the immediate host rocks (the upper portions of the Banded Mafic unit) which form the structural footwall to the quartz veining. The Banded Mafic unit becomes more siliceous proximal to

the quartz veins and cannot be distinguished from structurally overlying silicified felsic rocks.

In thin section increasing alteration within the Banded Mafic unit is marked by an enhancement of the banding. Chlorite dominated bands, up to 5 mm wide, are composed of parallel aligned, wispy chlorite, small patches of recrystallized quartz (less than 1 mm in diameter) and patches of carbonate overgrowths. The chlorite is typically Fe-rich and is similar to chlorite from mafic tuffaceous rocks throughout the Tulks Hill volcanics (see Figure 7.1). Chlorite from both the Banded Mafic unit and the mineralized quartz veins plot largely within the Ripidolite field of Hey (1954) (see Figure 3.2).

Two styles of quartz-dominated bands are developed within the Banded Mafic unit. The first style consists of recrystallized quartz, minor chlorite and trails of fine-grained pyrite. This style forms narrow bands which exhibit a reduction in grain size as the band margins are approached. The second style is comprised of quartz-rich bands with abundant feldspar. Feldspar in the groundmass is largely unaltered, however, larger crystals are variably saussuritized. The groundmass is cut by wispy bands of chlorite and sericite. In both styles pyrite appears to overgrow the groundmass. These alternating bands are believed to represent a highly flattened breccia comprised of felsic fragments represented by the quartz-feldspar bands and the breccia matrix

represented by the recrystallized quartz-chlorite bands.

Pyrite-rich bands or veins with coarser-grained chlorite and sericite mantling the pyrite grains are locally developed within the Banded Mafic unit.

5.2.2 PYRITIZATION (SULPHIDATION) AND CARBONATIZATION

Disseminated pyrite is a common constituent throughout all of the Tulks Hill volcanics with concentrations generally on the order of 1 to 2 percent. Pyrite is widely developed in the alteration zone associated with the gold mineralization at Midas Pond. It occurs as fine disseminations and coarse patches constituting from 1 to 5 percent of the rock in the structural hanging wall. In the Banded Mafic unit, the structural footwall to the mineralization, pyrite increases in abundance from 1 to 2 percent up to greater than 5 percent proximal to the gold-bearing quartz veins. Here the pyrite forms coarse irregular patches and subhedral crystals which carry anomalous gold values.

Carbonate is widely and variably developed throughout all of the altered rocks associated with the gold mineralization at Midas Pond. The carbonate occurs as patches and locally forms tiny, perfectly preserved rhombs which overprint the groundmass. In the lower portions of the mafic tuffaceous rocks (Unit 2) overlying the alteration zone, epidote is replaced by carbonate and chlorite and

hence constitutes the first indication of the alteration associated with the gold mineralization (Plates 5.6 and 5.7). Carbonate increases in abundance towards the gold-bearing quartz veins. In the banded mafic rocks carbonate also increases in abundance as the veining is approached as indicated by the prominent rusty weathering associated with these rocks.

Electron microprobe analyses indicated that the carbonate associated with the alteration and with the auriferous quartz veining is typically Fe-rich (ferroan dolomite) (Table 5.3).

5.3 Interpretation and Summary

An extensive alteration halo is associated with auriferous quartz veining at Midas Pond. The distribution of this alteration is controlled by the Midas Pond shear zone, however, the alteration is most strongly developed in the structural hanging wall to the mineralized veins. Three styles of alteration are preserved at Midas Pond and these record an evolving hydrothermal system in which earlier alteration assemblages were destroyed as the chemistry and temperature of the fluids changed.

The most prominent style of alteration is advanced argillic and alteration assemblages associated with this style are pyrophyllite, paragonite, quartz, albite, chlorite, fluorite, pyrite and locally sericite. The pyrophyllite and paragonite

locally overprint an earlier poorly preserved argillic alteration phase as indicated by the presence of kaolinite.

The formation of pyrophyllite as opposed to kaolinite could be a result of an increase in either the temperature or the CO_2 content of the hydrothermal fluid (Miyashiro, 1973). P-T conditions of the kaolinite-pyrophyllite stability fields are shown in Figure 5.2 (after Miyashiro, 1973). Limited fluid inclusion data (T.J. Reynolds personal communication, 1990) from the mineralized quartz veins indicate that the veins formed at approximately 250° to 300°C. Brittle-ductile transformation occurs at depths of 10 to 15 kms (Sibson, 1977) (see Chapter 4). The geobarametric pressure at these depths is between 2.5 and 4 kb (Winkler, 1976). Within this pressure range (Figure 5.2) the conversion of kaolinite to pyrophyllite would occur at temperatures in excess of 350°C which is higher than the temperature of the hydrothermal fluids. This indicates that the alteration and mineralization may have developed at depths shallower than 10 to 15 kms.

CO_2 can be generated by the breakdown of minerals during prograde dehydration and decarbonation during metamorphism (Rose and Burt, 1979). Thus, with continued metamorphism at depth there would be an increase in the amount of CO_2 available to a hydrothermal fluid; this would promote the formation of pyrophyllite and paragonite. The production of pyrophyllite and

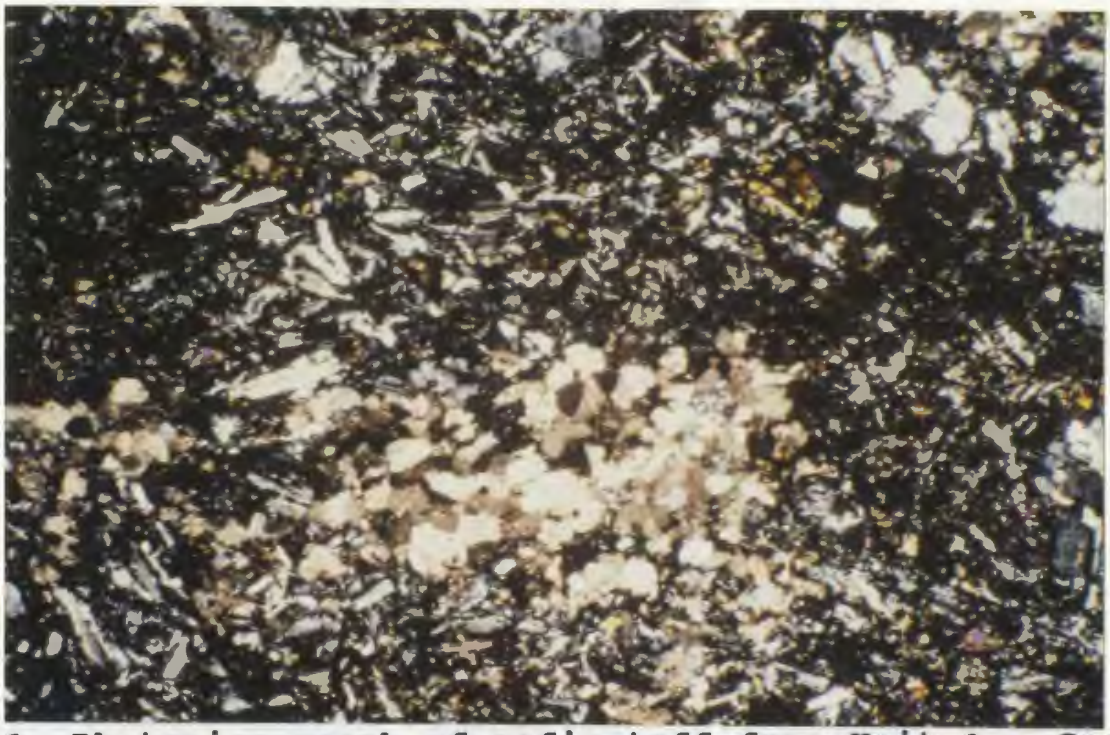

Plate 5.6 Photomicrograph of mafic tuff from Unit 2. Carbonate has partially overprinted the earlier greenschist facies chlorite and epidote. This is the first indication of the extensive carbonatization that overprints the alteration zone. Field of view is approximately 3.25 by 5 mm.

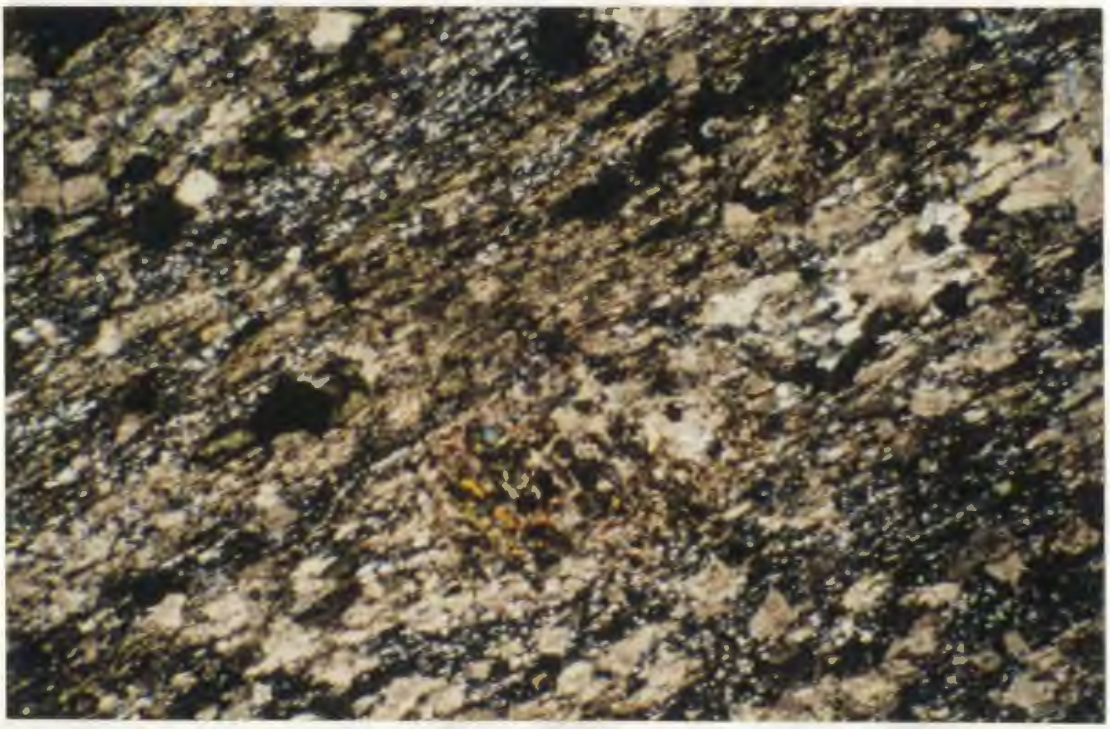

Plate 5.7 Photomicrograph of mafic tuff from Unit 2. Epidote in the groundmass has been totally replaced by carbonate and chlorite. Small patches of coarser epidote encased by chlorite remain. Field of view is approximately 3.25 by 5 mm.

	86-202	86-213-1	86-209	86-213-2	86-218
	(3)	(1)	(5)	(4)	(4)
MgO	0.2	21.44	14.6	20.4	19.2
CaO	61.97	30.76	28.55	29.6	29.8
MnO	0.73	0.39	0.47	0.78	0.69
FeO	0.41	3.8	12.14	3	5.2
SrO	0.15	0.09	0.03	0.07	0.05
Total	63.4	56.46	55.8	53.8	54.9
Au content of interval (ppb) from which sample was collected	Nil	1080	45-530	1080	2700-73000
Mg	0.3	37.9	26.2	37.9	35
Ca	98	54.6	51.2	55	54.3
Mn	1	0.7	0.8	1.5	1.3
Fe	0.6	6.7	21.8	5.6	9.5
Sr	0.2	0.2	0.44	0.13	0.09
Total	100	100	100	100	100

Table 5.3 Electron microprobe analyses of carbonates from Midas Pond; unmineralized vein, 86-202; host rock, 86-213-1; and, mineralized veins, 86-209, 86-213-2 and 86-218. Each analysis is an average, the number of analyses per grain is given immediately below the sample number.

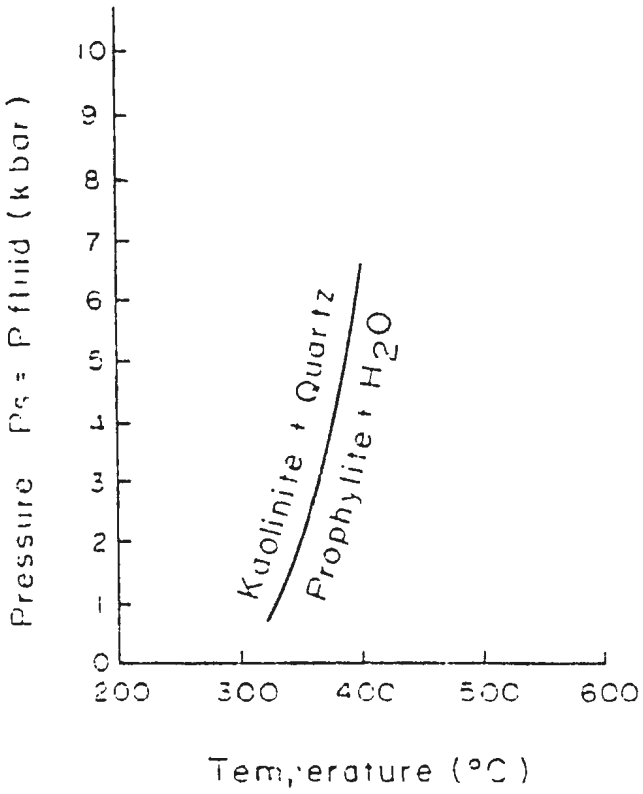

Figure 5.2 Experimentally determined equilibrium curves relevant to metamorphism of pelitic rocks (modified after Miyashiro, 1973). This diagram shows the stability field for kaolinite and pyrophyllite.

paragonite can be described by the following reactions (Miyashiro,1973):

$Al_2Si_2O_5(OH)_4 + 2SiO_2 = Al_2Si_4O_{10}(OH)_2 + H_2O$
Kaolinite + Quartz = Pyrophyllite

$NaAlSi_3O_8 + Al_2Si_2O_5(OH)_4 = NaAl_3Si_3O_{10}(OH)_2 + 2SiO_2 + H_2O$
Albite + Kaolinite = Paragonite + Quartz

$NaAl_3Si_3O_{10}(OH)_2 + 4SiO_2 = NaAlSi_3O_8 + Al_2Si_4O_{10}(OH)_2$
Paragonite + Quartz = Albite + Pyrophyllite

Silica remobilization and albitization accompanied the advanced argillic alteration, and is represented by zones and bands of quartz and feldspar. The presence of these minerals can be explained by the above reactions. Both the formation of pyrophyllite and paragonite would result in the formation of quartz and feldspar.

The presence of fluorite in the Midas Pond alteration halo indicates that the hydrothermal fluids not only were CO_2-rich but they also contained fluorine. Fluorine transport is favoured by low salinity, Ca^{2+} and CO_2-rich, high temperature fluids (Ellis, 1979). Precipitation of fluorine can occur as a result of an increase in pH and by mixing of Ca^{2+} ions with a solution rich in F^- (Barnes, 1979). F^- is typically considered to be a volatile

constituent which is concentrated during magma crystallization. However, F^- can also be liberated through the breakdown of OH-bearing minerals such as apatite and mica (Koritnig, 1972; Hanor, 1979). Since fluorite is not present within the auriferous veins and is restricted to the altered felsic rocks at Midas Pond, it may have been derived locally through the breakdown of OH mineral species rather than in the fluid source area. Alternatively F^- may have only been present in the hydrothermal fluids responsible for the advanced argillic alteration and not in the fluids which produced the auriferous quartz veins. This interpretation requires two separate hydrothermal fluids.

The final stage of alteration, Stage 3) involved sulphidation and finally carbonization. Sulphide haloes are a significant alteration phenomena characteristic of many Archean mesothermal gold deposits (Colvine et al., 1984; 1988; Roberts, 1988; Kerrich, 1989a). These haloes are often independent of, and overprint, other alteration assemblages. The pyrite is interpreted to result from the sulphidation of iron oxides and silicates in the host rocks. Sulphidation is a reducing process (Colvine et al., 1984; 1988; Kerrich, 1989a) which leaves the hydrothermal fluids relatively oxidized.

Carbonitization forms the final stage of alteration and resulted in the development of an extensive zone or halo of Fe-carbonate which largely overprints all other alteration

assemblages. Higher concentrations of CO_2 in the hydrothermal fluids would result in the breakdown of Ca-bearing silicate minerals producing Fe-carbonate (Miyashiro, 1978). This can be observed in the mafic tuffaceous rocks of Unit 2 immediately north of Midas Pond. With increasing alteration, epidote gradually diminishes and is replaced by carbonate and chlorite. Epidote is also lacking in the Banded Mafic unit, which is central to the shear zone and underwent extensive carbonitization.

CHAPTER 6

GEOCHEMISTRY

6.1 INTRODUCTION

Rocks within the alteration halo at Midas Pond comprise water-lain pyroclastic rocks or reworked tuffs that appear to be of mixed parentage. Superimposed upon these rocks is greenschist facies regional metamorphism, inhomogeneous deformation and alteration related to the auriferous quartz veins. Because of these factors the classical approach to studying the geochemistry of the alteration zone (ie. Gresen, 1967; Grant, 1986), in which the composition of altered rocks is compared to a least altered protolith, is not viable. Therefore, the approach in tnis study has been to make a qualitative study of element enrichment and depletion patterns within the alteration halo. Chemical analyses discussed in this chapter are presented in Tables 6.1 and 6.2. Analytical procedure, precision, accuracy and sample locations are presented in Appendix 2.

6.2 TECTONIC SETTING OF THE TULKS HILL VOLCANICS

It is not within the scope of this thesis to resolve or to discuss in detail the complicated geochemistry of all rocks within the Tulks Hill volcanics. The pillow lava associated with the main belt of felsic pyroclastic rocks have been interpreted to be

slightly to highly depleted (depleted in the incompatible HFSE) island-arc tholeiites (Kean and Evans, 1988a; Swinden et al., 1989). This interpretation is based on the assumption that the high field strength elements (Ti, Y, Zr and Nb) and the REE were relatively immobile during the prevalent regional greenschist facies metamorphism.

Felsic volcanic rocks within the Tulks Hill volcanics are considered to be rhyodacitic in composition (Kean and Jayasinghe, 1980) and are possibly analogous to felsic volcanic rocks (high-SiO_2 dacites and low-K rhyolites) in modern island arcs (Ewart, 1979). This may explain why the Tulks Hill felsic volcanic rocks are typically enriched in Na relative to K by a factor of 3 to 1 (Department of Mines and Energy unpublished data). Figure 6.1 (after LeMaitre, 1989) illustrates the low K content of the majority of the Tulks Hill felsic volcanic rocks. The purpose of this figure is to not to classify the felsic rocks but to emphasize the K deficiency. The mobility of both SiO_2 and K_2O preclude using these elements in a classification scheme involving ancient volcanic rocks. Similar rocks, which are associated with mafic volcanic rocks (depleted in the incompatible HFSE) of island-arc origin, have been identified within the Wild Bight Group, north-central Newfoundland (Swinden, 1987).

A plot of TiO_2 versus Zr (Figure 6.2) illustrates that three

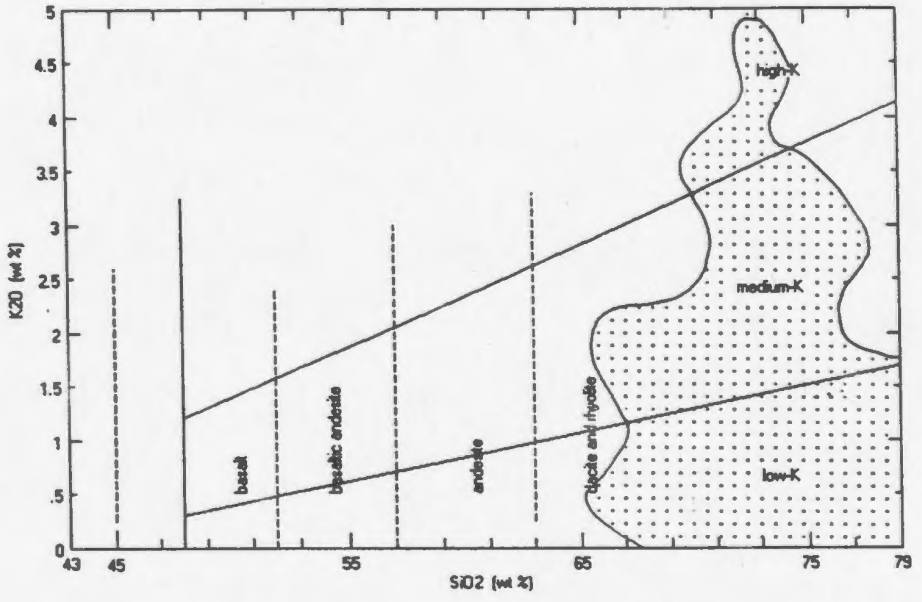

Figure 6.1 Discrimination diagram (after LeMaitre, 1989) used to emphasize the K-poor nature of the Tulks Hill felsic volcanic rocks (Department of Mines and Energy, unpublished data).

chemical subdivisions are present within the Tulks Hill volcanics (source Department of Mines and Energy, unpublished data). These subdivisions are: A) highly depleted pillow lava; B) depleted pillow lava; and C) felsic volcanic rocks. These elements are used below to illustrate relationships among the immobile HFSE in the Midas Pond alteration system.

Samples from the Midas Pond alteration zone, plotted on the same diagram (Figure 6.2), also form three distinct groups consisting of: Group 1) the mafic tuffaceous rocks, three banded mafic samples and one Al-rich sample; Group 2) the Banded Mafic unit and one Al-rich sample; and Group 3) the altered felsic rocks. Groups 1 and 3 are broadly comparable with the depleted pillow lava and felsic volcanic fields respectively and are considered to have been similar in original composition to the corresponding Tulks Hill rocks, assuming TiO_2 and Zr immobility. Group 2 does not correspond with any identified rocks within the Tulks Hill volcanics.

Group 1 samples plot partly within the field (Figure 6.2) defined by the slightly depleted pillow lava of the Tulks Hill volcanics suggesting that they were originally broadly basaltic in composition (Figure 6.3). The scatter observered within this group may be due to the fact that these rocks are tuffs. Two of the banded mafic samples (86-149d and 86-221) which plot with this group appear to form the structural base of the Banded Mafic

Sample Name	SiO2	TiO2	Al2O3	FeO*	MnO	MgO	CaO	Na2O	K2O	P2O5	LOI	V	Cu	Pb	Zn	Rb	Ba	Sr	Nb	Zr	Y	F
Mafic Tuffs																						
DE-86-76	51.66	0.87	19.65	8.99	0.18	6.69	6.61	4.31	0.98	0.08	6.53	274	9	<1	105	12	88	149	3.2	63	22	234.75
DE-87-01	50.52	1.01	19.26	10.48	0.17	2.63	9.75	5.89	0.21	0.07	4.17	388	0	5	79	0	77	180	2.1	46	21	na
DE-87-02	53.50	0.85	18.76	8.33	0.14	2.34	8.99	6.84	0.13	0.12	5.85	351	17	0	69	2	10	259	4.3	44	23	na
Banded Mafic Unit																						
DE-86-111b	62.46	1.22	15.24	9.50	0.06	7.05	0.27	3.85	0.18	0.16	5.38	447	16	0	83	2	0	29	6.4	113	34	504.36
DE-86-114b	61.62	1.28	15.76	8.54	0.09	4.81	3.07	4.64	0.09	0.11	5.94	345	4	2	67	0	5	76	3.2	110	43	537.30
DE-86-115b	57.81	1.31	15.42	12.59	0.09	7.69	3.01	1.66	0.22	0.21	6.94	524	4	<1	148	4	0	73	4.4	112	36	1035.05
DE-86-117d	82.50	0.62	7.07	7.50	0.01	0.40	0.03	1.35	0.43	0.10	3.25	211	5	4	16	6	122	46	2.0	54	19	297.62
DE-86-119f	65.83	1.13	15.09	8.40	0.07	5.12	0.77	3.23	0.23	0.12	4.68	398	25	<1	146	2	52	146	3.2	108	28	800.08
DE-86-120e	52.33	1.47	22.15	12.46	0.05	8.26	0.34	2.13	0.63	0.16	7.69	1166	259	<1	233	na	na	na	na	na	na	1441.99
DE-86-134c	58.44	1.30	16.86	12.34	0.03	6.18	0.31	4.15	0.16	0.22	5.04	585	9	<1	90	1	37	73	3.2	119	24	66.00
DE-86-146b	61.23	1.40	16.54	6.55	0.13	3.14	4.30	6.58	0.08	0.04	6.37	354	10	<1	66	0	19	170	4.5	120	58	430.90
DE-86-149d	59.09	1.25	15.03	11.35	0.09	5.02	4.28	3.71	0.01	0.17	6.12	163	6	<1	85	0	58	31	2.2	63	23	694.62
DE-86-198	62.83	1.18	14.89	10.40	0.11	5.56	1.22	3.59	0.02	0.20	3.81	338	12	<1	33	0	20	40	4.2	107	37	968.56
DE-86-221	53.89	1.14	15.41	14.83	0.11	6.32	4.98	3.21	0.02	0.10	5.79	495	9	<1	46	0	0	82	3.2	52	23	456.24
Sample Name	SiO2	TiO2	Al2O3	FeO*	MnO	MgO	CaO	Na2O	K2O	P2O5	LOI	V	Cu	Pb	Zn	Rb	Ba	Sr	Nb	Zr	Y	F
Al-rich rocks																						
DE-86-215	68.58	1.42	22.35	6.78	0.01	0.02	0.20	0.42	0.08	0.13	9.40	237	10	1	6	0	na	114	3.7	111	9	1273.89
DE-86-216	70.67	1.23	25.93	0.42	0.01	0.02	0.31	1.09	0.14	0.18	4.80	na	4	15	6	na	na	na	na	na	na	1700.00
DE-87-12	63.62	1.04	15.62	11.63	0.01	6.29	0.23	1.05	0.39	0.12	9.63	297	na	6	na	na	71	208	3.7	68	28	na
Altered Felsic Rocks																						
DE-86-90b	79.04	0.37	12.76	0.88	0.01	0.16	0.03	5.13	1.58	0.03	1.07	20	2	2	12	16	367	42	4.1	128	23	121.10
DE-86-128c	78.72	0.39	13.61	2.33	0.06	0.15	0.05	2.34	2.28	0.07	2.20	19	6	5	30	na	na	na	na	na	na	283.60
DE-86-129b	75.89	0.46	14.71	2.54	0.02	1.34	0.08	2.82	2.07	0.07	2.59	34	3	6	30	24	381	125	6.5	164	30	326.54
DE-86-142c	76.25	0.37	13.50	1.24	0.02	0.28	0.38	7.85	0.04	0.06	1.32	27	9	3	6	0	5	77	2.0	119	26	78.34
DE-86-144d	73.80	0.48	18.66	1.35	0.01	0.51	0.02	1.54	3.59	0.03	3.27	190	43	9	8	52	619	128	3.1	165	31	996.00
DE-86-154b	78.18	0.35	11.89	2.65	0.02	1.53	0.17	4.64	0.52	0.06	2.47	22	3	1	16	4	147	47	4.1	115	25	310.05
DE-86-184c	73.47	0.48	13.49	3.11	0.02	3.53	0.10	5.47	0.28	0.05	2.97	89	36	4	99	3	na	45	3.1	145	20	855.45
DE-86-187c	74.69	0.41	13.60	2.91	0.01	0.74	0.05	7.51	0.05	0.02	2.24	35	7	1	18	0	na	40	4.1	159	22	212.81
DE-86-189b	75.82	0.22	11.08	4.33	0.02	3.46	0.09	4.88	0.04	0.05	3.57	54	12	1	70	0	na	24	6.3	170	35	936.00
DE-86-219	84.79	0.29	14.09	0.12	0.01	0.01	0.11	0.42	0.10	0.05	2.99	82	3	18	3	0	16	80	4.3	161	13	1033.14
DE-86-220	75.37	0.52	13.51	1.64	0.03	0.54	1.89	6.30	0.11	0.06	3.17	33	3	12	4	0	49	106	3.3	183	9	258.03
DE-87-13	86.47	0.30	12.84	0.05	0.01	0.03	0.08	0.12	0.03	0.05	2.61	34	na	5	na	na	12	92	4.2	140	7	na
DE-87-18	82.11	0.18	9.06	5.64	0.01	0.77	0.27	1.58	0.34	0.03	4.11	114	na	5	na	na	126	169	3.3	179	27	na
DE-87-21	71.65	0.56	14.33	5.68	0.02	1.23	0.92	4.98	0.48	0.15	4.05	394	na	na	na	na	102	179	2.1	131	3	na
DE-87-27	75.10	0.60	16.15	2.97	0.01	0.63	0.28	2.46	1.69	0.11	3.32	56	0	10	4	25	573	133	5.5	129	42	na
DE-87-39	74.81	0.29	12.07	6.19	0.01	0.10	0.08	2.09	0.29	4.06	5.45	119	na	na	na	na	69	223	5.5	143	23	na
DE-87-41	74.48	0.61	16.00	3.30	0.03	0.98	1.03	2.42	1.02	0.14	4.24	46	0	2	11	10	403	128	4.5	147	32	na
DE-87-48	76.66	0.56	15.32	3.07	0.01	0.65	0.29	2.38	0.92	0.12	3.68	64	0	1	0	11	201	117	4.4	122	28	na
DE-87-49	71.05	0.36	11.40	6.07	0.04	3.38	2.42	5.06	0.12	0.10	6.01	126	4	0	38	0	18	57	4.5	151	48	na
DE-87-60	74.21	0.41	13.16	3.73	0.01	3.24	0.18	4.54	0.41	0.11	3.45	57	0	5	53	5	71	66	5.5	123	38	na

Table 6.1 Chemical analyses, major oxide and selected trace elements (recalculated to 100% anhydrous), for mafic tuffs, banded mafic and altered felsic rocks from Midas Pond. (na, not analyzed).

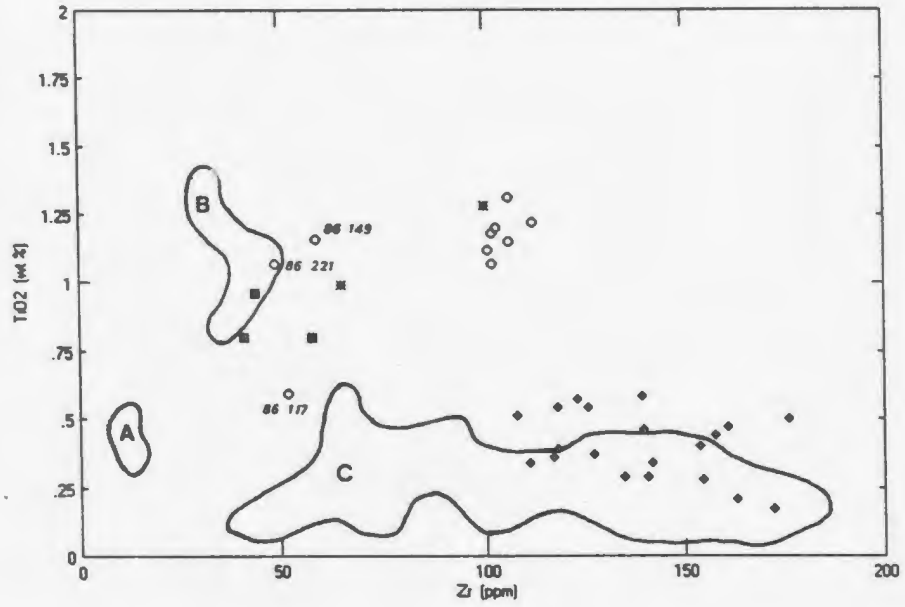

Figure 6.2 A plot of TiO_2 versus Zr which exhibits the distribution of samples from Midas Pond relative to fields defined by the Tulks Hill volcanics (data for the Tulks Hill volcanics, Department of Mines and Energy, unpublished data). Midas Pond area/: ▪ mafic tuffs, o banded mafic rocks, * Al-rich rocks, ♦ altered felsic volcanic rocks. Tulks Hill fields, A) highly depleted pillow lava, B) slightly depleted pillow lava, and C) rhyodacites.

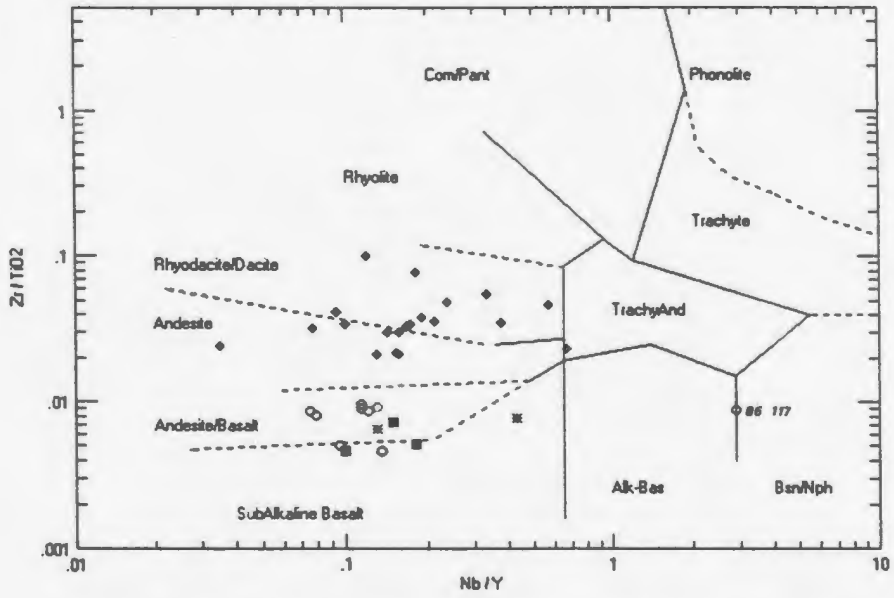

Figure 6.3 Discrimination diagram exhibiting rock types present within the Midas Pond area (after Winchester and Floyd, 1977). Symbols are the same as in Figure 6.1.

Sample	DE-87-18	DE-87-21	DE-87-27	DE-87-32	DE-87-46	DE-87-53	DE-86-219A	DE-87-02	DE-86-216
Ba	140	121	655	10	16	259	15	22	25
Sr	103	105	120	77	82	89	74	0	159
Ta	0.09	0.17	0.15	0.07	0.13	0.16	0.13	0.04	0.10
Nb	0.5	1.9	1.3	1.0	2.2	2.3	1.3	0.8	1.0
Hf	2.37	1.95	2.09	2.94	3.11	3.58	4.33	1.04	3.47
Zr	163	125	127	93	95	110	149	33	106
Y	15	22	22	34	33	38	12	22	13
Th	0.94	4.08	3.17	1.61	2.14	6.61	7.37	0.71	4.01
La	1.72	11.50	8.73	6.47	8.31	8.31	13.42	4.38	14.41
Ce	4.63	23.77	19.45	16.48	21.74	19.14	26.36	10.35	33.12
Pr	0.71	3.12	2.65	2.36	3.05	2.49	2.99	1.53	4.27
Nd	3.71	13.34	11.33	11.05	14.92	11.65	11.05	7.64	18.77
Sm	1.25	3.30	3.11	3.64	4.48	3.60	2.33	2.50	5.10
Eu	0.30	0.83	0.88	1.01	1.08	0.85	0.69	0.87	1.80
Gd	1.92	3.52	3.38	4.80	5.32	5.36	1.78	3.48	4.17
Tb	0.32	0.57	0.56	0.86	0.91	0.91	0.28	0.53	0.50
Dy	2.27	3.80	3.70	6.01	6.18	6.68	2.04	4.05	2.73
Ho	0.53	0.82	0.82	1.30	1.31	1.45	0.47	0.82	0.54
Er	1.64	2.51	2.48	4.05	3.86	4.52	1.67	2.45	1.68
Tm	0.25	0.38	0.37	0.58	0.61	0.69	0.29	0.34	0.26
Yb	1.73	2.56	2.51	3.98	4.02	5.03	2.19	2.26	1.77
Lu	0.32	0.38	0.39	0.63	0.64	0.76	0.39	0.34	0.30

Table 6.2 Selected trace element and REE data for rocks from the Midas Pond area. Siliceous alteration (87-18, 87-53 and 86-219a), altered felsic volcanic rocks (87-21 and 87-27), Banded Mafic unit (87-32 and 87-46), Al-rich alteration (86-216), Mafic tuff (87-02).

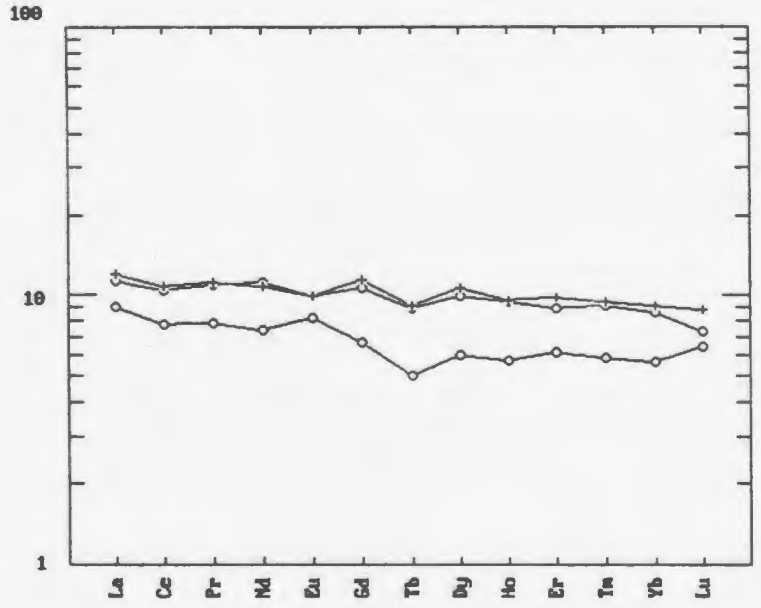

Figure 6.4 Chondrite normalized REE plot which compares mafic tuff sample 87-02 (+) to the field defined by the slightly depleted Tulks Hill mafic volcanic rocks (O) (source Department of Mines and Energy, unpublished data; normalization values after Taylor and McLennan, 1985; see Appendix 2).

unit. If the protolith to the Banded Mafic unit was a volcanic breccia comprised of large felsic fragments in a mafic matrix then these two samples may represent the composition of the matrix. Banded mafic sample 86-117d, which contains 82.5 percent SiO_2, was collected proximal to the mineralized quartz veins and is strongly silicified. For this reason it plots well outside of the other samples on both Figures 6.2 and 6.3.

REE concentrations within mafic tuffaceous rocks (Table 6.2) are strikingly similar to the REE concentrations of the slightly depleted mafic volcanic rocks of the Tulks Hill volcanics (Department of Mines and Energy, unpublished data) (Figure 6.4). The mafic tuff, sample 87-02, exhibits a fairly flat REE pattern at approximately 10X chondrite, with a slight negative Eu anomaly.

Group 2, which comprises the majority of the banded mafic samples, has quite distinct TiO_2 and Zr compositions from other two groups and from relatively unaltered volcanic rocks elsewhere in the Tulks Hill volcanics (Figure 6.2). On Figure 6.3, the banded mafic samples are classified as andesites, a lithology which has not yet been identified within the Tulks Hill volcanics.

The altered felsic rocks, Group 3, have similar TiO_2 and Zr compositions to the felsic rocks of the Tulks Hill volcanics (Figure 6.2) and plot mainly within the dacite/rhyodacite field (Figure 6.3). Based on these similarities the altered felsic

volcanic rocks at Midas Pond are assumed to have had low-K concentrations similar to the Tulks Hill felsic volcanic rocks.

6.3 ALTERATION GEOCHEMISTRY

A total of 35 samples from the alteration halo were analyzed for major and selected trace elements (Table 6.1). Twenty-four of these samples consist of variably altered felsic volcanic rocks collected from the structural hangingwall to the auriferous quartz veins. The remainder of the samples were collected from the Banded Mafic unit in the structural footwall. Nine samples were selected for REE analyses (Table 6.2).

6.3.1 GEOCHEMISTRY OF THE ALTERED FELSIC VOLCANIC ROCKS

The rocks which occupy the structural hanging wall to the gold mineralization at Midas Pond are dominated by variably deformed and altered felsic crystal tuffs. Alteration in these rocks varies from argillic to advanced argillic alteration assemblages. Mineral components include quartz, pyrophyllite, paragonite, kaolinite, plagioclase, pyrite, Fe-carbonate and minor chlorite.

A visual comparison of geochemical data from the Tulks Hill felsic rocks (average values calculated from Newfoundland Department of Mines and Energy, unpublished data; Appendix 2) with data for the felsic rocks from the Midas Pond alteration zone

indicates significant variation in the elemental compositions of this latter group, particularly in the major oxide (eg. SiO_2, Na_2O and K_2O) concentrations.

Within the altered felsic rocks at Midas Pond three chemical groupings can be identified (Figure 6.5). These groups, which are illustrated on the plots of Na_2O versus K_2O (Figure 6.5a) and SiO_2 versus Na_2O (Figure 6.5b) are as follows: 1) a Na-enriched group; 2) a K-enriched group; and 3) a silica-enriched group. This latter group is defined by samples with low concentrations of both Na_2O and K_2O. Sample 86-90b has relatively high and equal concentrations of both Na_2O and K_2O which is anomalous with respect to the other samples.

The three groupings are further subdivided on a plot of Na_2O versus Zr (Figure 6.5c). Except for samples 86-142c, 86-187c and 86-220, which exhibit strong Na enrichment, and sample 86-144d, which exhibits strong K enrichment, the bulk of the altered felsic rocks plot as two groups, a Na-rich group and a K-rich group. Both of which exhibit weak positive correlations between Na_2O and Zr. These groups may represent the least altered of the felsic rocks. The two groupings are aligned roughly parallel and vary by approximately 2 percent NaO_2.

Since the felsic rocks were initially K-poor and no appreciable K was added to the alteration zone (except for sample

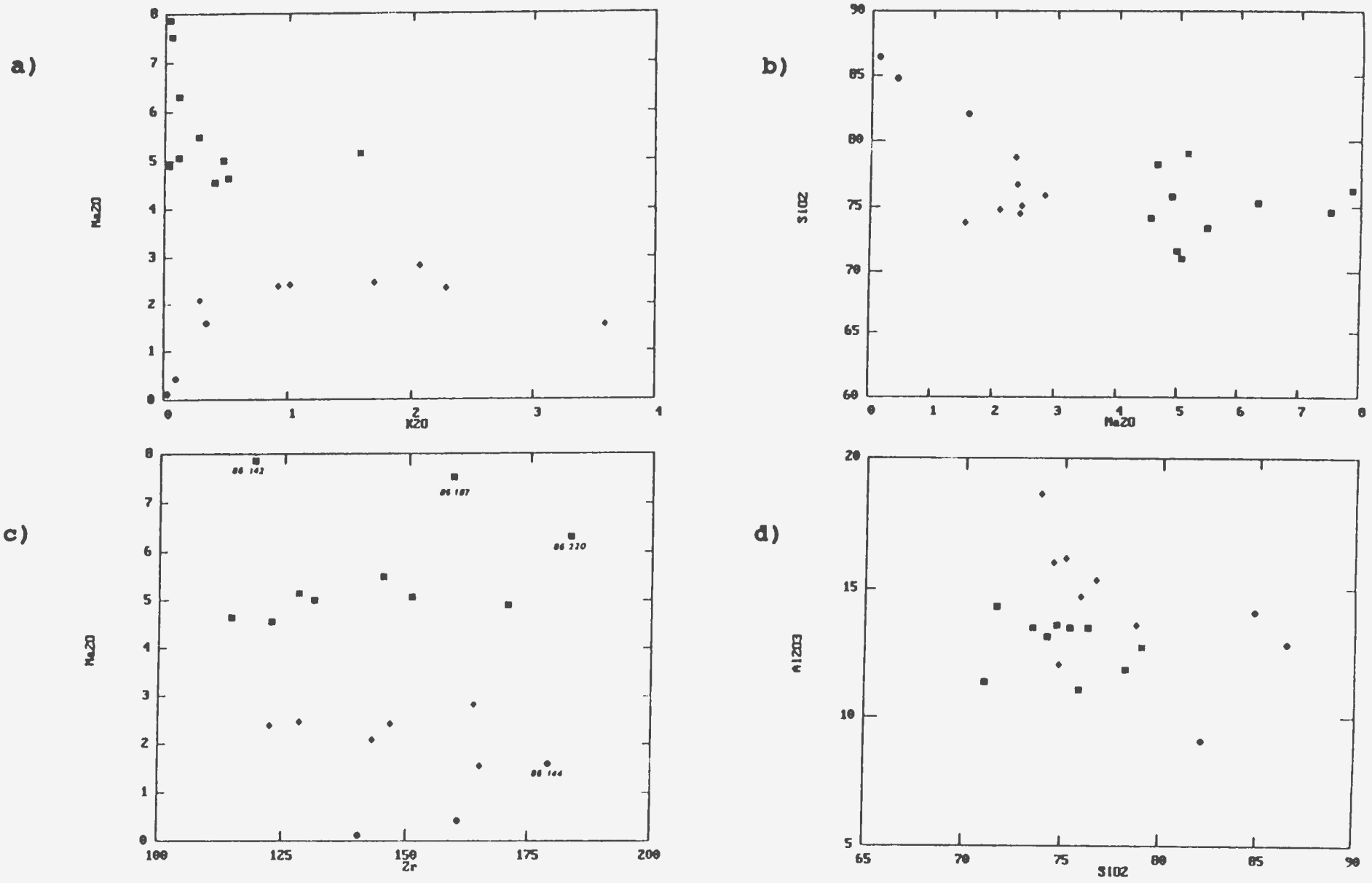

Figure 6.5 Plots illustrating the three chemical groupings present within the altered felsic rocks at Midas Pond: a) Na_2O versus K_2O; b) SiO_2 versus Na_2O; c) Na_2O versus Zr; and d) Al_2O_3 versus SiO_2. Symbols: • silica-enriched rocks; ▪ Na-enriched rocks; ♦ K-enriched rocks; and ★ 86-90b.

DE-86-144d) then the hydrothermal fluids appear to have remobilized both K and Na from within the zone affected by the alteration. Localized stripping of Na and K probably occurred during the breakdown of primary igneous and greenschist facies metamorphic minerals such as feldspar and mica.

Samples 86-142c, 86-187c and 86-220, which exhibit the highest concentrations of Na_2O, are the most altered samples within the Na-enriched group. These samples appear to have undergone significant Na addition, possibly through the formation of paragonite related to advanced argillic alteration.

Only one sample (86-144d), a sericite schist, appears to exhibit significant K-enrichment. K-metasomatism leading to extreme K-enrichment appears to have been a relatively localized and rare phenomenon.

Al_2O_3 concentrations exhibit little significant variation in any of the three groups, however, the K-enriched group has slightly more elevated Al_2O_3 concentrations then the other two groups (Figure 6.5d). The concentrations of FeO*, MgO and CaO (Table 6.1) are more variable and appear to reflect local concentrations of pyrite, Fe-carbonate and chlorite.

The trace elements Sr, Rb and Ba exhibit consistent trends within the alteration zone (Figure 6.6). Sr concentrations appear

to be more elevated in the K-enriched group relative to the other groupings (Figure 6.6a). However, one silica-rich sample (87-18), two Na-rich samples (86-220 and 87-21) and one K-rich sample (87-39) exhibit elevated Sr concentrations relative to the other samples in these groups (Table 6.1). Sr can substitute for Ca in plagioclase and for K in K-feldspar; however, it does not readily substitute for K within mica (Stueber, 1978). In hydrothermal alteration zones Sr can occur within carbonate and fluorite (Faure, 1978). Slightly elevated Sr concentrations within portions of the Midas Pond alteration zone must be related to the substitution of Sr within plagioclase, carbonate and possibly fluorite. Rb concentrations are elevated in a number of the K-enriched samples (Figure 6.6b) indicating substitution of K by Rb. Rb readily substitutes for K within mica (Heier, 1978).

Ba concentrations are also elevated in some of the samples from the K-rich group. Significant concentrations of Ba can occur within feldspar and mica (Puchelt, 1978). F does not appear to exhibit any consistent enrichment trends within the alteration zone, however, this assumption is based on a limited amount of data (Figure 6.6d). The sporadic nature of the fluorite within the altered rocks and its absence from within the auriferous quartz veins suggests that the fluorite may have been locally derived, possibly through the breakdown of OH minerals.

REE concentrations within the altered felsic rocks vary

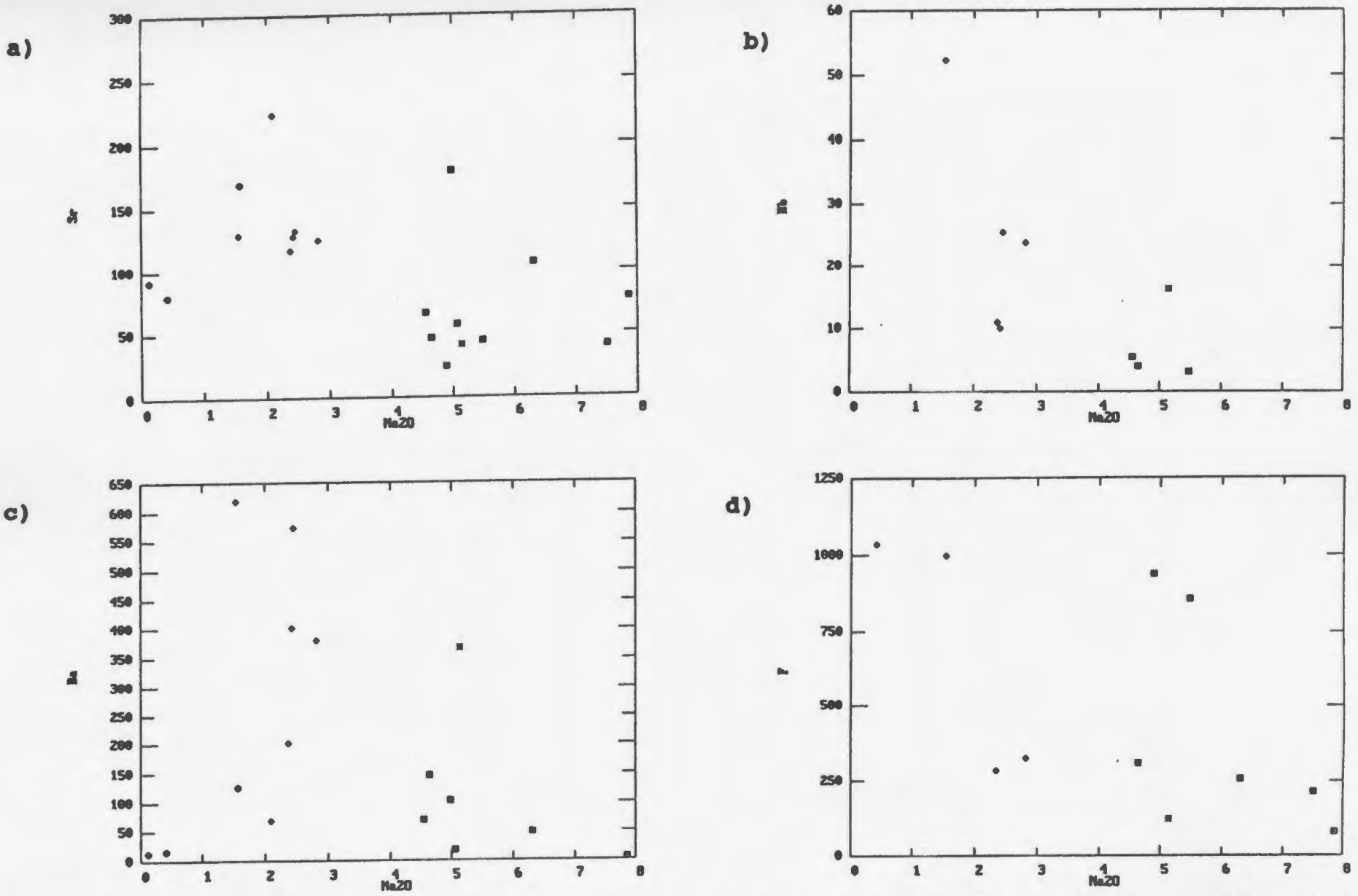

Figure 6.6 Plots of Sr, Rb, Ba and F versus Na_2O for the altered felsic rocks at Midas Pond. Symbols are the same as in Figure 6.4.

considerably with the style of alteration. Figure 6.7 is a chondrite-normalized REE plot of two altered felsic volcanic rocks from Midas Pond. Sample 87-27 is considered to be the least altered sample analyzed based on a comparison of the major oxide data for this sample with the average concentration for the Tulks Hill volcanics (Appendix 2). It has a slightly concave-upward pattern and a small negative Eu anomaly. REE concentrations vary between approximately 20X chondrite for the LREE to 10X for the mid to HREE.

Sample 87-18 (Figure 6.7) is considered to have been silicified (see discussion above) which resulted in an overall reduction in REE abundances and a marked depletion in the LREE and a prominent negative Eu anomaly. The mid to heavy REE exhibit a pattern similar to sample 87-27 but with abundances of only 7X to 9X chondrite. LREE depletion as exhibited by this sample maybe the result of Cl^- complexing and removal by hydrothermal fluids (Taylor and Fryer, 1982).

6.3.2 THE AL-RICH GROUP

The Al-rich samples (86-215, 86-216 and 87-12) have TiO_2 values of between 1.04 and 1.42 percent (Table 6.1) which are considerably higher than the altered felsic samples. The Ti and Zr contents of two of the samples are similar to that of the mafic tuffs and the Banded Mafic unit respectively indicating that these

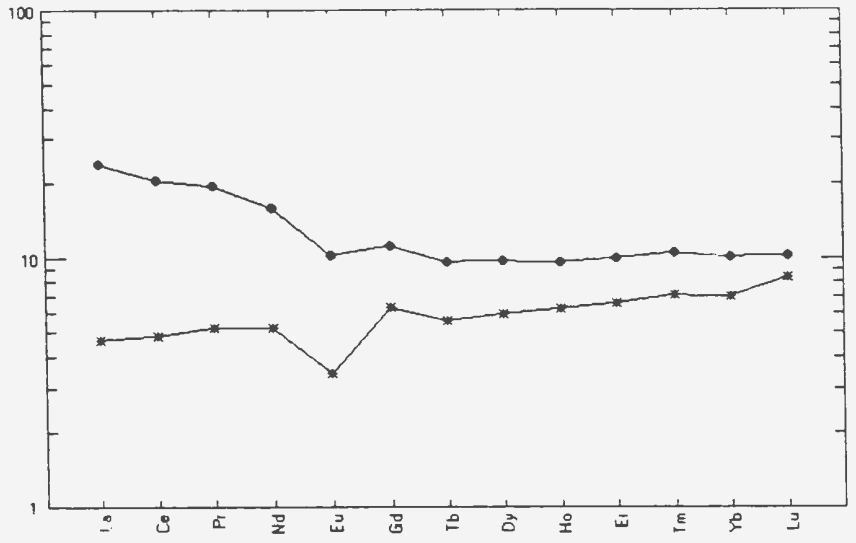

Figure 6.7 Chondrite normalized REE plot for altered felsic volcanic rocks from Midas Pond. • DE-87-27 (least altered sample), * DE-87-18 (silica-rich sample) (normalization values after Taylor and McLennan, 1985; see Appendix 2).

rocks may be altered equivalents of these mafic units.

The extremely high Al_2O_3 concentrations in samples 86-215 and 86-216 and the low concentrations of Na_2O, K_2O, CaO and MgO (Table 6.1) indicate that these rocks were subjected to intense alteration.

Figure 6.8 is a chondrite-normalized REE plot which illustrates the REE abundances of sample 86-216, an Al-rich sample, and two banded mafic samples from Midas Pond. Sample, 86-216, exhibits a sigmoidal shaped REE pattern which is unlike the patterns produced by either the banded mafic samples or the Midas Pond mafic tuff (Figure 6.4). REE concentrations within sample 86-216 range from 30X chondrite for the LREE to 7 to 8X chondrite for the mid to HREE. If the Al-rich rocks are altered equivalents of either the banded mafic unit or the mafic tuff (Figure 6.2) than the Al-rich rocks must have been subjected to substantial remobilization of the REE. Sample 86-216 exhibits an apparent increase in the LREE abundances and Eu relative to both the banded mafic samples and the mafic tuffs. However, the mid to HREE appear to have been preferentially leached by the hydrothermal fluids. Based on the presence of CO_2-rich fluid inclusions (see Section 7.2.1) in the mineralized veins and the presence of fluorite in the most intensely altered portions of alteration zone it is believed that the mineralizing fluids were CO_2- and possibly F-rich. Scavenging by carbonate and fluorine ion complexes, which are

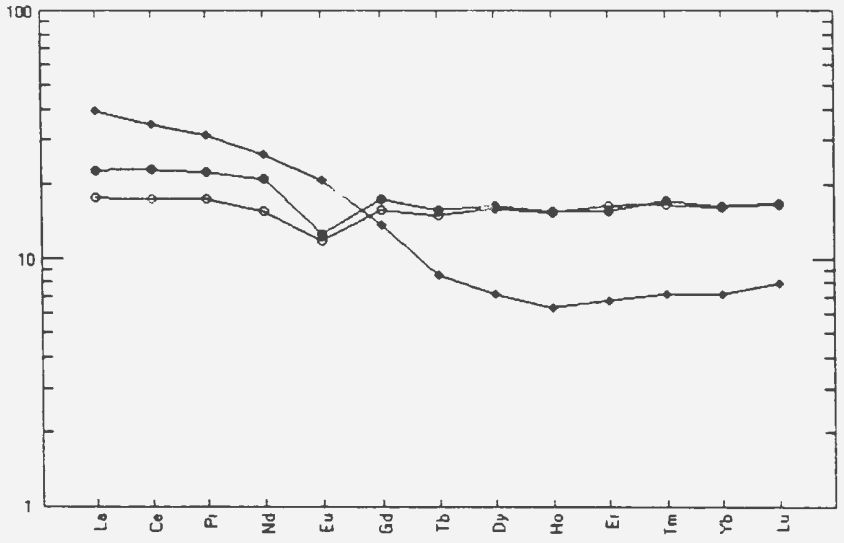

Figure 6.8 Chondrite normalized REE plot for banded mafic samples 87-32 (○) and 87-46 (●) and Al-rich sample 86-216 (♦) (normalization values after Taylor and McLennan, 1985; see Appendix 2).

thought to be responsible for the mobilization of the heavy REE (Taylor and Fryer, 1982), may have resulted in the REE pattern exhibited by sample 86-216. This interpretation, however, is only based on one analysis.

6.3.3 GEOCHEMISTRY OF THE BANDED MAFIC UNIT

Chemically and lithologically the andesitic rocks of the Banded Mafic unit are distinct from all other rock types within the alteration zone. Concentrations of FeO*, MgO CaO, TiO_2 and V are amongst the highest of any rock type within the alteration halo at Midas Pond. The FeO*, MgO and CaO concentrations all exhibit slight to moderate increases with increasing silica content (Table 6.1). The higher values for these elements are attributed to the abundant Fe-carbonate and pyrite developed proximal to the auriferous quartz veins.

The majority of Banded Mafic samples exhibit only slight variation in element concentrations (Table 6.1). Only three samples 86-117d, 86-149d and 86-221 exhibit any significant variation in element abundances. Samples 86-149d and 86-221 have Zr concentrations which are similar to the Midas Pond mafic tuffs (see Figure 6.2) and are therefore possible correlatives of these rocks. The V contents of these two samples are somewhat similar to the mafic tuffs, however, sample 86-221 is slightly elevated.

Sample 86-117d is considered to be the most intensely altered sample analyzed from within the banded mafic unit. The silica concentration of this sample is 82.5 weight percent as compared to a range of approximately 52 to 66 weight percent for the remainder of the banded mafic samples.

Figure 6.8 is a chondrite-normalized REE plot of two banded mafic samples from Midas Pond. REE concentrations within the Banded Mafic unit do not exhibit any consistent variation as a result of alteration. Samples 87-32 and 87-46 exhibit fairly flat, slightly concave upward patterns, with negative Eu anomalies. REE concentrations are approximately 11X chondrite.

HREE concentrations within the banded mafic samples are significantly higher than in any other rock type within the Midas Pond area. This evidence together with the apparent lack of significant alteration within the Banded Mafic unit implies that a genetic link does not exist between this unit and the mafic/felsic tuffaceous rocks at Midas Pond (ie. the unit does not plot along a mixing line between the felsic and mafic rocks, see Figure 6.2). However, this does not rule out the possibility that the Banded mafic unit is a hybrid pyroclastic rock, a mixture of either the mafic or felsic tuffs and an unidentified rock type of alkalic composition.

An alternate hypothesis, which may explain the chemical

uniqueness of the Banded Mafic unit, is that the unit may be a highly deformed dyke. This interpretation is not supported by field observations such as the presence of angular felsic fragments.

6.4 SUMMARY

Most of the rocks within the Midas Pond area are highly altered water-lain pyroclastics, that bear striking resemblance both lithologically and geochemically to the rest of the Tulks Hill volcanics. The mafic rocks have HFSE and REE concentrations which are similar to depleted island-arc tholeiites from the Tulks Hill volcanics.

The felsic rocks are interpreted to have been rhyodacitic in composition and exhibit characteristics (HFSE abundances and Na/K ratios) similar to the rest of the Tulks Hill felsic volcanics.

Chemically and lithologically the Banded Mafic unit is a distinct rock type within the Midas Pond alteration zone. The unit is interpreted to be a hybrid mixture of the mafic or felsic tuffs present at Midas Pond and some unidentified alkalic rock. The possibility that the Banded Mafic unit is a deformed dyke is not supported by field observations. The Banded mafic unit appears to have been largely unaffected by the alteration related to the auriferous quartz veins. However, elevated concentrations of FeO*,

CaO and MgO are present proximal to the veins and these are related to the presence of abundant Fe-carbonate and pyrite.

Alteration at Midas Pond involved mainly: 1) the addition silica, resulting in slightly silica-enriched rocks (SiO_2 in excess of 80 weight/percent), and 2) localized stripping and remobilization of Na, K and F. This remobilization resulted in Na-enriched/K-depleted rocks, slightly K-enriched rocks and sporadically developed fluorite. Na redistribution was accomplished through albitization and the formation of paragonite. The lack of significant K-enrichment in these rocks is a result of the low primary concentrations of K in the felsic volcanic rocks. Variations in the concentrations of MgO, CaO and FeO and the trace elements Sr, Rb, Ba are related to the concentrations of the various alteration assemblages such as pyrite, Fe-carbonate, chlorite, feldspar, fluorite and mica.

Variation in REE concentrations among altered felsic volcanic rocks from the structural hanging wall are attributed to CO_2^{2-}, F^- and possibly Cl^- complexing. These complexes are considered to be successful scavenging agents of the REE.

CHAPTER 7

AURIFEROUS QUARTZ VEINS

7.1 INTRODUCTION

The gold is hosted by a series of quartz veins which are developed along the contact between the Banded Mafic unit and the structurally overlying altered felsic volcanic rocks. The veins cut grey to greyish-green, sheared and siliceous rocks of both the Banded Mafic unit and the felsic volcanic rocks (Plate 7.1).

The auriferous zone has a strike length of approximately 800 m and is sporadically mineralized over a width of 10 to 12 m. The zone appears to increase in width with depth. The gold is associated with pyrite and occurs largely as elemental gold with subordinate amounts of electrum and gold tellurides. Thin pyrite veinlets (Plate 7.2), pyrophyllite and sericite/paragonite seams are common within the quartz veins. The veins also contain Fe-carbonate, pyrite, fine-grained tourmaline, paragonite and plagioclase.

Three sets of gold-bearing quartz veins are present within the mineralized zone, the structural origin of these veins was discussed in Section 4.5. The earliest veins (V_1) are boudinaged and parallel the shear zone foliation. They contain coarse-grained, milky-white

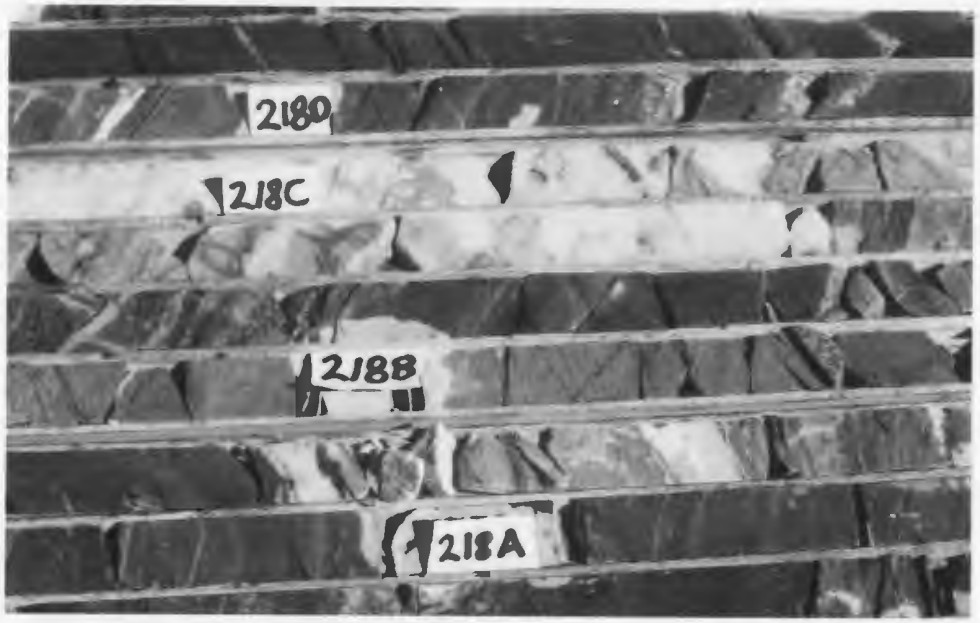

Plate 7.1 Mineralized section from diamond drill hole GP-21. Sample 218A (base of section) is a banded mafic rock with abundant coarse patches of pyrite which carry anomalous gold. Sample 218B is silicified banded mafic rock. Sample 218C is mineralized quartz veining. Sample 218D is silicified felsic volcanic rock.

Plate 7.2 Close up of sample 218C showing dilational nature of veining and abundant stringers of fine-grained pyrite. This section assayed 7.3 g/t over 0.9 m.

quartz, rusty carbonate and minor pyrite. A penetrative foliation defined by sericite/paragonite is commonly developed within the boudins. A grab sample from one of these veins exposed in Trench 46+00 assayed 1150 ppb. gold.

Second and third generation quartz veins (V_2 and V_3) consist of milky-white, coarsely crystalline quartz with locally developed comb structures and vuggy quartz-lined cavities. The veins are generally thin, less than 1 cm, but locally may reach up to 1 m in thickness. Sections with multiple veins are up to 7 m thick.

The V_2 and V_3 veins contain large patches of Fe-carbonate, pyrite, chlorite, fine-grained pale-green paragonite, pyrite and fine needles of tourmaline.

7.2 MINERALOGY OF THE VEINS

In diamond drill core it is not possible to distinguish between V_1 and V_2-V_3 veins. Petrographic descriptions are of samples collected from outcrop. Thin section analyses of V_1 veins indicate that these veins contain deformed and recrystalized quartz and minor wispy mica and small oxidized pyrite cubes. The quartz occurs as large rounded crystals with undulatory extinction and seriate margins and as patches of fine grained crystals. Tourmaline was not observed in thin section, however, it was observed in some hand samples. Surface exposure of the V_1 veins is

limited, therefore, making petrographic comparisons with the V_2-V_3 veins is difficult.

Mineralogically the V_2 and V_3 veins are the same. Thin section analyses indicate that both vein sets contain coarse crystals of quartz, Fe-carbonate, paragonite, pyrite, plagioclase, chlorite, tourmaline and minor pyrophyllite.

7.2.1 QUARTZ

The quartz is variably deformed. Veins exposed in Trench 46+00 contain coarse quartz crystals which have ragged almost seriate boundaries. These quartz crystals exhibit undulatory extinction and locally contain fine wisps of pyrophyllite and paragonite. Patches of fine granular quartz are developed along some of the quartz crystal boundaries and locally form narrow bands. In less strained zones, as intersected by diamond drill hole GP-21, the veins lack the fine-grained recrystallized quartz.

Abundant CO_2-rich fluid inclusions (Plate 7.3) are present in the large quartz crystals. At least two distinct populations of inclusions are present, liquid-rich and vapour-rich which exhibited homogenization temperatures of 290 and 250-270 °C respectively (T.J. Reynolds pers. comm., 1990). Abundant low salinity, CO_2-rich inclusions are indicative of lode gold occurrences and while CO_2-rich inclusions occur in a wide range of deposit types they are

ubiquitous in lode gold deposits (Colvine et al., 1984; Kerrich, 1989a). The presence of significant concentrations of CO_2-rich inclusions is believed to indicate that the hydrothermal fluids responsible for the vein system originated at relatively deep crustal levels (Kerrich, 1989a; Reynolds, 1990).

7.2.2 CARBONATE

Carbonate generally occurs along the vein margins and within the wallrock adjacent to the veins. It forms rhombohedral crystals and large patches up to a few millimetres in size (Plate 7.4). These exhibit rhombohedral cleavage and high birefringence.

Electron microprobe analyses indicate that the carbonate within the quartz veins and in the immediate host rocks is Fe-carbonate (ferroan dolomite ?) (Table 5.3). A weak correlation exists between the Fe content of the carbonate and the gold value of the mineralized zone from which the carbonate was taken (Table 5.3). Carbonate samples with higher Fe contents appear to come from zones with higher gold concentrations. However, sample DE-86-209 (collected from outcrop) has a high Fe content and the zone from which it was taken has a relatively low gold content, this may reflect weathering of both the carbonate minerals and possible leaching of gold by surface waters.

Non-auriferous quartz veins, containing pyrite and carbonate, are exposed in the southern end of a trench on line 52+00 south of

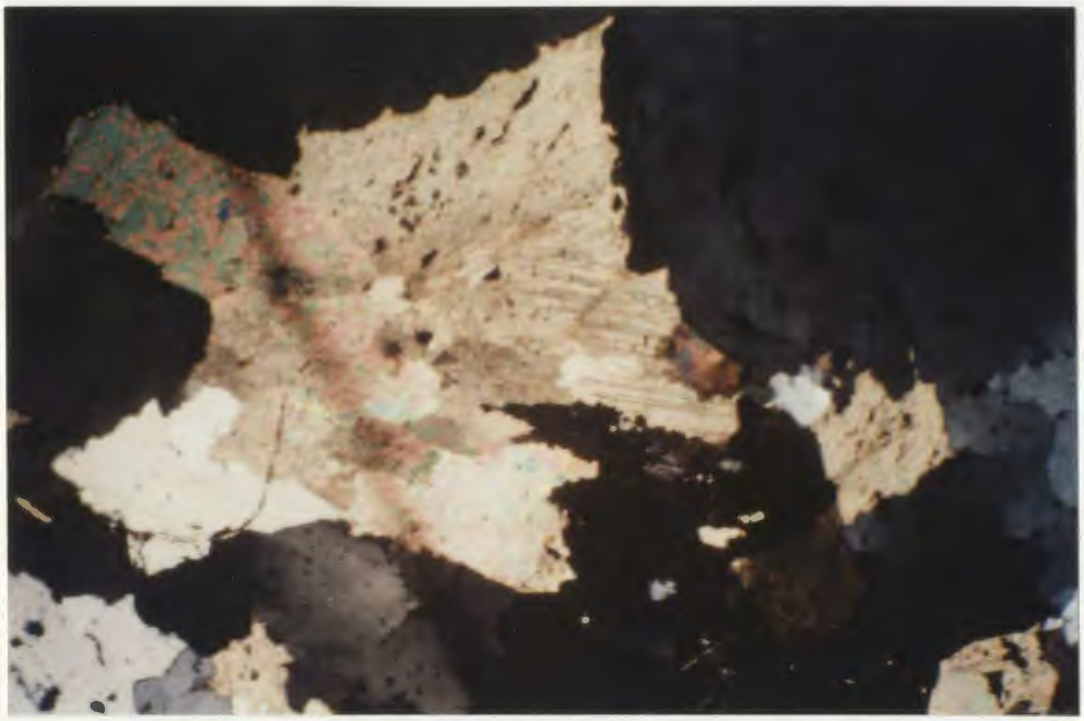

Plate 7.3 Photomicrograph of coarse Fe-carbonate patch developed within mineralized quartz vein. Field of view is approximately 3.25 by 5 mm.

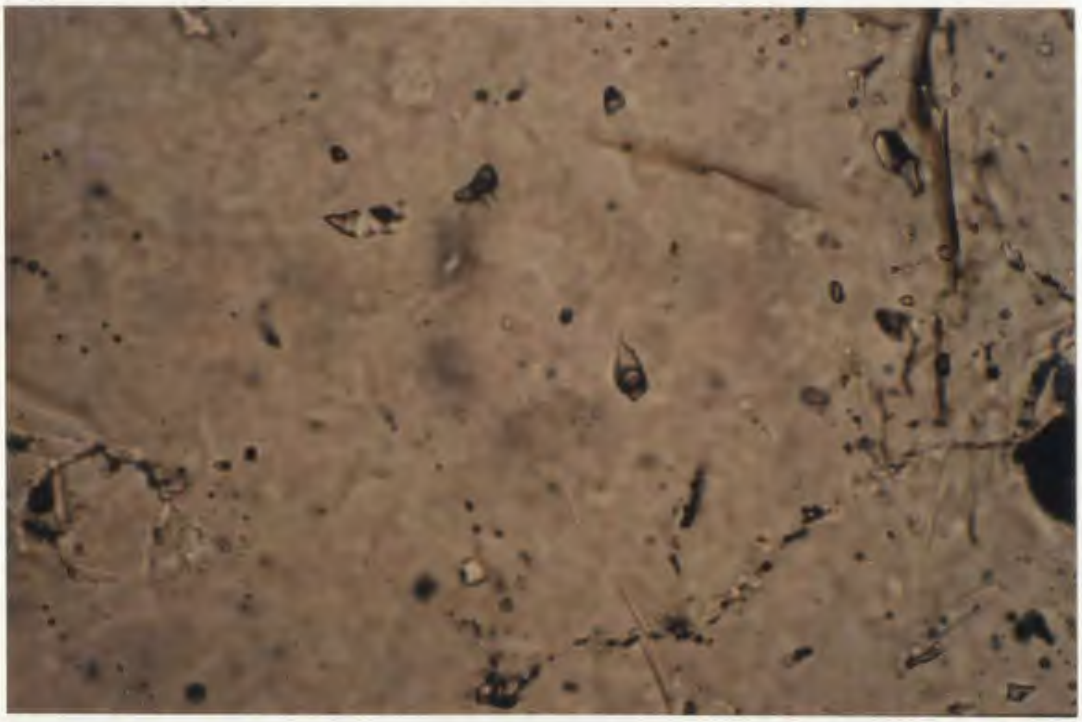

Plate 7.4 Photomicrograph of a quartz crystal from a mineralized vein which contains abundant CO_2 vapour-rich fluid inclusions. Width of picture is approximately 0.35 mm.

Muskegone Pond. These veins are developed along the contact between mafic feldspar crystal tuff (Unit 2) and altered felsic crystal tuff (Unit 3). The setting of this veining is similar to the auriferous veining from the mineralized zone at Midas Pond, however, the carbonate in these veins is calcite (Table 5.3) as opposed to Fe-carbonate (ferroan dolomite ?) in the mineralized veins.

7.2.3 CHLORITE

Olive-green chlorite forms dense masses and patches of tiny circular structures with radiating textures that have pervasively overprinted large portions of the veins, including quartz (Plate 7.5).

Electron microprobe analyses indicate that this chlorite and chlorite from the immediate host rocks are relatively more enriched in Mg than chlorite from the mafic tuffs outside the alteration zone (Table 7.1; Figure 3.2). However, these Mg-enriched chlorites plot midway between the chlorite from the mafic tuffs and the Mg-rich chlorites associated with the massive sulphide alteration zones on an Al-Fe-Mg diagram (Figure 7.1). High fluid/rock ratios dominated by seawater are responsible for the more Mg-rich chlorite associated with the volcanogenic massive sulphide deposits (Mottl, 1983). Chlorite from the quartz veins plot within the Ripidolite field on Hey's chlorite nomenclature diagram (Hey, 1954; see Figure

Plate 7.5 Photomicrograph of radiating worm-like chlorite overprinting a mineralized quartz vein. Field of view is approximately 3.25 by 5 mm.

Table 7.1 Microprobe analyses (see next page) for chlorite from the auriferous quartz veins (86-116D and 86-116d-2) and the host rocks (86-119D, 86-125, 86-125A and 86-179E) are listed on the next page. The computed cation proportions are based on 28 oxygen atoms. Each analysis is an average, the number of analyses per grain is given immediately below the sample number.

	86-116D (3)	86-116D-2 (3)	86-119A-1 (3)	86-119A-2 (3)	86-119D-1 (3)	86-119D-2 (3)	86-119D-3 (2)	86-125-1 (3)	86-125-2 (3)	86-125A-1 (3)	86-125A-2 (3)	86-179E (1)
Na_2O	.05	.04	.04	.03	.08	.13	.12	.04	.04	.02	.01	.01
MgO	18.94	19.16	18.02	18.55	20.42	20.87	20.59	17.73	17.63	17.54	17.90	21.00
Al_2O_3	21.32	21.21	21.76	21.13	21.95	21.77	22.21	22.68	22.21	21.98	22.16	22.33
SiO_2	25.82	26.02	26.23	25.76	26.30	27.27	26.87	27.07	26.70	26.57	27.09	26.94
K_2O	.01	.01	.03	.00	.05	.07	.06	.04	.04	.00	.01	.00
CaO	.00	.00	.01	.01	.01	.01	.00	.00	.02	.02	.01	.00
TiO_2	.03	.04	.02	.02	.01	.02	.02	.02	.02	.04	.05	.00
Cr_2O_3	.00	.00	.01	.03	.00	.02	.03	.02	.01	.01	.02	.00
MnO	.09	.14	.11	.09	.04	.09	.08	.06	.09	.08	.09	.08
FeO*	19.89	19.96	20.68	20.04	16.73	16.95	16.47	22.00	22.61	22.52	22.05	16.46
NiO	.00	.01	.00	.02	.02	.03	.02	.01	.01	.03	.04	.03
Total	86.14	86.59	86.90	85.68	85.60	87.22	86.48	89.67	89.35	88.79	89.42	86.95
Na	.018	.012	.012	.006	.030	.047	.042	.012	.012	.006	.000	.035
Mg	5.886	5.926	5.556	5.803	6.264	6.284	6.234	5.315	5.330	5.340	5.382	6.322
Al	5.237	5.189	5.307	5.224	5.322	5.181	5.322	5.374	5.312	5.286	5.270	5.314
Si	5.378	5.396	5.429	5.409	5.413	5.507	5.459	5.445	5.419	5.423	5.405	5.444
K	.000	.000	.006	.000	.012	.018	.012	.006	.006	.000	.000	.000
Ca	.000	.000	.000	.000	.000	.000	.000	.000	.000	.000	.000	.000
Ti	.000	.000	.000	.000	.000	.000	.000	.000	.000	.000	.006	.000
Cr	.000	.000	.000	.000	.000	.000	.000	.000	.000	.000	.000	.000
Mn	.012	.024	.018	.012	.006	012	.012	.006	.012	.012	.012	.012
Fe	3.463	3.459	3.577	3.518	2.875	2.863	2.798	3.703	3.834	3.841	3.718	2.781
Ni	.000	.000	.000	.000	.000	.000	.000	.000	.000	.000	.006	.000
Total	19.995	20.007	19.904	19.972	19.921	19.912	19.878	19.860	19.924	19.908	19.858	19.09

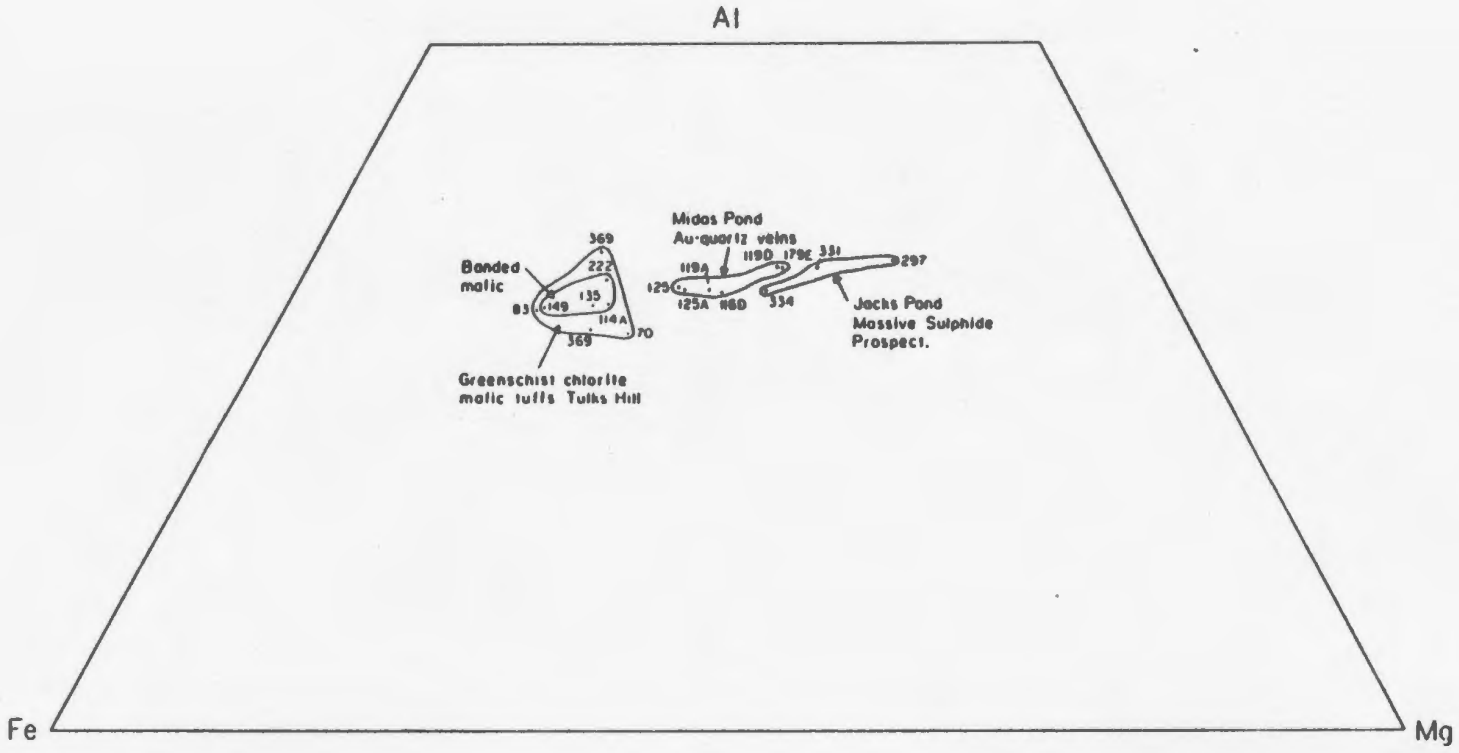

Figure 7.1 Chlorite compositions plotted on an Al-Mg-Fe molecular proportion diagram. The field defined as Midas Pond Au-quartz veins also includes samples from the wall rock. Data for the Jacks Pond field and Tulks Hill mafic tuffs are from Evans (1986).

3.2).

7.2.4 PYRITE

Pyrite within the occurs as fine disseminations, coarse-grained patches and as single euhedral crystals up to 1 to 2 cm in diameter. As seen in thin section pyrite forms stringers which cross-cut the quartz veins. Patches and single crystals of pyrite occur along the vein margins.

7.2.5 MINOR MINERAL PHASES

Paragonite is commonly developed proximal to the vein margins. Small crystals of plagioclase (andesine ?) were observed in a couple of thin sections. The plagioclase occurs along the quartz vein margins and exhibits albite, pericline and Carlsbad twining.

Pyrophyllite and paragonite occur as small patches and wisps within and as fine stringers which cross-cut the quartz veins. Tourmaline occurs as tiny blue-green needles.

7.2.6 GOLD

Gold values are sporadic along the strike length of the mineralized zone (Figure 7.2). Selected gold assays include 7.3 g/t over 0.9 m from diamond drill hole GP-21 and 14.74 g/t over

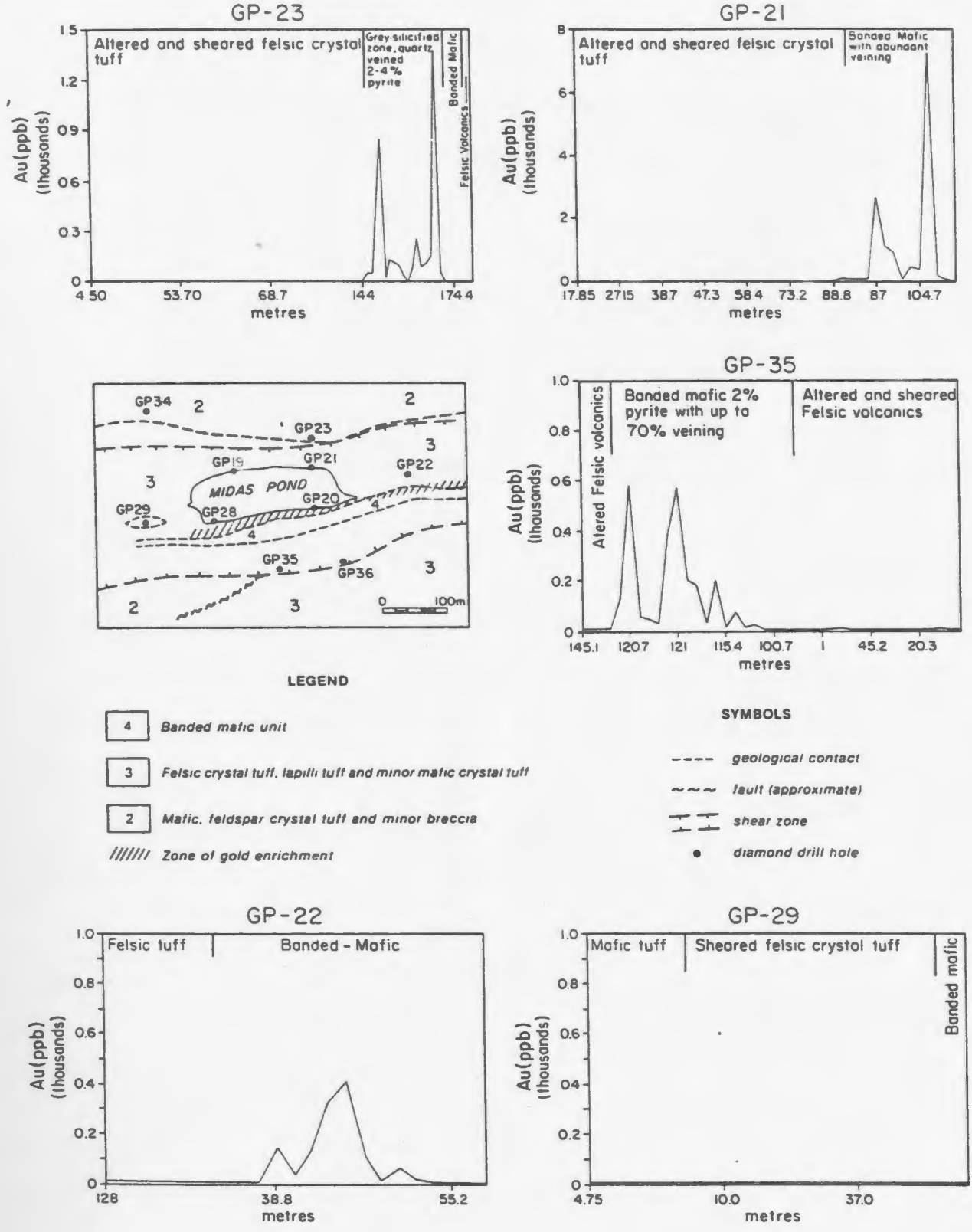

Figure 7.2 Drill sections showing the distribution of gold mineralization at Midas Pond. Also shown are the host rocks. All holes were drilled at approximately 45 degrees.

1.15 m in Trench 45+10 (Barbour et al., 1988). Background gold values in both mafic and felsic units outside of the mineralized zone are generally less than 5 ppb. Host rocks to the quartz vein have slightly elevated gold values associated with pyrite.

The gold is intimately associated with pyrite, and as such pyrite contents locally reflect the gold grade of the quartz veins. SEM analyses indicate that the gold occurs as: inclusions within pyrite; veinlets developed along fractures (Plate 7.6); and as patches developed along the margins of the pyrite grains (Plate 7.7).

The gold is generally pure, however minor gold tellurides (Plate 7.8) and electrum (Plate 7.9) are locally present (Figure 7.3). The silver content of the gold-rich zones is low and assay values for the quartz veins are generally on the order of 0.2 to 0.4 ppm. However, the section which assayed 7.3 g/t gold also contained 1.2 ppm silver.

7.3 ISOTOPIC STUDIES

Isotopic analyses were undertaken on galena, pyrite and carbonate separates from the auriferous quartz veins in an attempt to characterize the hydrothermal fluid and to discriminate between possible fluid source areas. Analytical procedures are outlined in Appendix II.

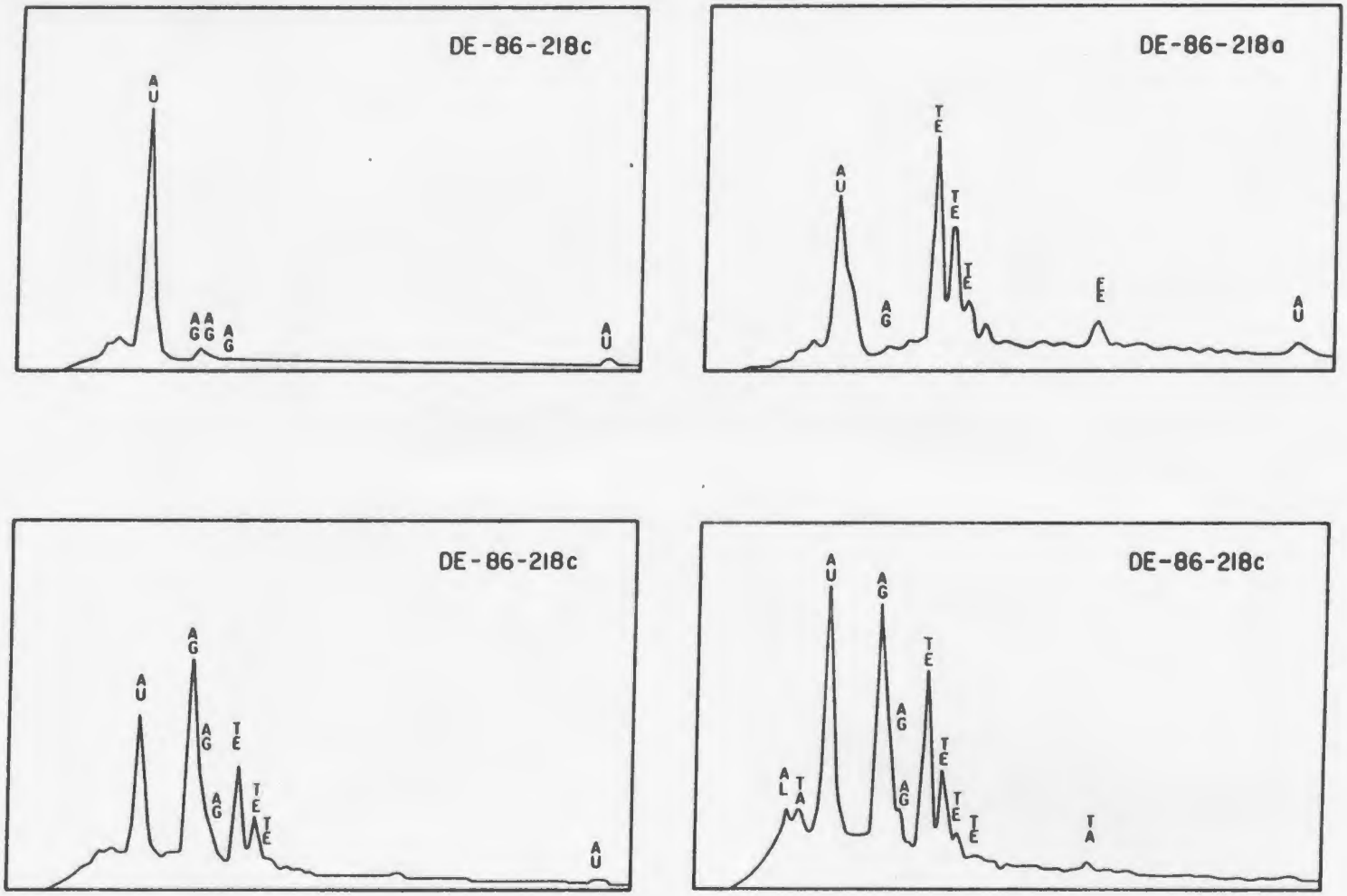

Figure 7.3 Scanning electron microscope (SEM) spectra of gold grains which exhibit the variation in gold mineralogy from the Midas Pond area (SEM operating techniques are outlined in Appendix 4).

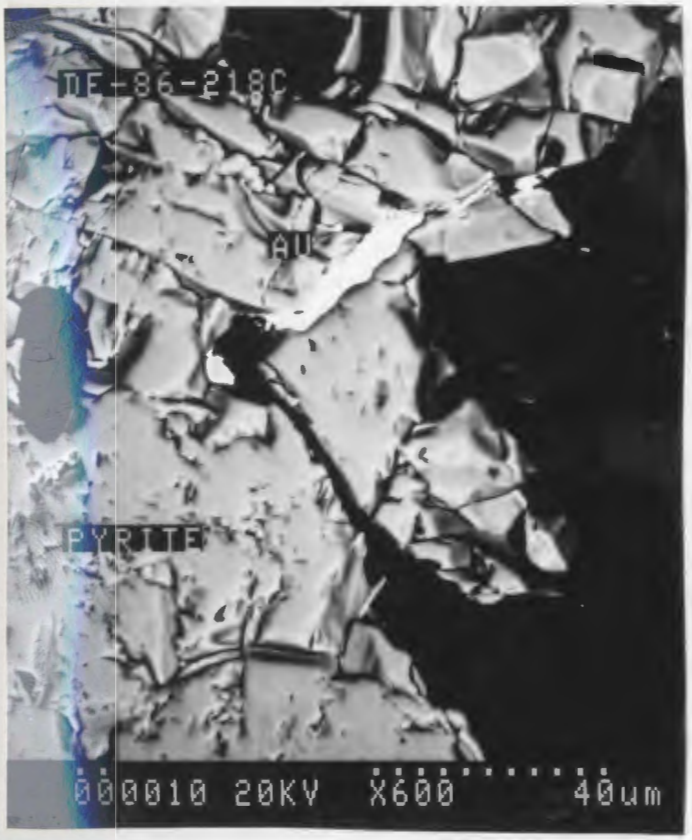

Plate 7.6 SEM backscatter photograph of gold developed along a fracture within a pyrite grain. Sample is from the vein shown in Plate 7.1.

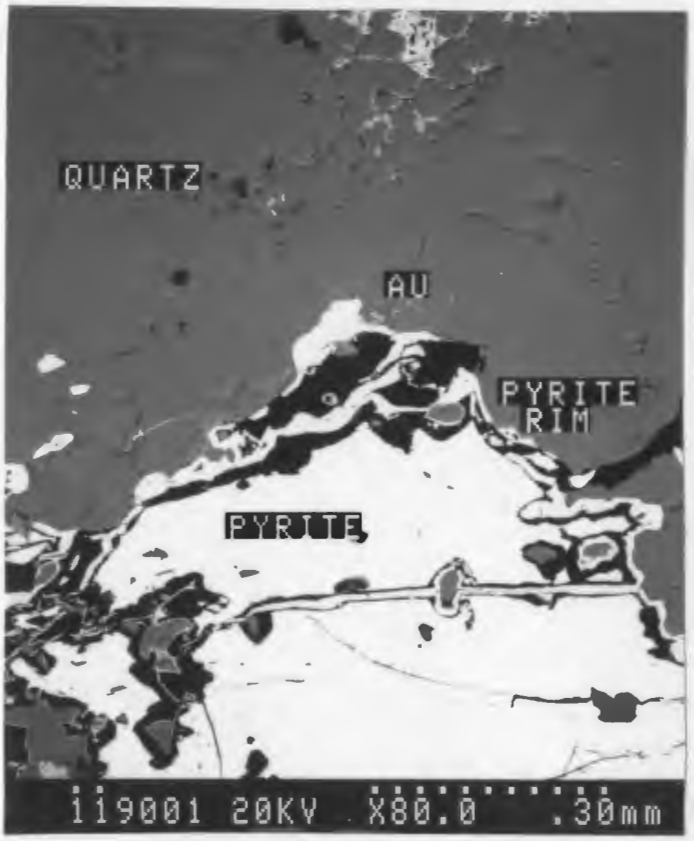

Plate 7.7 SEM backscatter photograph of gold, intergrown with pyrite, forming a rim around an earlier pyrite grain.

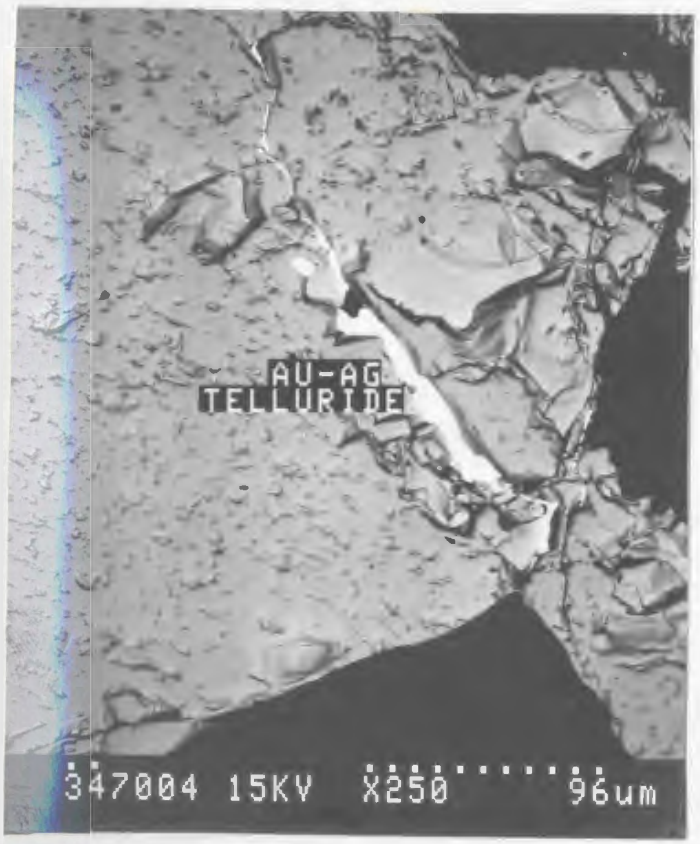

Plate 7.8 SEM backscatter photograph of a Au-Ag telluride mineral developed along a fracture in a pyrite grain.

Plate 7.9 SEM backscatter photograph of electrum developed along a fracture within a pyrite grain.

7.3.1 LEAD ISOTOPES

A small amount of galena and possibly sphalerite were observed in drill hole GP-26 (65.5m) . The galena occurs in a narrow quartz-carbonate vein which assayed 1350 ppb gold. This galena along with samples from the Road and West Tulks gold prospects, which also occur within the Victoria Lake Group, were collected for lead isotope analyses and compared with data obtained for a number of massive sulphide deposits (Table 7.2). The analyses were performed by Geospec Consultants Limited of Alberta.

The isotopic data (Table 7.2) define two distinct groups as the lode gold deposits are more radiogenic than the massive sulphides. Model lead ages (Figure 7.4), based on Stacey and Kramers (1975) for the massive sulphide deposits within the Victoria Lake Group are in general significantly younger than the precise U/Pb zircon ages (Evans et al., 1990) of the host rocks by approximately 100 Ma. Likewise interpreting model ages for the gold mineralization based on lead isotope data is just as tenuous. However, it is sufficient to say that the lode gold occurrences are indeed younger than the massive sulphide mineralization.

As can be seen from Figure 7.4 the lead from the Victoria Lake lode gold and the massive sulphide prospects have relatively similar $^{207}Pb/^{204}Pb$ ratios but the gold prospects have higher $^{206}Pb/^{204}Pb$ ratios relative to the massive sulphides. Higher

Prospect	Mineral	$^{206}Pb/^{204}Pb$	$^{207}Pb/^{204}Pb$	$^{208}Pb/^{204}Pb$	μ
Gold Mineralization					
West Tulks	Galena	18.226	15.598	38.074	9.71
Road Showing	Galena	18.206	15.575	37.965	9.61
Midas Pond	Galena	18.231	15.579	38.053	9.62
Volcanogenic Massive Sulphide Mineralization					
Side of the Hill (a)	Galena	18.156	15.584	37.954	9.67
Tulks Hill (a)	Galena	18.144	15.571	37.957	9.62
Side of the Hill (b)	Galena	18.287	15.581	38.097	9.62
Tulks Hill (b)	Galena	18.267	15.571	38.107	9.59

Table 7.2 Lead isotope data for gold and massive sulphide mineralization within the Victoria Lake Group. Isotopic values for Side of the Hill (b) and Tulks Hill (b) were calculated using the closed system evolution equations of Doe and Zartman (1979) (T_1 = 75 Ma). μ values were calulated using the model of Stacey and Kramer (1975). Data for Tulks Hill was taken from Swinden and Thorpe (1984).

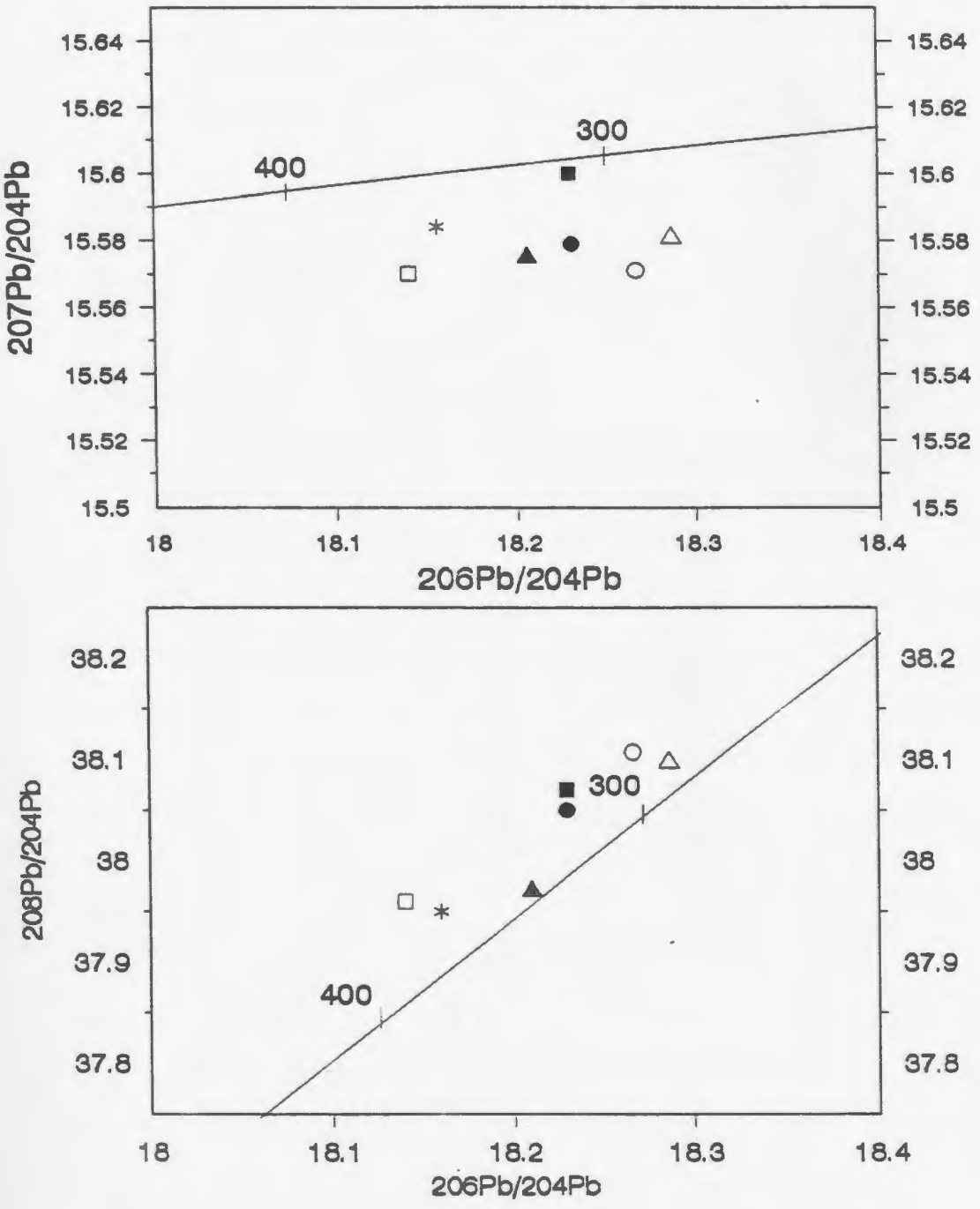

Figure 7.4 $^{207}Pb/^{204}Pb$ and $^{208}Pb/^{204}Pb$ versus $^{206}Pb/^{204}Pb$ diagram for selected lode gold (West Tulks ■ , Road Showing ▲, and Midas Pond ●) and volcanogenic massive sulphide prospects (Side of the Hill (a) *, Tulks Hill (a) □, Side of the Hill (b) △, and Tulks Hill (b) ○) within the Victoria Lake Group. Data for Tulks Hill, Burnt Pond and Tally Pond is from Swinden and Thorpe (1984).

$^{206}Pb/^{204}Pb$ ratios would be expected for the gold occurrences for two reasons: 1) the gold occurrences are younger than the volcanogenic massive sulphide mineralization; and 2) the isotopic source reservoirs were different for the two styles of mineralization.

The subseafloor setting of volcancgenic massive sulphide mineralization within the Victoria Lake Group and the importance of seawater in their formation indicates that its lead isotopic characteristics would be derived from island arc-type rocks and at fairly high crustal levels. The age of this mineralization is interpreted to coeval with the host lithologies which in the Tulks Hill volcanics have been dated at 498+6-4 Ma (Evans et al.,1990).

Regicnal interpretations (Evans et al., 1990) suggest that the gold mineralization within the Victoria Lake area is pre 400 Ma based on $^{40}Ar/^{39}Ar$ ages of sericite from hydrothermal alteration zones. Auriferous quartz veins located at the Valentine Lake prospect (Barbour, 1990) cut the Rogerson Lake conglomerate which is interpreted to be Silurian. Therefore, the age of gold mineralization within the Victoria Lake area appears to be approximately 75 Ma years younger than the volcanogenic massive sulphide deposits.

Using the closed-system evolution equations of Doe and Zartman

(1979) page 24, it is possible to calculate the lead isotopic ratios present at any given time assuming a constant source area (orogene). Calculations based on the isotopic ratios from the volcanogenic massive sulphide mineralization at 498 Ma produce a much more radiogenic lead at 425 Ma than the measured ratios for the gold occurrences (Table 7.2). This indicates the possibility of separate isotopic source reservoirs for the two styles of mineralization.

Lead isotopic studies of auriferous quartz veins at Cape Ray, Newfoundland (Wilton and Strong, 1986) and of carbonate-hosted deposits in western Newfoundland (Swinden et al., 1988b) suggest a Grenvillian crustal component in the derived lead. Grenvillian rocks are depleted in U/Pb relative Th/Pb, which results in relatively non-radiogenic lead (Doe and Zartman, 1979; Fletcher and Farquhar, 1982). Deep seismic studies indicate that Grenvillian crust may actually extend under a substantial portion of the Dunnage Zone (Keen et al., 1986). It is therefore quite plausible that the less radiogenic lead associated with the gold mineralization at Midas Pond could have been extracted from a mixed source which may have included Grenvillian crust.

7.3.2 SULPHUR ISOTOPES

Sulphur isotopic studies involve the examination of variations in $^{34}S/^{32}S$ ratios of sulphide minerals. Sulphur isotopic

compositions are expressed as a $\delta^{34}S$ value which is the $^{0}/_{00}$ per mil deviation of the $^{34}S/^{32}S$ ratio of the mineral relative from that of the Canyon Diablo meteorite standard (Ohmoto and Rye, 1979). Figure 7.5 summarizes sulphur isotopic variation in nature, sulphides from igneous systems cluster close to $^{0}/_{00}$.

Figure 7.6 is a compilation of average $\delta^{34}S$ values for sulphide minerals from a variety of lode gold deposits. The majority of Archean mesothermal gold deposits have $\delta^{34}S$ values between +1 to +9 per mil with most clustering between +1 to +6 per mil (Kerrich, 1989b). Sulphur of this composition would likely have been derived from a magmatic source or through dissolution and/or desulphidation of primary, or remobilized, magmatic sulphides. Large negative values for some Canadian and Australian deposits are attributed to oxidation of the hydrothermal fluids (Kerrich, 1989b).

Sulphur isotopic analyses from the Cape Ray gold deposits located in southwestern Newfoundland range between -5.2 to 6.9 per mil (Wilton and Strong, 1986). The sulphur is considered to be of magmatic (granitic) derivation.

Meguma Group lode gold deposits are unique with respect to their sulphur isotopic compositions (Kontak and Smith, 1989). $\delta^{34}S$ values range between 9 to 25 per mil which are considerably higher than typical auriferous quartz vein systems (Figure 7.6). Such

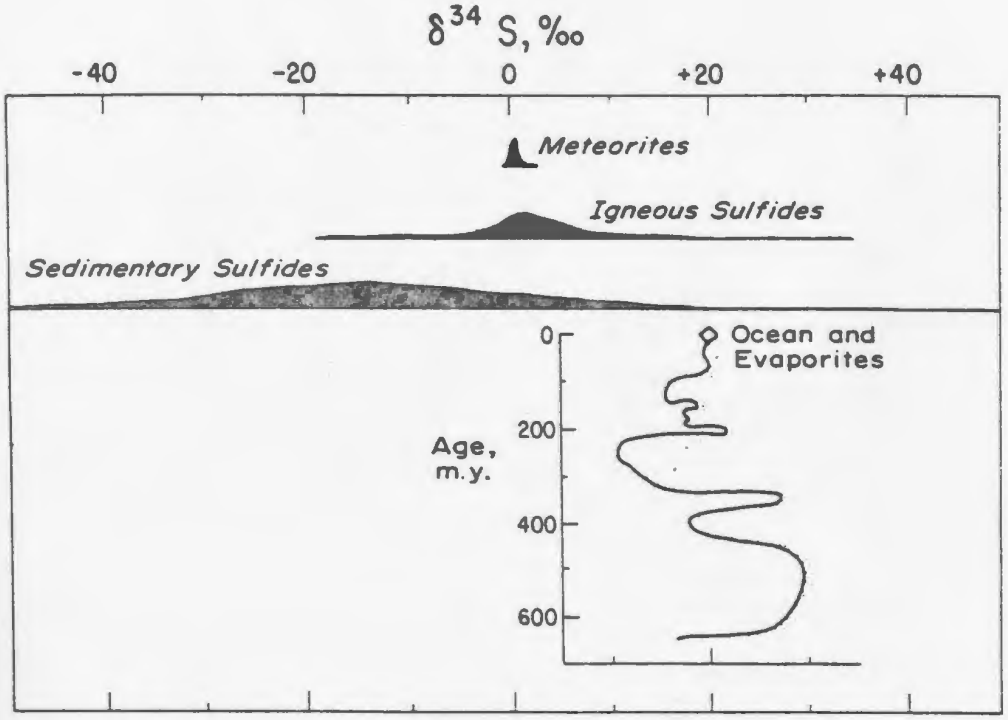

Figure 7.5 Sulphur isotopic variation in nature (from Ohmoto and Rye, 1979).

SAMPLE NUMBER	LOCATION	$\delta^{34}S$ RATIO
DE-86-119F	45+10W, 38+60N	+4.5 per mil
DE-86-157C	GP-35 129m	+4.6 per mil
DE-86-157D	GP-35 129m	+4.4 per mil

Table 7.3 $\delta^{34}S$ data for pyrite separates from auriferous quartz veins, Midas Pond.

extreme positive values are attributed to modification of the hydrothermal fluids during transport from the source area (Kontak and Smith, 1989). Sulphur isotopic values in the source area are considered to have been originally closer to 0 per mil.

$\delta^{34}S$ ratios in the Midas Pond pyrite samples collected from V_2 and V_3 veins (Table 7.3) are slightly enriched in the heavy sulphur isotope and have positive $\delta^{34}S$ values. These analyses are consistent with the data compiled for Archean and younger lode gold deposits (Kerrich, 1989b; Kontak and Smith, 1989) (Figure 7.6). The ratios appear to be comparable with sulphur derived from an igneous source, possibly by leaching of igneous sulphides.

Under acidic conditions an aqueous fluid could decompose igneous pyrite to produce H_2S. This is illustrated in the following equation.

$$3\ FeS_2 + 2\ H_2O + 6\ H^+ \rightarrow 3\ Fe^{2+} + 5\ H_2O + SO_2$$

The resulting hydrothermal fluid would have $\delta^{34}S$ values nearly identical to that of magmatic sulphur (Ohmoto and Rye, 1979). H_2S in the hydrothermal fluid would also be significant with respect to the transport of dissolved gold. A number of authors (Phillips and Groves, 1983; Seward, 1984) suggest that gold can be transported in hydrothermal fluids as $Au(HS)^{2-}$ complexes at low temperatures.

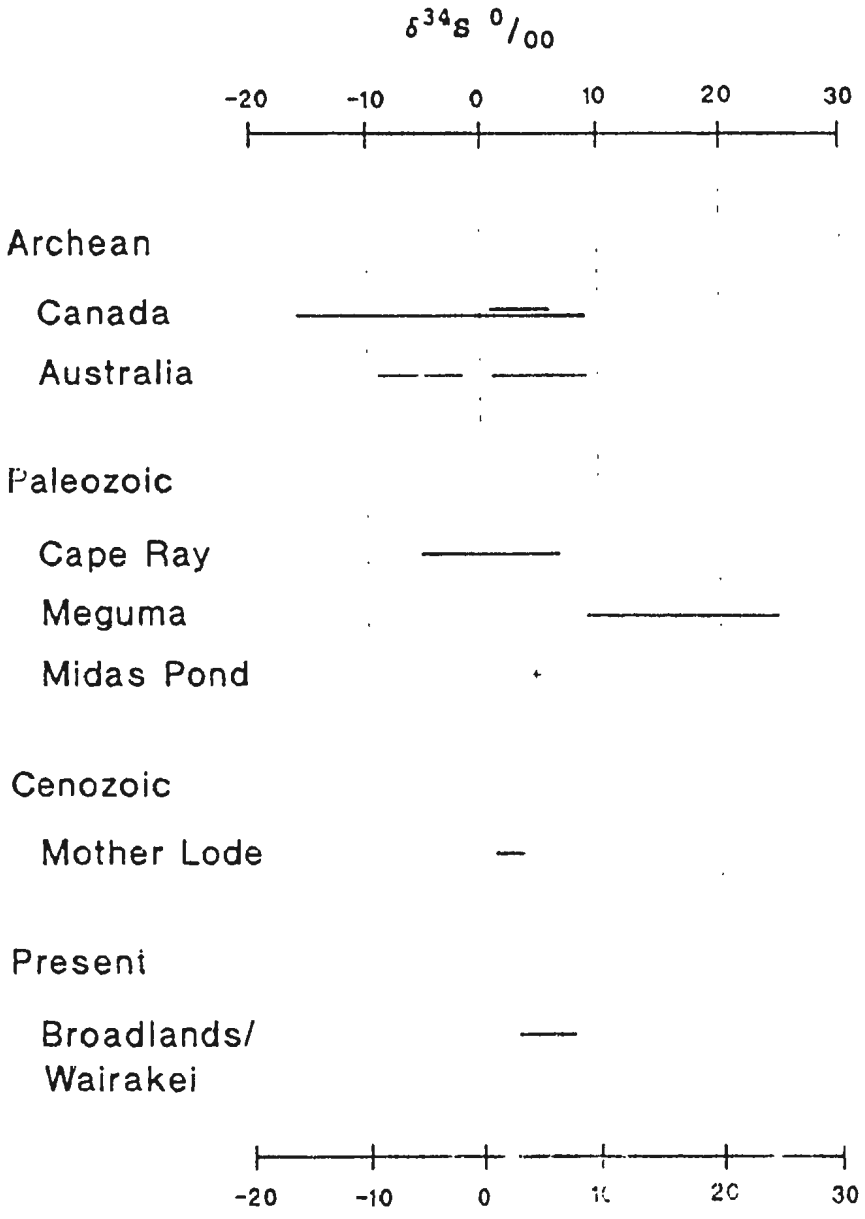

Figure 7.6 Compilation of average $\delta^{34}S$ values for Archean, Paleozoic and Cenozoic lode gold deposits and the Broadlands epithermal system (data from compilation of Kerrich (1989b) and Kontak and Smith (1989). Data for the Cape Ray deposits is taken from Wilton and Strong (1986).

7.3.3 CARBON/OXYGEN ISOTOPES

In carbon isotopic studies two isotopes, ^{13}C and ^{12}C , are measured. The ratio of $^{13}C/^{12}C$ is compared relative to a known standard (PDB) (Ohmoto and Rye, 1979) and is reported as $\delta^{13}C$. Carbon isotopes derived from igneous sources have an average $\delta^{13}C$ value of -5.5 per mil. However, because of the possible large isotopic fractionation between oxidized and reduced carbon species there can be significant local variation in the $\delta^{13}C$ values. The proportions of oxidized and reduced species in the hydrothermal fluid is affected by changes in the physiochemical conditions at the time of carbonate precipitation (Ohmoto and Rye, 1979)

Oxygen isotopic data is reported as $\delta^{18}O$ and this value is obtained as follows:

$$\delta^{18}O = \left(\frac{R_{sample}}{R_{SMOW}} - 1\right) 1000$$

where R_{sample} is $^{18}O/^{16}O$ of the sample and R_{SMOW} is Standard Mean Ocean Water (Taylor, 1979).

Lode gold deposits within Archean greenstone belts and Phanerozoic mesothermal systems worldwide are characterized by abundant, typically Fe-rich, hydrothermal carbonate (Kerrich, 1989a). To form carbonate minerals, the hydrothermal fluid must contain an oxidized carbon species such as CO_2 (Ohmoto and Rye, 1979). The carbonate is thought to form through the interaction of

wallrock Ca, Fe, Mg, Mn-bearing silicate minerals with the CO_2-rich hydrothermal fluids.

The source of these CO_2-rich fluids is controversial and a number of theories have emerged with respect to possible fluid sources. These sources include: 1) mantle; 2) magmatic; 3) metamorphism (oxidation of reduced carbon such as graphite); and 4) leaching of pre-existing sedimentary and igneous carbonates by hydrothermal fluids (Ohmoto and Rye, 1979; and see review given by Kerrich, 1989a; 1989b). Figure 7.7 illustrates carbon isotopic variation in nature. A thorough overview of carbon isotopic systematics is given by Kerrich (1989b) and based on this review he indicates that the source, or sources, of carbon cannot be resolved with certainty.

Most volcanic and plutonic rocks have $\delta^{18}O$ values of 5.5 to 10.0 per mil (Taylor, 1979). Regional metamorphism produces fluids which have $\delta^{18}O$ values of 5 to 25 per mil. This wide range of values reflects the fact that fluids derived from metamorphosed sedimentary and igneous rocks tend to preserve the oxygen isotopic characteristics of these rocks (Taylor, 1979). Metamorphism of igneous rocks, sandstones, greywackes, arkoses and volcanogenic sedimentary rocks tend to produce fluids with $\delta^{18}O$ values of 5 to 13 per mil.

Kerrich (1989b) defined the range of $\delta^{13}C$ and $\delta^{18}O$ values for

a number of Archean and Phanerozoic mesothermal gold deposits as being between -9 to 0.4 per mil and 9.1 to 15.4 per mil respectively. He states that on a deposit scale there is generally a tight clustering of $\delta^{13}C$ values which suggests that the ore forming fluids had uniform carbon isotopic compositions within individual deposits. At larger scales variations in the carbon isotopic composition of the source rocks is reflected in differences in average $\delta^{13}C$ values between deposits.

Isotopic analyses of ankerite from the Stog'er Tight gold prospect on the Baie Verte Peninsula indicate a range in $\delta^{13}C$ and $\delta^{18}O$ values of -5.0 to -6.5 and +11 to +12 per mil respectively (Ramezani et al., 1992). These values were considered to be typical of Archean and younger mesothermal gold deposits.

Fe-carbonate mineral separates from Midas Pond have $\delta^{13}C$ and $\delta^{18}O$ values ranging from -8.9 to -4.2 per mil and 12.1 to 17.6 per mil respectively (Table 7.4). Samples DE-87-23 (drill hole GP-23) and DE-87-57 (drill hole GP-25) were collected from quartz carbonate veins developed in the altered felsic volcanic rocks which form the structural hanging wall to the mineralized zone. These two samples have $\delta^{13}C$ and $\delta^{18}O$ values which plot within the Archean-Phanerozoic mesothermal gold field defined by Kerrich (1989b) (Figure 7.8). The samples also fall within the range of isotopic data presented by Wilton et al. (1989,1990) for carbonate samples collected from gold-bearing vein systems within the

Victoria Lake area. These two samples, together with those of Wilton et al. (1989,1990), cluster around a $\delta^{13}C$ value of -5 per mil which suggests possible leaching of carbon from pre-existing igneous or metamorphic carbonate. The $\delta^{18}O$ values for the these two samples indicates a metamorphic source for the hydrothermal fluids.

Sample DE-87-29 plots outside the isotopic field defined by Kerrich (1989b) (Figure 7.8). This sample was collected from an auriferous quartz-carbonate vein which cuts the Banded Mafic unit in drill hole GP-21. Variations in the physiochemical conditions of the hydrothermal fluid as discussed above may explain the isotopic variation observed within this sample. Alternatively the lower $\delta^{13}C$ and $\delta^{18}O$ values for this sample may indicate an element of isotopic exchange between the hydrothermal fluid and silicate and pre-existing carbonate minerals within the Banded Mafic unit.

7.4 SUMMARY

Gold mineralization at Midas Pond occurs within structurally controlled quartz veins developed along the contact between the Banded mafic unit and the structurally overlying felsic volcanic rocks. Three sets of auriferous quartz veins, genetically related to variations in the structural regime active within the shear zone are present. The origin of these veins was addressed in Chapter 4.

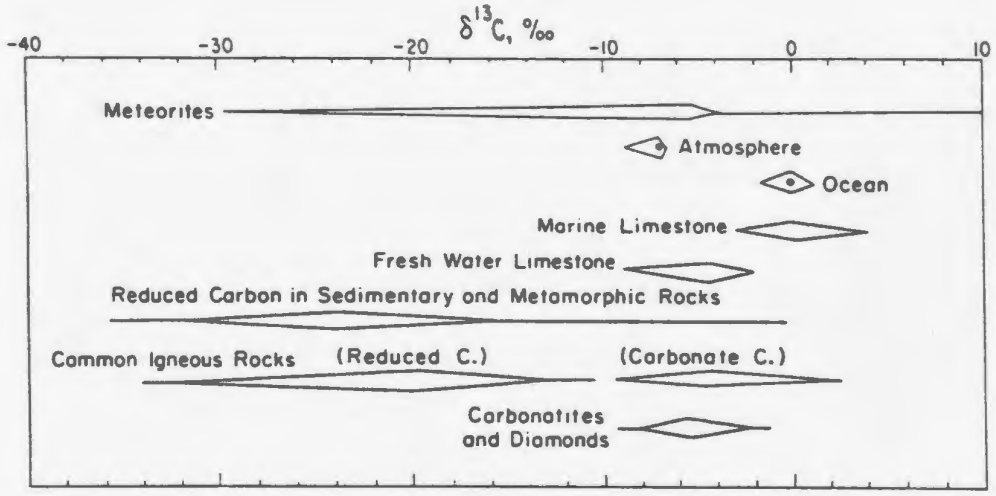

Figure 7.7 Carbon isotopic variation in nature (from Ohmoto and Rye, 1979).

SAMPLE NUMBER	LOCATION	$\delta^{13}C$ (PDB)	$\delta^{18}O$ (SMOW)
DE-87-23	GP-23 50.6m	-4.702	+12.115
DE-87-29	GP-21 91.7m	-8.917	+17.634
DE-87-57	GP-25 47.5m	-4.181	+12.212

Table 7.4 $\delta^{13}C$ and $\delta^{18}O$ data for Fe-carbonate separates from the auriferous quartz veins, Midas Pond.

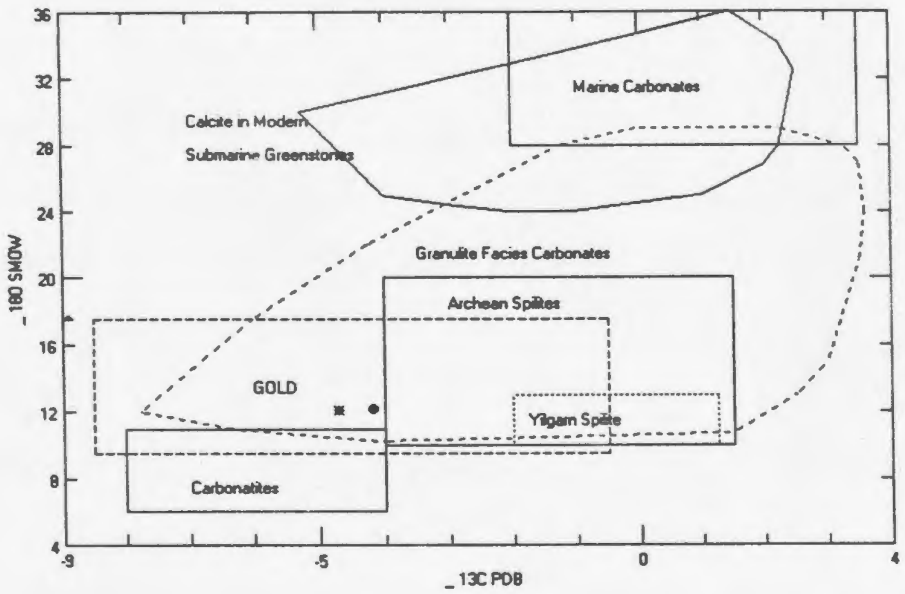

Figure 7.8 Plot of $\delta^{18}O$ vs $\delta^{13}C$ for lode gold mineralization within the Victoria Lake Group. The isotope field defined by Kerrich (1989b) is based on average values for Archean and Phanerozoic mesothermal gold deposits worldwide. * DE-87-23, ▲ DE-87-29, ○ DE-87-57 • other Victoria Lake Group lode gold occurrences (from Wilton et al. 1990).

The quartz veins contain pyrite, Fe-carbonate (ferroan dolomite ?), paragonite, chlorite, minor pyrophyllite and plagioclase. The chlorite within the mineralized zone at Midas Pond is more Mg-rich than chlorite from outside the zone. This maybe the result of competition for Fe^{2+} between pyrite, carbonate and chlorite which were forming within the veins at approximately the same time. Therefore, the chlorite would be relatively more enriched in Mg relative to Fe, since Fe was being deposited in pyrite and carbonate "sinks".

At Midas Pond gold was precipitated as the hydrothermal fluids came in contact with the structurally prepared, relatively Fe-rich Banded Mafic unit. The gold is intimately associated with the pyrite and occurs as tiny inclusions, small fracture-controlled veinlets and as coatings around pyrite grains. Coarse pyrite grains developed within the host rocks to the quartz veins also carry anomalous gold.

Isotopic studies conducted on galena, pyrite and Fe-carbonate separates from the Midas Pond auriferous quartz veins suggests a deep seated, metamorphic origin for the hydrothermal fluids based on the following:

1) Lead isotopic analyses suggest a possible Grenvillian crustal influence;

2) $\delta^{34}S$ ratios are comparable to sulphur leached from pre-existing igneous sulphides; and,

3) $\delta^{18}O$ and $\delta^{13}C$ ratios are typical of carbonate produced through the leaching of igneous rocks by metamorphic fluids.

CHAPTER 8

SUMMARY AND CONCLUSIONS

8.1 INTRODUCTION

The Midas Pond prospect is one of a number of significant gold occurrences located within the southwest portion of the Victoria Lake Group. These occurrences, discussed in Chapter 2, are either hosted by shear zones or rocks deformed by nearby shears. This chapter will review models of lode gold mineralization and summarize and characterize the Midas Pond prospect.

8.2 REVIEW OF MESOTHERMAL LODE GOLD MINERALIZATION

Mesothermal lode gold occurrences, particularly within the Archean, are an extensively studied and best documented style of gold deposit. Recent workers (including. Colvine et al., 1984, 1988; Groves and Phillips, 1987; Groves et al., 1988; Barley et al., 1989; Barley and Groves, 1990; Burrows et al., 1986; Colvine, 1989; Eisenlohr et al., 1989; Hodgson, 1989; Kerrich, 1989a; Kerrich, 1989b; Kerrich and Feng, 1992) have compiled tremendous amounts of data for this style of mineralization which they have combined with their own detailed structural and isotopic studies to produce metallogenic models. These models although differing with respect to the original source of the hydrothermal fluids are all similar with regards to the setting and style of the lode gold

mineralization. The fundamental characteristics of mesothermal gold systems as defined by the authors listed above are reveiwed in Table 8.1.

8.3 MIDAS POND, SUMMARY AND MODEL

The Victoria Lake Group is a structurally complex assemblage of Cambro-Ordovician island arc and back arc volcanic, volcaniclastic and epiclastic rocks (Evans et al, 1990). The volcanic rocks form two linear belts referred to as the Tally Pond and Tulks Hill volcanics. The Midas Pond gold prospect is located within the southern extremity of the Tulks Hill volcanics and rocks in the Midas Pond area are typical of the Tulks Hill volcanics both lithologically and chemically. They comprise waterlain felsic and mafic volcanic rocks that have been metamorphosed in the lower greenschist facies and subjected to inhomogeneous deformation and metasomatism. Aspects of the alteration and mineralization are reviewed in Table 8.2.

The Midas Pond prospect is typical of the pyritiferous quartz vein class of gold mineralization developed with the Victoria lake Group. A comparision of Tables 8.1 and 8.2 indicates that the Midas Pond prospect exhibits many of the features that are typical of the mesothermal-style of lode gold mineralization. These similarities include:

MESOTHERMAL VEINS
SETTING -spatially-related to major structural breaks formed in part by tectonic shortening -localized along 2nd order or higher structures where brittle/ductile deformation predominates -irregular distribution of Au deposits along these structures indicating focused fluid flow due to local extensional features -shear zone must exhibit little displacement, be active and permeable for an extended period and open to a large volume of fluids -late syn to post regional metamorphism
HOST ROCKS -occur in all rock types; mafic rocks (ie. Fe-rich) favoured -some are spatially associated with felsic intrusives
VEIN GEOMETRY -simple shear strain predominates resulting in (1) shear fracture veins within R (low angle Riedel shears), R' (high angle Riedel shears), P (pressure shears), D (central shears)shears (2) extensional fractures, T (tensional) veins -geometry of veins controlled by shear zone and rheology and orientation of the host lithology -1-10s of m wide with strike lengths of 10s -100s of m -part of larger anastomosing structure (kms long, up to 2 km deep) with individual shears hosting a vein system -vein formation and deformation synchronous -overall vertical extent of mineralizing system maybe on the order of 10-15 km deep
VEIN CHARACTERISTICS -coarse, milky white to grey quartz, often cherty-like -laminated indicating multiple fluid injections -gangue minerals (albite, Fe-carbonate, tourmaline, sericite, chlorite, pyrite, pyrrhotite, arsenopyrite, galena, sphalerite, chalcopyrite, molybdenite, stibnite, tellurides and tungsten) -CO_2-rich, low salinity fluid inclusions.
ALTERATION -an extensive outer chlorite/calcite zone, often linear shaped due to shear zone control -inner carbonate zone comprised of Fe-dolomite, sericite, pyrite and quartz -forms haloes 1 to 10s of m around vein systems, often overlap and merge to produce a broad zone -intensity of Fe-carbonate alteration depends on the availability of Fe in the host rock

Table 8.1 Summary of the major characteristics of Archean lode gold mineralization.

MIDAS POND GOLD PROSPECT
SETTING -localized within a 200 m wide brittle-ductile shear zone -the shear zone is a D_1 structure considered to be a splay of the Tulks Valley fault -D_2 deformation resulted in flexuring (Z-shaped flexures) of the shear zone
HOST ROCKS -the auriferous quartz veins are localized along the contact between the andesitic Banded Mafic unit and the structurally overlying altered rhyodacitic rocks -the rhyodacites originally had low concentrations of K (typical of island arcs)
STRUCTURES CONTROLLING MINERALIZATION -three auriferous vein sets are present: V_1 boudinaged veins developed parallel to the shear zone fabric (C-shears) V_{2-3} extensional fracture veins related to D_2 deformation, these veins locally contain comb structures and quartz lined cavities
ALTERATION -broad halo, dominated by advanced argillic alteration and overprinted by sulphidation and carbonitization, intensifies proximal to the auriferous quartz veins -alteration assemblages include quartz, pyrophyllite, mica, plagioclase, chlorite, pyrite, Fe-carbonate and leucoxene -distribution controlled by the shear zone with shearing and alteration overlapping -alteration resulted in a remobilization of silica and sodium and the addition of F, S, and C.
VEIN CHARACTERISTICS -coarse, milky white veins with abundant CO_2-fluid inclusions V_1 veins contain stringers of pyrophyllite and mica, V_{2-3} veins locally contain altered blocks of wall rock. -gangue minerals include: Fe-carbonate, pyrite, chlorite, plagioclase, paragonite and tourmaline
GOLD MINERALIZATION -mainly elemental but minor tellurides and electrum are present -precipitated on pre-existing and similtaneously crystallizing pyrite
FLUID CHARACTERISTICS -250-300°C -initially slightly acidic to produce argillic alteration -CO_2-rich, suggests metamorphic source -contained F, however, fluorite is lacking in the quartz veins, the source of this F is unknown -Pb isotopes suggest that the veins younger than, and accessed a fluid source different from the volcanogenic massive sulphide mineralization -C, O and S isotopic analyses indicate either a magmatic or metamorphic source -gold possibly carried as a $Au(HS)^{2-}$ complex

Table 8.2 Summary of the Midas Pond gold prospect.

1) A spatial association with brittle-ductile and ductile shear zones. The larger, regionally extensive ductile shears are considered to form conduits which focus large volumes of fluid from deep crustal sources.

2) The alteration and mineralization developed at Midas Pond appears to be late-syn regional metamorphism and deformation.

3) A spatial association with Fe-rich rocks. Pyrite, with which the gold is associated, developed as a result of the the breakdown of Fe-silicate minerals in the Banded Mafic unit.

4) An extensive Fe-carbonate and pyrite alteration halo.

5) The gold occurs within quartz veins which are structurally controlled.

6) Abundant CO_2-rich fluid inclusions within the quartz veins.

7) A metamorphic source for the hydrothermal fluids involving elements of island arc and possible Grenvillian crust is favoured. Metamorphic dehydration and decarbonation reactions would provide both the abundant CO_2, as observered in the fluid inclusions, and account for the carbon and sulphur isotopic ratios.

Based on this comparsion the Midas Pond prospect is interpreted to be a mesothermal lode gold prospect. The presence of comb structures and vuggy cavities in the mineralized quartz

veins may argue for a fairly shallow mesothermal system. A schematic model outlining the formation of the alteration and mineralization at Midas Pond is shown in Figure 8.1. This model involves the focusing of CO_2-rich fluids, most likely of metamorphic derivation, into deep seated, regionally extensive ductile shear zone. These fluids are further focused into secondary structures where, given the right combination of physiochemical and structural conditions, alteration and mineralization occurs. Mafic rocks because of their iron rich character are a favoured site for gold precipitation. Fe derived form the breakdown of mafic minerals combines with sulphur from the hydrothermal fluids to produce sulphide minerals (sulphidation). Sulphide minerals, particularly pyrite, are important sites for gold precipitation (Colvine et al., 1984).

The widespread argillic alteration (kaolinte, pyrophyllite and mica) associated with the Midas Pond prospect, while not typical of mesothermal gold deposits in general, is one of the most prevalent styles of alteration associated with mineral deposits in acidic rocks (Evans, 1980). At Midas Pond felsic volcanic rocks with low concentrations of K, Fe and Mg undoubtly influenced the style of alteration developed within the shear zone. This style of alteration may also indicate that the mineralizing system was fairly shallow, perhaps transitional between between mesothermal and epithermal.

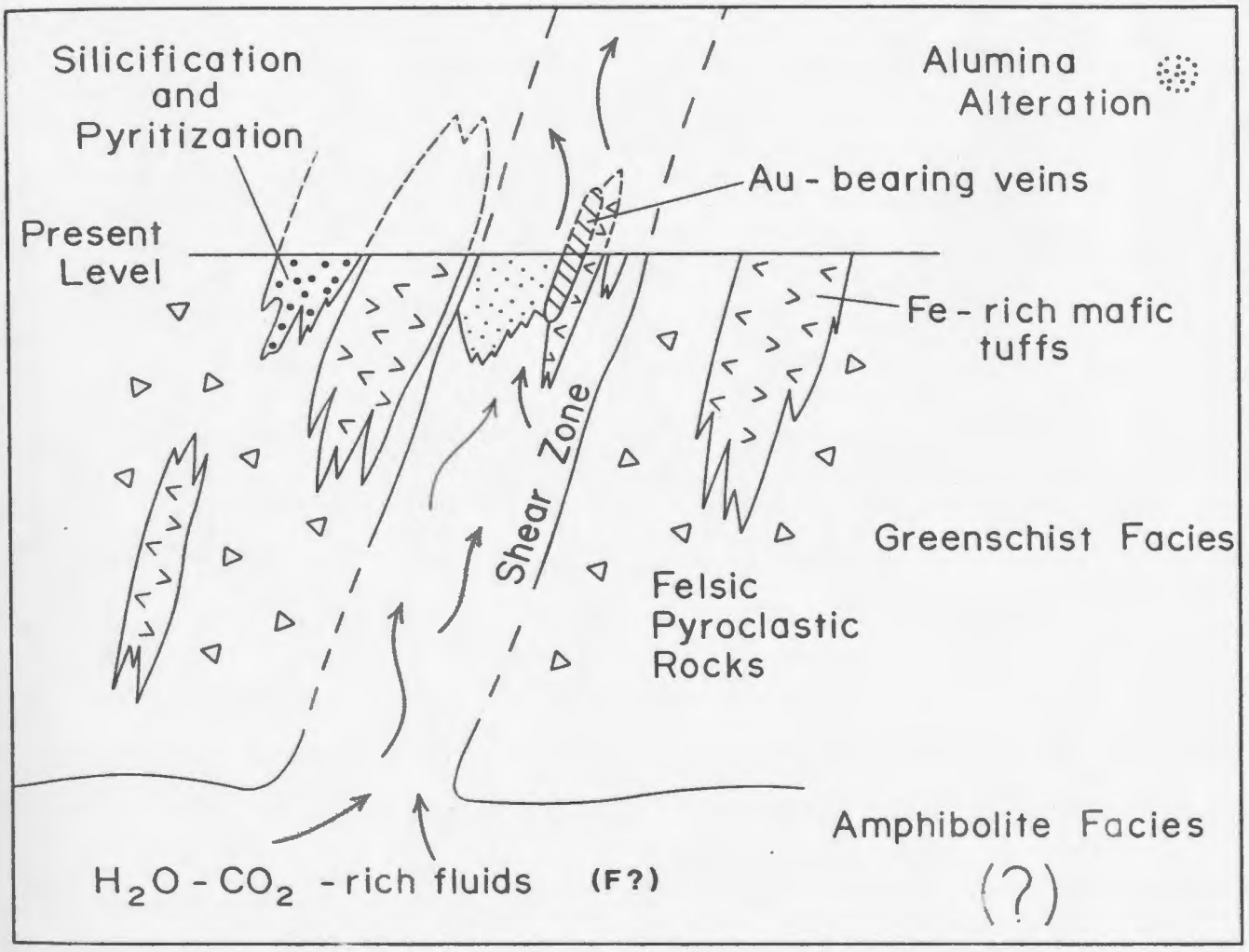

Figure 8.1 Schematic model for the development of alteration and gold mineralization at Midas Pond.

The presence of fluorite within the alteration zone at Midas Pond is an enigma. The lack of fluorite in the mineralized veins suggests that either F solubility was unaffected during vein formation or that the fluids responsible for the veins contained no F. If the latter is the case, then the fluorite may have already been present when the veins were formed suggesting the possibility of a two stage alteration mineralizing event.

8.4 REGIONAL GOLD MODEL

Gold mineralization within the Victoria Lake area is considered to be epigenetic and as discussed in Chapter 2 can be subdivided into five subclasses. This mineralization occurs in a wide range of rock types of widely varying age, from Cambro-Ordovician at Midas Pond, to the Silurian (?) cover sequence at Valentine Lake. The gold appears to be restricted to the more deformed sections of the group, particularly the southern portion of the Tulks Hill volcanics (Figure 8.2). Deformation would create an effective plumbing system which would facilitate fluid migration.

Regional U/Pb age dating studies (Dunning et al., 1990) defined the widespread, penetrative regional deformation, metamorphism, batholith emplacement and subaerial volcanicity as the product of a Silurian orgeny. The younger limit for this regional deformation and metamorphism is defined as 396 +6/-3 Ma,

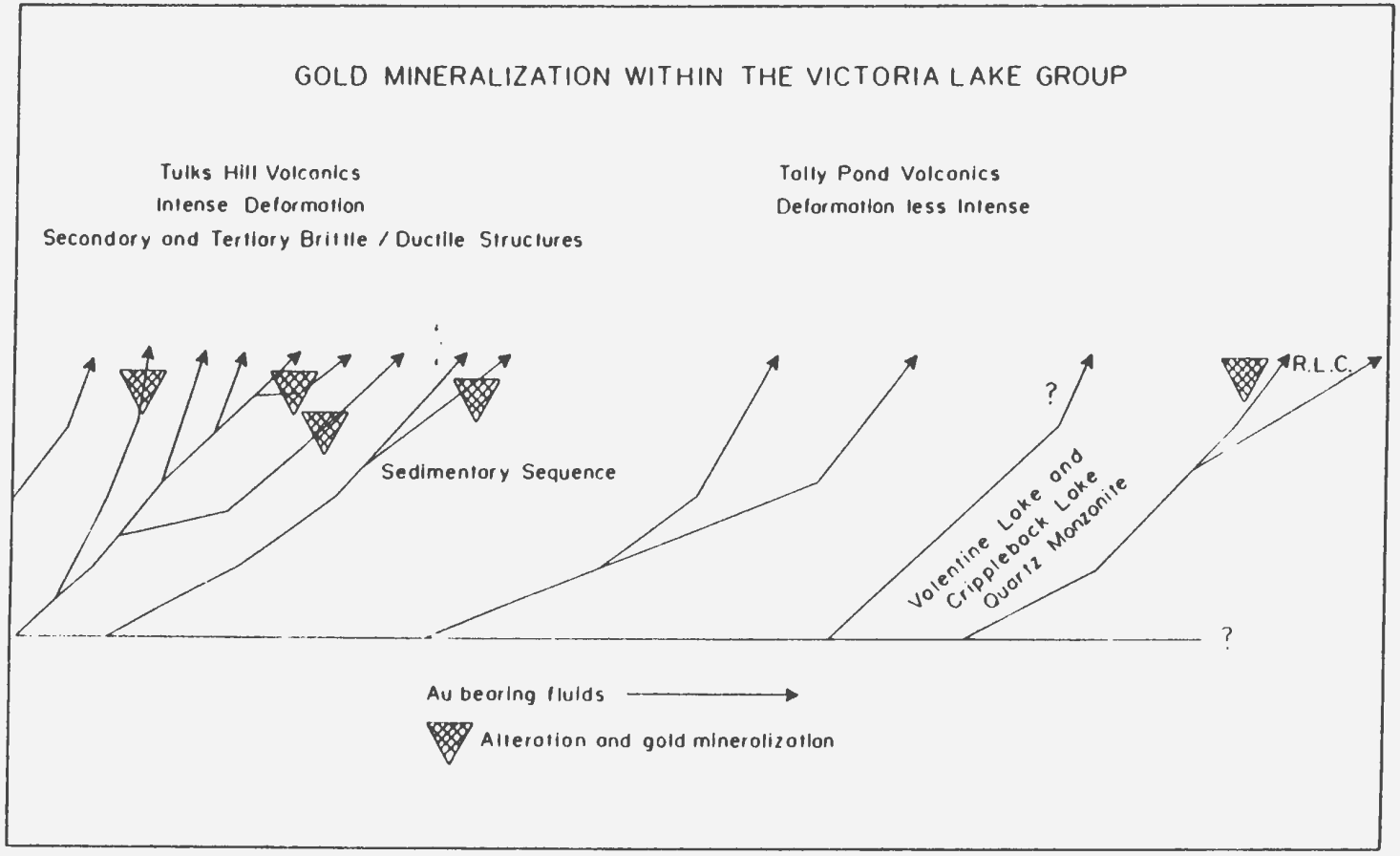

Figure 8.2 Gold mineralization model within the Victoria lake area (after Evans et al., 1990). Auriferous fluids migrated upwards through the ductile shears and were focused into secondary and tertiary brittle-ductile structures where alteration and mineralization developed.

the age of a granite from the North Bay Granite Suite. As suggested previously, a possible minimum age for deformation within the Victoria Lake Group, based on $^{40}Ar/^{39}Ar$ dating, is in the range of 395 to 380 Ma (Evans et al. 1990). This deformation roughly coincides with the upper limit defined by Dunning et al. (1990). Within the Victoria Lake area there is a spatial association between gold and regionally extensive linear structures. Some of these structures are interpreted to be related to southeast-directed thrusting active during regional deformation. If the gold mineralization is related to this deformational event and if, as appears to be typical of mesothermal systems in general, the gold is late syn- to post peak regional metamorphism then these ages would provide a minimum albeit poorly constrained age for the gold mineralization.

8.5 UNRESOLVED QUESTIONS

1) What is the sense of shear movement within the Midas Pond shear zone?

2) What is the temporal relationship between D_1 and D_2; are they related or are they separate deformational events? If so what is the age of D_2?

3) What is the temporal relationship between V_1 and V_2 and V_3 veins? How long was the system active?

4) What is the age of the gold mineralization at Midas Pond?

5) What is the protolith to the Banded mafic unit? Lithologically it is considered to have been a pyroclastic breccia comprised of felsic fragments in a mafic matrix, however, geochemically it bears no direct relationship to either the mafic or felsic rocks. Compositionally the unit can be classifed as andesitic.

6) What is the source and significance of the fluorite developed within the altered felsic rocks?

7) Do quartz vein shoots exist along the flexure hinges and if so how are they oriented?

REFERENCES

Barbour, D.M.
1990: Valentine Lake gold prospect. In Metallogenic framework of base and precious metal deposits, central and western Newfoundland. Edited by H.S. Swinden, D.T.W. Evans and B.F. Kean. Eighth IAGOD Symposium Field Trip Guidebook. Geological Survey of Canada, Open File 2156, pages 73-76.

Barbour, D.M. and Thurlow, J.G.
1982: Case histories of two massive sulphide discoveries in central Newfoundland. In Prospecting in areas of glaciated terrain. Edited by P.H. Davenport. Canadian Institute of Mining and Metallurgy Geology Division, Montreal, pages 300-320.

Barbour, D.M., Desnoyers, D.W., Gubins, A., McKenzie, C.B., Thurlow, J.G. and Woods, G.
1988: Assessment report on geological, geochemical, geophysical and diamond drilling exploration for 1987 submission on Reid Lots 227-229, 231-235 and 247 and Crown Lease Lot B in the Valentine Lake, Tulks River, Victoria River and Horseshoe Pond areas, Newfoundland. BP Resources Canada Limited, Unpublished report, 1368 pages.

Barley, M.E., Eisenlohr, B.N., Groves, D.I., Perring, C.S. and Vearncombe, J.R.
1989: Late Archean convergent margin tectonics and gold mineralization: A new look at the Norseman-Wiluna Belt, Western Australia. Geology, Volume 17, pages 826-829.

Barley, M.E. and Groves, D.I.
1990: Mesothermal gold mineralization in the Yilgarn Craton, Western Australia, the result of late Archean convergent tectonics? Chronique de la recherche miniere, Number 498, pages 3-13.

Barnes, H.L.
1979: Solubilities of ore minerals. In Geochemistry of Hydrothermal Ore Deposits, Second Edition. Edited by H.L. Barnes. A Wiley-Interscience Publication, John Wiley and Sons, pages 404-460.

Belt, E.S.
1969: Newfoundland Carboniferous stratigraphy and its relation to the Maritimes and Ireland. In North Atlantic - Geology and Continental Drift. Edited by M. Kay. American Association of Petroleum Geologists, Memoir 12, pages 734-735.

Bence, A.E. and Albee, A.L.
1968: Empirical correction factors for the electron microanalysis of silicates and oxides. Journal of Geology, Volume 76, pages 382-403.

Berthe, D., Choukroune, P., and Jegouzo, P.
1979: Orthogneiss, mylonite and non-coaxial deformation of granites: the example of the South Armoricain shear zone. Journal of Structural Geology, Volume 1, pages 31-42.

Besaw, D.M.
1972: Geology of Halfway Pond area, central Newfoundland: Unpublished B.Sc. thesis, Memorial University of Newfoundland, St. John's.

Blackwood, R.F.
1982: Geology of the Gander Lake (2D/15) and Gander River (2D/2) area: Nfld. Dept. Mines and Energy, Mineral Development Division, Report 82-4, 56 pages.

1985: Geology of the Grey River area, southwest coast of Newfoundland. In Current Research, Newfoundland Department of Mines and Energy, Mineral Development Division, Report 85-1, pages 617-629.

Brown, N.E.
1952: Geology of the Buchans Junction area, Newfoundland. Unpublished M.Sc. thesis, McGill University, Montreal, Quebec, 83 pages.

Burrows, D.R., Wood, P.C. and Spooner, E.T.C.
1986: Carbon isotope evidence for a magmatic origin for Archean gold-quartz vein ore deposits. Nature, Volume 321, pages 851-854.

Bursnall, J.T.
1989: Introduction: Review of mechanical principles, deformation mechanism and shear zone rocks. In Mineralization and Shear Zones. Edited by J.T Bursnall. Geological Association of Canada, Short Course Notes, Volume 6, pages 1-30.

Clarke, D.
1990: Newpet: geochemical data handling and plotting computer program. Memorial University of Newfoundland, Centre for Earth Resources Research.

Collins, M.J.
1964: Geology of Jacks Pond area. Unpublished B.Sc. thesis Memorial University of Newfoundland, St.John's, 24 pages.

Colman-Sadd, S.P.
1980: Geology of south-central Newfoundland and evolution of the eastern margin of Iapetus. American Journal of Science, Volume 280, pages 991-1017.

1987: Geology of the Snowshoe Pond (12A/7) map area. In Current Research. Newfoundland department of Mines and Energy, Mineral Development Division, Report 88-1, pages 127-134.

Colman-Sadd, S.P., and Swinden, H.S.
1984: A tectonic window in Central Newfoundland? Geological evidence that the Appalachian Dunnage Zone may be allochthonous. Canadian Journal of Earth Sciences, Volume 21, pages 1349-1367.

Colvine, A.C.
1989: An empirical model for the formation of Archean gold deposits: products of final cratonization of the Superior Province, Canada. In Geology of Gold Deposits: The Prospective in 1988. Edited by R.R. Keays, W.R.H. Ramsay and D.I. Groves. Economic Geology Monograph Six, pages 37-54.

Colvine, A.C., Andrews, A.J., Cherry, M.E., Durocher, M.E., Fyon, A.J., Lavigne, M.J., Jr., MacDonald, A.J., Marmont, S., Poulsen, K.H., Springer, J.S., and Troop, D.G.
1984: An integrated model for the origin of Archean lode gold deposits, Ontario Geological Survey Open File Report 5524, 98 pages.

Colvine, A.C., Fyon, J.A., Heather, K.B., Marmont, S., Smith, P.M., and Troop, D.C.
1988: Archean lode gold deposits in Ontario: Part I. A depositional model; Part II. A genetic model. Ontario Geological Survey Miscellaneous Paper 139, 136 pages.

Cooper, G.E.
1967: The geology of the Tulks Hill area, central Newfoundland. Unpub. M.Sc. thesis, Memorial Univ. of Nfld., St. John's 112 pages.

Coyle, M. and Strong, D.F.
1987: Geology of the Springdale Group: a newly recognized Silurian epicontinental-type caldera in Newfoundland: Canadian Journal Earth Sciences, Volume. 24, pages 1135-1148.

Coward, M.P.
1966: The geology of the mineral belt, southeast of Red Indian Lake, central Newfoundland: Unpublished B.Sc. thesis, Royal School of Mines, Imperial Collage, London, 21 pages.

Dallmeyer, R.D., Kean, B.F., Odom, A.L. and Jayasinghe, N.R.
1983: Age and contact-metamorphic effects of the Overflow Pond Granite: an undeformed pluton in the Dunnage Zone of the Newfoundland Appalachians. Canadian Journal of Earth Science, Volume 20, pages 1639-1645.

Davenport, P.H., Nolan, L.W., Honarvar, P. and Hogan, A.P.
1990: Gold and associated elements in lake sediment from regional geochemical surveys in the Red Indian Lake map area (NTS 12A). Newfoundland department of Mines and Energy, Mineral Development Division, Open File 12A/561.

Dean, P.L.,
1978: The volcanic stratigraphy and metallogeny of Notre Dame Bay: Memorial University of Newfoundland, St. John's, Geology Report 7, 204 pages.

Desnoyers, D.
1990a: Victoria Mine prospect. In Metallogenic framework of base and precious metal deposits, central and western Newfoundland. Edited by H.S. Swinden, D.T.W. Evans and B.F. Kean. Eighth IAGOD Symposium Field Trip Guidebook. Geological Survey of Canada, Open File 2156, pages 65-67.

1990b: Bobby's Pond alteration zone. In Metallogenic framework of base and precious metal deposits, central and western Newfoundland. Edited by H.S. Swinden, D.T.W. Evans and B.F. Kean. Eighth IAGOD Symposium Field Trip Guidebook. Geological Survey of Canada, Open File 2156, pages 65-67.

Dimmel, P.
1986: A case history of the discovery and geophysical and geochemical signatures of the Burnt Pond sulphide prospects, Noel Paul's Brook, central Newfoundland, NTS 12A/9. Unpublished B.Sc. thesis, University of New Brunswick, 56 pages.

Doe, B.R. and Zartman, R.E.
1979: Plumbotectonics, the Phanerozoic. In Geochemistry of Hydrothermal Ore Deposits, Second Edition. Edited by H.L. Barnes. A Wiley-Interscience Publication, John Wiley and Sons, pages 22-70.

Douglas, G.V., Williams, D., Rove, O.N., and others
1940: Copper deposits of Newfoundland. Geological Survey of Newfoundland, Bulletin 20, 176 pages.

Dunning, G.R.
1986: Precise U-Pb zircon geochronology applied to Newfoundland ophiolites, granitoid and felsic volcanic rocks (abstract). Program with Abstract, Newfoundland Section,

Geological Association of Canada, Annual Meeting, pages 11-12.

Dunning, G.R., Kean, B.F., Thurlow, J.G. and Swinden, H.S.
1987: Geochronology of the Buchans, Roberts Arm and Victoria Lake Groups and Mansfield Cove Complex, Newfoundland. Canadian Journal of Earth Sciences, Volume 24, pages 1175-1184.

Dunning, G.R. and Krogh, T.E.
1985: Geochronology of ophiolites of the Newfoundland Appalachians. Canadian Journal of Earth Sciences, Volume 22, pages 1659-1670.

Dunning, G.R., Krogh, T.E., Kean, B.F., O'Brien, S. and Swinden, H.S.
1986: U/Pb ages of volcanic groups from the central mobile belt, Newfoundland. (Abstract); In Geological Association of Canada, Annual Meeting, Program with Abstracts, Volume 11, pages 66.

Dunning, G.R., O'Brien, S.J., Colman-Sadd, S.P., Blackwood, R.F., Dickson, W.L., O'Neil, P.P. and Krogh, T.E.
1990: Silurian orogeny in the Newfoundland Appalachians. Journal of Geology, Volume 98, pages 895-913.

Dunning, G.R., Swinden, H.S., Kean, B.F., Evans, D.T.W. and Jenner, G.A.
1991: A Cambrian island arc in Iapetus: geochronology and geochemistry of the Lake Ambrose Volcanic Belt, Newfoundland Appalachians. Geological Magazine, Volume 128, pages 1-17.

Eisenlohr, B.N., Groves, D. and Partington, G.A.
1989: Crustal-scale shear zones and their significance to Archean gold mineralization in Western Australia. Mineral Deposita, Volume 24, pages 1-8.

Ellis, A.J.
1979: Explored geothermal systems. In Geochemistry of Hydrothermal Ore Deposits, Second Edition. Edited by H.L. Barnes. A Wiley-Interscience Publication, John Wiley and Sons, pages 632-683.

Evans, A.M.
1980: An Introduction To Ore Geology. Elsevier, New York. Geoscience Texts, Volume 2, 231 pages.

Evans, D.T.W.
1986: The geology, geochemistry, alteration and sulphide petrology of the Lower Ordovician Jacks Pond pyritic volcanogenic massive sulfide prospects, central Newfoundland. Unpublished B.Sc.(Hon.) thesis, MUN., St. John's, Newfoundland, 113 pages.

1990: Midas Pond gold prospect. In Metallogenic framework of base and precious metal deposits, central and western Newfoundland. Edited by H.S. Swinden, D.T.W. Evans and B.F. Kean. Eighth IAGOD Symposium Field Trip Guidebook. Geological Survey of Canada, Open File 2156, pages 70-72.

1992: Gold metallogeny of the eastern Dunnage Zone, central Newfoundland. In Current Research. Newfoundland Department of Mines, Mineral Development Division, Report 92-1, pages 231-243.

1993: Gold metallogeny of the eastern Dunnage Zone, central Newfoundland. In Current Research. Newfoundland Department of Mines, Mineral Development Division, Report 9_-1, pages 339-350.

Evans, D.T.W. and Kean, B.F.
1986: Geology of the Jacks Pond volcanogenic sulphide prospects, Victoria Lake Group, central Newfoundland. In Current Research. Newfoundland Department of Mines and Energy, Mineral Development Division, Report 86-1, pages 59-64.

1987: Gold and massive sulphide mineralization in the Tulks Hill volcanics, Victoria Lake Group, Central Newfoundland. In Current Research. Newfoundland Department of Mines and Energy, Mineral Development Division, Report 87-1, pages 103-111.

1990: Geology and Mineral Deposits of the Victoria Lake Group. In Metallogenic framework of base and precious metal deposits, central and western Newfoundland. Edited by H.S. Swinden, D.T.W. Evans and B.F. Kean. Eighth IAGOD Symposium Field Trip Guidebook. Geological Survey of Canada, Open File 2156, pages 46-55.

Evans, D.T.W., Kean, B.F. and Dunning, G.R.
1990: Geological studies, Victoria Lake Group, central Newfoundland. In Current Research. Newfoundland Department of Mines, Geological Survey Branch, Report 90-1, pages 144.

Ewart, A.
1979: A review of the mineralogy and chemistry of Tertiary-Recent dacitic, latitic, rhyolitic and related sialic volcanic rocks. In Trondhjemites, Dacites and Related Rocks. Edited by F. Barker. Elsevier, New York, pages 13-121.

Faure, G.
1978: Strontium: 38-F. Behavior in magmatogenic processes. In K.H. Wedepohl, Executive Editor. Handbook of Geochemistry, Volume II/4. Springer-Verlag, New York, page 38-F-1.

Fletcher, I.R and Farquhar, R.M.
1982: The protocontinental nature and regional variability of the Central Metasedimentary Belt of the Grenville Province: lead isotope evidence. Canadian Journal of Earth Sciences, Volume 19, pages 239-253.

Ford, K.L.
1991: Airborne geophysical survey of the Tulks volcanic belt, Red Indian Lake area, Newfoundland. Geological Survey of Canada, Open File 2481.

Geological Survey of Canada
1985a: Aeromagnetic vertical gradient map, Badger, Newfoundland, 1:50,000 scale: Geophysics Series, Map C40096G.

1985b: Aeromagnetic vertical gradient map, Star Lake, Newfoundland, 1:50,000 scale: Geophysics Series, Map C41137G.

1985c: Aeromagnetic vertical gradient map, Lake Ambrose, Newfoundland, 1:50,000 scale: Geophysics Series, Map C41138G.

1985d: Aeromagnetic vertical gradient map, Noel Pauls Brook, Newfoundland, 1:50,000 scale: Geophysics Series, Map C41139G.

1985e: Aeromagnetic vertical gradient map, Victoria Lake, Newfoundland, 1:50,000 scale: Geophysics Series, Map C41140G.

Govindaraju, K.
1989: 1989 compilation of working values and sample description for 272 geostandards. Geostandards Newsletter, Volume 13, Special Issue, 113 pages.

Grant, J.A.
1986: The Isocon Diagram- a simple solution to Gresen's equation for metasomatic alteration. Economic Geology, Volume 81, pages 1976-1982.

Gresens, R.L.
1967: Composition-volume relationships of metasomatism. Chemical Geology, Volume 2, pages 47-55.

Grimes-Graeme, R.
1934: Report on a geological reconnaissance survey for Terra Nova properties Lloyd's and Victoria Lakes, Newfoundland: Hans Lundberg Ltd., Montreal, Buchans Mining Company Ltd., unpublished report, 32 pages.

Groves, D.I. and Phillips, G.N.
1987: The genesis and tectonic control on Archean gold deposits of the Western Australian Shield-a metamorphic replacement model. Ore Geology Reviews, Volume 2, pages 287-322.

Groves, D.I., Ho, S.E., McNaughton, N.J., Mueller, A.G., Perring, C.S., Rock, N.M.S. and Skwarnecki, M.S.
1988: Genetic models for Archean lode gold deposits in Western Australia. In Advances in Understanding Precambrian Gold deposits. Edited by S.E. Ho and D.I. Groves. Geology Department and University Extension, University of Western Australia, Publication 11, pages 1 -22.

Hammond, B.R.
1962: Geology and mineralization of the Long Lake prospect, central Newfoundland. Unpublished B.Sc. thesis, Royal School of Mines, Imperial Collage, London, 113 pages.

Hanor, J.S.
1979: The sedimentary genesis of hydrothermal fluids. In Geochemistry of Hydrothermal Ore Deposits, Second Edition. Edited by H.L. Barnes. A Wiley-Interscience Publication, John Wiley and Sons, pages 137-172.

Hanmer, S. and Passchier, C.
1991: Shear-sense indicators: a review. Geological Survey of Canada, Paper 90-17, 72 pages.

Haq, B.U. and Van Eysinga, F.W.B.
1987: Geological Time Table. Elsevier Science Publishers B.V., Amsterdam.

Heald, P., Foley, N.K. and Hayba, O.
1987: Comparative anatomy of volcanic-hosted epithermal deposits: acid-sulfate and adularia-sericite types. Economic Geology, Vol. 82, No.1, pages 1-26.

Heier, K.S.
1978: Rubidium: 37-D. Rubidium abundance in rock-forming minerals. In K.H. Wedepohl, Executive Editor. Handbook of Geochemistry, Volume II/4. Springer-Verlag, New York, pages 37-D-1-37-D-4.

Hey, M.H.
1954: A new review of the chlorites. Mineralogical Magazine, volume 30, pages 272-292.

Hobbs, B.E., Means, W.D. and Williams, P.F.
1976: An Outline Of Structural Geology. John Wiley and Sons,Incorporated, New York, 571 pages.

Hodgson, C.J.
1989: Patterns of mineralization. In Mineralization and Shear Zones. Edited by J.T. Bursnall. Geological Association of Canada, Short Course Notes, Volume 6, pages 51-88.

Howse, A.F.
1992: Barite resources of Newfoundland. Newfoundland Department of Mines and Energy, Mineral Development Division. Mineral Resources Report 6, 48 pages.

Jambor, J.L.
1984a: Mineralogy of the Tulks Zn-Pb-Cu massive sulphide deposit, Buchans area, Newfoundland. Canmet, Energy, Mines and Resources Canada, Division Report MRP/MSL 84-22(IR), 49 pages.

1984b: Mineralogy and Predictive Metallogeny of the Tally Pond Pyritic Massive Sulphide Deposit, Buchans Area, Newfoundland. Canmet, Energy Mines and Resources Canada, Report. MRP/MSL 84-164 (TR), 35 pages.

Jambor, J.L. and Barbour, D.M.
1987: Geology and mineralogy of the Tulks deposit. In Buchans Geology, Newfoundland. Edited by R.V. Kirkham. Geological Survey of Canada, Paper 86-24, pages 219-226.

Jenner, G.A., Longerich, H.P., Jackson, S.E. and Fryer, B.J.
1990: ICP-MS-a powerful tool for high precision trace element analysis in earth sciences: evidence from analysis of selected USGS reference samples. Chemical Geology, Volume 83, pages 133-148.
1990:

Kean, B.F.
1977: Geology of the Victoria Lake map area (12A/6), Newfoundland. Newfoundland Department of Mines and Energy, Mineral Development Division, Report 77-4, 11 pages.

1979a: Star Lake map area, Newfoundland. Newfoundland Department of Mines and Energy, Mineral Development Division, Map 79-1 (with descriptive notes).

1979b: Buchans map area, Newfoundland. Newfoundland Department of Mines and Energy, Mineral Development Division, Map 79-125 (with descriptive notes).

1983: Geology of the King George IV Lake map area (12A/4). Newfoundland Department of Mines and Energy, Mineral Development Division, Report 83-4, 67 pages.

1985: Metallogeny of the Tally Pond volcanics, Victoria Lake Group, central Newfoundland. In Current Research. Newfoundland Department of Mines and Energy, Mineral Development Division, Report 85-1, pages 89-93.

Kean, B.F., Dean, P.L., and Strong, D.F.
1981: Regional geology of the Central Volcanic Belt of Newfoundland. Geological Association of Canada, Special Paper 22, pages 65-78.

Kean, B.F. and Evans, D.T.W.
1986: Metallogeny of the Tulks Hill volcanics, Victoria Lake Group, central Newfoundland. In Current Research Newfoundland Department of Mines and Energy, Mineral Development Division, Report 86-1, pages 51-57.

Kean, B.F. and Evans, D.T.W.
1988a: Regional metallogeny of the Victoria Lake Group, central Newfoundland, In Current Research. Newfoundland Department of Mines, Mineral Development Division, Report 88-1, pages 319-330.

1988b: Geology and mineral deposits of the Victoria Lake Group, In The Volcanogenic Sulphide Districts of Central Newfoundland. Edited by H.S. Swinden and B.F. Kean. Geological Association of Canada, Mineral Development Division, pages 144-156.

Kean, B.F. and Jayasinghe, N.R.
1980: Geology of the Lake Ambrose (12A/10) and Noel Paul's Brook (12A/9) map areas, Newfoundland. Newfoundland Department of Mines and Energy, Mineral Development Division, Report 80-2, 29 pages.

1982: Geology of the Badger map area (12A/16), Newfoundland. Newfoundland Department of Mines and Energy, Mineral Development Division, Report 81-2, 37 pages.

Kean, B.F. and Mercer, N.L.
1981: Grand Falls map, area (2D/13), Newfoundland. Newfoundland Department of Mines and Energy, Mineral Development Division, Map 8199 (with descriptive notes).

Kean, B.F. and Strong, D.F.
1975: Geochemical evolution of an Ordovician island arc of the Central Newfoundland Appalachians. American Journal of Science, Volume 275, pages 97-118.

Kean, B.F., and Thurlow, J.G.
1975: Geology, mineral deposits and mineral potential of the Buchans volcanic belt: A report submitted to the Buchans Task Force, 50 pages.

1976: Geology, mineral deposits and mineral potential of the Buchans volcanic belt, St. John's. Government of Newfoundland and Labrador, Mining Subcommittee Report to the Buchans Task Force, pages A4-1 - A4-63.

Keen, C.E., Keen, M.J., Nichols, B., Reid, I., Stockmal, G.S., Colman-Sadd, S.P., O'Brien, S.J., Miller, H., Quinlan, G., Williams, H. and Wright, J.
1986: Deep seismic reflection profile across the northern Appalachians. Geology, Volume 14, pages 141-145.

Kerrich, R.
1989a: Geodynamic setting and hydraulic regimes: shear hosted mesothermal gold deposits. In Mineralization and Shear Zones. Edited by J.T. Bursnall. Geological Association of Canada, Short Course Notes, Volume 6, pages 89-128.

1989b: Geochemical evidence on the sources of fluids and solute for shear zone hosted mesothermal Au deposits. In Mineralization and Shear Zones. Edited by J.T. Bursnall. Geological Association of Canada, Short Course Notes, Volume 6, pages 129-197.

Kerrich, R. and Feng, R.
1992: Archean geodynamics and the Abitibi-Pontiac collision: implications for advection of fluids at transpressive collisional boundaries and the origin of giant quartz vein systems. Earth-Science Reviews, Volume 32, pages 33-60.

Kontak, D.J. and Smith, P.K.
1989: Sulphur isotopic composition of sulphides from the Beaver Dam and other Meguma Group-hosted gold deposits, Nova Scotia: implications for genetic models. Canadian Journal of Earth Sciences, Volume 26, pages 1617-1629.

Koritnig, S.
1972: Fluorine. In K.H. Wedepohl editor, Handbook of Geochemistry, Springer-Verlag, New York.

LeMaitre, R.W.
1989: A Classification of Igneous Rocks and Glossary of Terms. Blackwell, Oxford, 193 pages.

MacKenzie, A.C.
1988: An overview of the geology and tectonic setting of the Boundary volcanogenic massive sulphide deposit, Tally Pond

volcanics, central Newfoundland. In The Volcanogenic Sulphide Districts of Central Newfoundland. Edited by H.S. Swinden and B.F. Kean. Geological Association of Canada, Mineral Development Division, St. John's, pages 157-164.

MacKenzie, A.C., Squires, G. and MacInnis, D.
1988: The geology of the Duck Pond deposit, central Newfoundland. Geological Association of Canada-Canadian Society of Petroleum Geologists, Joint Annual Meeting, Program with Abstracts, Volume 13, page A77.

Martin, W.
1983: Once Upon a Mine: Story of Pre-Confederation Mines on the Island of Newfoundland. Canadian Institute of Mining and Metallurgy, Special Volume 26, 98 pages.

McCrea, J.M.
1950: On the isotope chemistry of carbonates and a paleotemperature scale. Journal of Chemistry and Physics, Volume 18, pages 849-857.

McKenzie, C., Desnoyers, D., Barbour, D. and Graves, M.
1990: Contrasting VMS styles in the Tulks Belt, central Newfoundland. Canadian Institute of Mining, District 1 Annual Meeting, St. John's, Newfoundland, Program with Abstracts, page 10.

Mihychuk, M.
1985: Drift prospecting in the Victoria and Tally Pond areas, central Newfoundland. Newfoundland Department of Mines and Energy, Mineral Development Division, Report 85-1, pages 99-104.

Mineral Occurrence Data System (MODS).
Newfoundland Department of Mines and Energy, mineral occurence data files for NTS 12A.

Miyashiro, A.
1978: Metamorphism and Metamorphic Belts. George Allen and Unwin, Great Britain, 492 pages.

Moreton, C.
1984: The Tulks Hill massive sulphide deposit, Newfoundland. Unpub. M.Sc. thesis, Memorial University of Newfoundland, 320 pages.

Mottl, M.J.
1983: Metabasalts, axial hot springs, and the structure of hydrothermal systems at mid-ocean ridges. Geological Society of America, Bulletin, Volume 94, pages 161-180.

Mullins, W.J.
1961: Geology of the Noel Paul's Brook area, central Newfoundland: Unpublished M.Sc. thesis, Memorial University of Newfoundland, St John's, Newfoundland, 97 pages.

Murray, A.
1872: Survey of Exploits River and Red Indian Lake. Geological Survey of Newfoundland, Report for 1871.

Murray, A. and Howley, J.P.
1881: Geological Survey of Newfoundland. Edward Stanford, London, 536 pages.

Neary, G.N.
1981: Mining history of the Buchans area. In The Buchans Orebodies: Fifty Years of Geology and Mining. Edited by E.A. Swanson, J.G. Thurlow and D.F. Strong. Geological Association of Canada, Special Paper 22, pages 1-64.

Newhouse, W.H.
1931: Geology and ore deposits of Buchans, Newfoundland. Economic Geology, Volume 26, pages 399-414.

O'Brien, S.J., Dickson, W.L. and Blackwood, R.F.
1986: Geology of the central portion of the Hermitage Flexure area, Newfoundland. In Current Research. Newfoundland Department of Mines and Energy, Mineral Development Division, Report 86-1, pages 189-208.

Ohmoto, H. and Rye, R.O.
1979: Isotopes of sulfur and carbon. In Geochemistry of Hydrothermal Ore Deposits, Second Edition. Edited by H.L. Barnes. A Wiley-Interscience Publication, John Wiley and Sons, pages 509-567.

Phillips, G.N. and Groves, D.I.
1983: The nature of Archean gold-bearing fluids as deduced from gold deposits of Western Australia. Journal of the Geological Society of Australia, Volume 30, pages 25-39.

Puchelt, H.
1978: Barium: 56-D. Abundance in rock-forming minerals (I) and barium minerals (II). In K.H. Wedepohl, Executive Editor. Handbook of Geochemistry, Volume II/4. Springer-Verlag, New York, pages 56-D-1- 56-D-18.

Ramezani, J., Dunning, G.R. and Wilson, M.R.
1992: Geochemical and isotopic study of the Stog'er Tight gold prospect, Baie Verte Peninsula, Newfoundland. Geological Association of Canada-Mineralogical

Association of Canada, Joint Annual Meeting, Abstracts Volume, Volume 17, page A93.

Ramsey, J.G.
1967: Folding and Fracturing of Rocks. McGraw-Hill, 568 pages.

1980: Shear zone geometry: a review. Journal of Structural Geology, Volume 2, pages 83-99.

Ramsey, J.G. and Graham, R.H.
1970: Strain variation in shear belts. Canadian Journal of Earth Sciences, Volume 7, pages 786-813.

Reynolds, T.J.
1990: Course notes for Workshop on application of fluid inclusions to mineral exploration. 53 pages.

Riley, G.C.
1957: Red Indian Lake (west half), Newfoundland. Geological Survey of Canada, Map 8-1957 (with descriptive notes).

Roberts, R.G.
1988: Archean lode gold deposits. In Ore Deposit Models. Edited by R.G. Roberts and P.A. Sheahan. Geoscience Canada, Reprint Series 3, pages 1-19.

Romberger, S.B.
1988: Disseminated gold deposits. In Ore Deposit Models. Edited by R.G. Roberts and P.A. Sheahan. Geoscience Canada, Reprint Series 3, pages 21-30.

Rose, A.W. and Burt, D.M.
1979: Hydrothermal alteration. In Geochemistry of Hydrothermal Ore Deposits. Second Edition. Edited by H.L. Barnes. A Wiley-Interscience Publication, John Wiley and Sons, pages 173-235.

Seward, T.M.
1984: The transport and deposition of gold in hydrothermal systems. In Gold '82. Edited by R.P. Foster. A.A. Balkema, Rotterdam, pages 165-181.

Sibson,R.H.
1977: Fault rocks and fault mechanisms. Journal of the Geological Society of London, Volume 133, pages 191-213.

1989: Earthquake faulting as a structural process. Journal Structural Geology, Volume 11, pages 1-14.

Sparkes, B.
1985: Quaternary mapping, Central Volcanic Belt. In

Current Research. Newfoundland Department of Mines and Energy, Mineral Development Division, Report 85-1, pages 94-98.

Squires, G.C., MacKenzie, A.C. and MacInnis, D.
1990: Geology and genesis of the Duck pond volcanogenic massive sulphide deposit. In Metallogenic framework of base and precious metal deposits, central and western Newfoundland. Edited by H.S. Swinden, D.T.W. Evans and B.F. Kean. Eighth IAGOD Symposium Field Trip Guidebook. Geological Survey of Canada, Open File 2156, pages 56-64.

Stacey, J.S. and Kramers, J.D.
1975: Approximation of terrestrial lead isotope evolution by a two stage model. Earth and Planetary Science Letters, Volume 26, pages 207-221.

Strickland, R.
1971: Geology of the Long Lake area, central Newfoundland: Unpublished B.Sc. thesis, Memorial University of Newfoundland, 69 pages.

Strong, D.F.
1980: Granitoid rocks and associated mineral deposits of Eastern Canada and Western Europe. In The Continental Crust and its Mineral Deposits. Edited by D.W. Strangway. Geological Association of Canada, Special Paper 20, pages 741-769.

Stueber, A.M.
1978: Strontium: 38-D. Abundance in rock-forming minerals; strontium minerals. In K.H. Wedepohl, Executive Editor. Handbook of Geochemistry, Volume II/4. Springer-Verlag, New York, pages 38-D-1-38-D-17.

Swinden, H.S.
1987: Ordovician volcanism and mineralization in the Wild Bight Group, central Newfoundland: a geological, petrological, geochemical and isotopic study. Unpub. Ph.D. thesis, Memorial University of Newfoundland, St. John's, Newfoundland, 452 pages.

1990: Regional geology and metallogeny of central Newfoundland. In Metallogenic framework of base and precious metal deposits, central and western Newfoundland. Edited by H.S. Swinden, D.T.W. Evans and B.F. Kean. Eighth IAGOD Symposium Field Trip Guidebook. Geological Survey of Canada, Open File 2156, pages 1-27.

Swinden, H.S., Kean, B.F. and Dunning, G.R.
1988a: Geological and paleotectonic settings of volcanogenic sulphide mineralization in central Newfoundland, In The

Volcanogenic Sulphide Districts of Central Newfoundland. Edited by H.S. Swinden and B.F. Kean. Geological Association of Canada, Mineral Development Division, pages 5-26.

Swinden, H.S., Lane, T.E. and Thorpe, R.I.
1988b: Lead-isotope compositions of galena in carbonate-hosted deposits of western Newfoundland: evidence for diverse lead sources. Canadian Journal of Earth Sciences, Volume 25, pages 593-602.

Swinden, G.A., Jenner, G.A., Kean, B.F. and Evans, D.T.W.
1989: Volcanic rock geochemistry as a guide for massive sulphide exploration in central Newfoundland. In Current Research. Newfoundland Department of Mines and Energy, Geological Survey Branch, Report 89-1, pages 201-219.

Swinden, H.S., and Thorpe, R.I.
1984: Variations in style of volcanism and massive sulfide deposition in Early to Middle Ordovician Island arc sequences of the Newfoundland Central Mobile Belt. Economic Geology, Volume 79, pages 1596-1619.

Szybinski, Z.A., Swinden, H.S., O'Brien, F.H.C., Jenner, G.A. and Dunning, G.R.
1990: Correlation of Ordovician volcanic terranes in the Newfoundland Appalachians: lithological, geochemical and age constraints (abstract): Geological Association of Canada, Program with Abstracts, Volume 15, page A128.

Taylor, H.P.
1979: Oxygen and hydrogen isotope relationships in hydrothermal mineral deposits: In Geochemistry of Hydrothermal Ore Deposits, Second Edition. Edited by H.L. Barnes. A Wiley-Interscience Publication, John Wiley and Sons, pages 236-277.

Taylor, R.P. and Fryer, B.J.
1982: Rare earth element geochemistry as an aid to interpreting hydrothermal ore deposits. In Metallization Associated with Acid Magmatism. Edited by A.M. Evans. John Wiley and Sons Ltd., pages 357-365.

Taylor, S.R. and McLennan, S.M.
1985: The Continental Crust: Its Composition and Evolution. Blackwell, Oxford, 312 pages.

Thorpe, R.I., Guha, J., Franklin, J.M. and Loveridge, W.D.
1984: Use of the Superior Province lead isotope framework in interpreting mineralization stages in the Chibougamou District. In Chibougamou-Stratigraphy and Mineralization. Edited by J.Guha and E.H. Chown. Canadian Institute of

Mining and Metallurgy, Special Volume 34, pages 496-516.

Thurlow, J.G.
1978: Geology of the Old Victoria mine, Central Newfoundland (Abstract). Canadian Institute of Mining and Metallurgy, District 1 Annual Meeting, St. John's, Newfoundland, Program with Abstracts, pages 7-8.

Thurlow, J.G. and Barbour, D.
1982: 1981 exploration report on the Anglo Newfoundland Development Company Charter and associated Reid Lots for work done between Jan. 1 and Dec. 31, 1981, Abitibi-Price Inc. unpublished report, 9 pages.

1985: Assessment report on geochemical exploration and diamond drilling exploration for 1984 submission for the Anglo Newfoundland Development Company Charter, and Reid Lots 228, 229, 232, 233 and 247 in the Buchans area, Newfoundland. Abitibi-Price Inc. unpublished report, 91 pages.

Thurlow, J.G., Barbour, D., Desnoyers, D.W. and Burton, G.B.
1987: 1986 Newfoundland mineral exploration report on the A.N.D. Charter and Reid Lots 227, 228, 229, 231, 232, 233, 234, 235, 247, Crown Lease Lots A, B, E, F, J, N, O, P, Q, R and Fee Simple Lots Vol. 1, Fol. 43; Vol. 1, Fol. 61; Vol. 1, Fol. 62; Vol. 1, Fol. 110; Vol. 2, Fol. 23; Vol. 2, Fol. 25; Vol. 2, Fol. 29; Sp. Vol. 2, Fol. 307: for work period 1986-01-01 to 1986-12-31, BP Resources Canada Ltd., Selco Division, unpublished report, 28 pages.

Tod, J.
1986: VLF-EM investigations in insular Newfoundland. In Current Research. Newfoundland Department of Mines and Energy, Mineral Development Division, Report 86-1, pages 239-250.

Tuach, J., Dean, P.L., Swinden, H.S., O'Driscoll, C.F., Kean, B.F. and Evans, D.T.W.
1988: Gold mineralization in Newfoundland: a 1988 review. In Current Research. Newfoundland Department of Mines, Mineral Development Division, Report 88-1, pages 279-306.

Twenhofel, W.H. and MacClintock, P.
1940: Surfaces of Newfoundland; Geological Society of America Bulletin, volume 51, pages 1665-1728.

Wagenbaur, H.A., Riley, C.A. and Dawe, G.
1983: Geochemical laboratory. In Current Research. Newfoundland Department of Mines, Mineral Development Division, Report 83-1, pages 133-137.

Williams, H.
1964: The Appalachians in Newfoundland - a two-sided symmetrical system. American Journal of Science, Volume 262, pages 1137-1158.

1970: Red Indian Lake (east half), Newfoundland. Geological Survey of Canada, Map 1196A.

1979: Appalachian Orogen in Canada. Canadian Journal of Earth Sciences, Volume 16, pages 792-807.

Williams, H., Colman-Sadd, S.P. and Swinden, H.S.
1988: Tectonic-Stratigraphic subdivisions of central Newfoundland. In Current Research, Part B. Geological Survey of Canada, Paper 88-1B, pages 91-98.

Wilton, D.H.C., Evans, D.T.W., Fryer, B.J., and Wilson, M.R.
1989: Preliminary report on the geochemical and isotopic study of mineralized faults and their extensions along the Lithoprobe East Vibroseis Transect. Lithoprobe East Report of Transect Meeting, Oct. 19-20, 1989, Memorial University of Newfoundland, St. John's. pages 37-39.

Wilton, D.H.C., Evans, D.T.W., and Fryer, B.J.
1990: Comparison of the geochemical, mineralogical and isotopic composition of mineralized fault systems in the Humber-Dunnage and Gander-Dunnage Zones. Lithoprobe East Report of Transect Meeting, October 24-25, 1990, Memorial University of Newfoundland, St. John's. pages 169-180.

Wilton, D.H.C. and Strong, D.F.
1986: Granite-related gold mineralization in the Cape Ray Fault Zone of southwestern Newfoundland. Economic Geology, Volume 81, Number 2, pages 281-295.

Winchester, J.A. and Floyd, P.A.
1977: Geochemical discrimination of different magma series and their differentiation products using immobile elements. Chemical Geology, Volume 20, pages 325-343.

Winkler, G.F.
1976: Petrogenesis of Metamorphic Rocks. Fourth Edition. Springer-Verlag, New York, 334 pages.

APPENDIX 1

ELECTRON MICROPROBE OPERATING TECHNIQUE AND STANDARDS

A1.1 ELECTRON MICROPROBE OPERATING TECHNIQUE AND STANDARDS

Chlorite, carbonate, paragonite/sericite, pyrophyllite and kaolinite were analyzed using a JEOL JX-5A electron probe microanalyser located at the Department of Earth Sciences, Memorial University. The analyser has three automated wavelength dispersive spectrometers run by the Krisel control system.

A beam current of 0.220 mA and an operating voltage of 15 kv were used to perform all analyses. The Krisel Alpha program which uses the Bence and Albee (1968) correction method was used for all data reduction. Pyroxene standard ACPX (Kakanui augite) was used for calibration.

Table A1.1 shows the results of replicate standard analyses with standard deviation of the oxide and homogeneity index. The homogeneity index is a measure of the homogeneity of distribution of each element in the grain. An index value of less than three is taken to indicate homogeneous element distribution in the grain. Since this calculation does not take background counts into consideration elements present in small amounts will show inhomogeneous distribution.

	Ave 3	SD	HI		AVE 3	SD	HI
SiO_2	48.59	1.11	4.19	SiO_2	50.51	.20	2.20
Al_2O_3	7.77	.08	1.28	Al_2O_3	7.90	.03	.42
FeO	6.50	.10	1.31	FeO	6.42	.10	1.33
MgO	15.90	.20	1.30	MgO	16.28	.13	1.11
CaO	15.25	.25	1.98	CaO	15.68	.32	3.71
Na_2O	1.30	.05	.78	Na_2O	1.28	.05	1.30
K_2O	.00	.00	.00	K_2O	.01	.00	5.57
TiO_2	.76	.01	.75	TiO_2	.74	.05	3.99
MnO	.13	.04	6.00	MnO	.13	.02	2.13
Cr_2O_3	.13	.02	8.35	Cr_2O_3	.14	.01	3.07
NiO	.03	.02	15.06	NiO	.04	.02	5.48
Total	96.36			Total	99.13		
Si	1.832			Si	1.837		
Al	.345			Al	.338		
Fe	.205			Fe	.194		
Mg	.893			Mg	.882		
Ca	.615			Ca	.610		
Na	.094			Na	.089		
K	.000			K	.000		
Ti	.021			Ti	.019		
Mn	.003			Mn	.003		
Cr	.003			Cr	.004		
Total	4.009			Total	3.979		

Table A1.1 Replicate analyses of ACPX pyroxene standard (SD - standard deviation, HI - homogeneity index).

APPENDIX 2

ANALYTICAL PROCEDURES, PRECISION, ACCURACY AND SAMPLE LOCATIONS

A2.1 SAMPLE PREPARATION AND ANALYTICAL PROCEDURES

Samples were prepared at the Newfoundland Department of Mines and Energy laboratory. All weathered surfaces were removed prior to crushing. Samples were crushed in a steel jaw crusher which was cleaned by air gun, steel brush and methanol between samples. The samples were than pulverized in a ceramic bowl and puck and stored in clean plastic viles. The ceramic bowl was cleaned with silica between samples.

Major element oxides and selected trace elements were determined at the Newfoundland Department of Mines and Energy laboratory. Sample dissolution techniques are outlined by Wagenbauer et al., (1983). This technique has been modified to include sample dissolution using $LiBo_2$ fusion. Analyses were determined using ICP-ES. Cu, Pb and Zn concentrations were determined using AAS.

F concentrations were determined by ISE using the procedure outlined by Wagenbauer et al. (1983).

Trace element data were determined by X-Ray fluorescence spectrometry at Memorial University. Samples (10 g mixed with 1.5 g of bakelite binder) were pelletized and baked at 200°C for twenty minutes. The pellets were analyzed using a Phillips 1450 X-Ray fluorescence spectrometer.

REE were determined by inductively coupled plasma mass spectrometry (ICP-MS) at Memorial University using the method described by Jenner et al., (1990).

Geochemical manipulation and plots were made using the NEWPET computer program (Clarke, 1990)

Total iron was recalculated as follows:

$$FeO_{Total} = FeO + Fe_2O_3 \times 0.89981$$

Major Elements	DE-86-63b		DE-86-123a		DE-86-152c		DE-86-196d		DE-87-12	
SiO2	76.5	76.95	65.45	65.55	81.9	82.6	65.35	65.05	60.65	60.45
TiO2	0.26	0.27	0.4	0.38	0.19	0.17	0.9	0.89	0.99	1
Al2O3	13.14	13.02	16.2	16.46	8.37	8.5	11.69	11.61	14.89	14.92
FeO*	1.34	1.36	5.88	5.81	2.23	2.23	7.65	7.72	11.09	11.65
MnO	0.01	0.01	0.08	0.08	0.01	0.01	0.02	0.01	0.01	0.01
MgO	0.23	0.23	1.86	1.86	0.87	0.86	2.42	2.36	0.07	0.07
CaO	0.04	0.05	0.21	0.23	0.03	0.03	0.22	0.23	0.22	0.23
Na2O	6.54	6.48	7.12	7.1	3.95	3.96	5.61	5.58	1	0.99
K2O	0.86	0.84	0.15	0.15	0.08	0.08	0.03	0.03	0.37	0.37
P2O5	0.02	0.01	0.11	0.12	0.02	0.03	0.12	0.12	0.1	0.1
LOI	1.15	1.24	1.7	1.76	1.64	1.64	4.36	5.28	9.63	9.45

Trace Elements	DE-86-63b		DE-86-123a		DE-86-152c		DE-86-196d	
Pb	3	3	1	1	1	1	1	1
Cu	3	3	4	3	3	3	7	6
Zn	6	6	103	104	9	7	12	11
Mo	3	3	2	4	6	5	4	4
F	84	79	216	189	346	334	765	716

Precision (P) Major and Trace Element analyses

Major Elements	P(mean)	Std	N
SiO2	0.36	0.14	5
TiO2	4.43	3.69	5
Al2O3	0.99	0.53	5
FeO*	1.7	1.69	5
MnO	13.33	26.67	5
MgO	0.73	1	5
CaO	8.04	7.65	5
Na2O	0.57	0.35	5
K2O	0.47	0.94	5
P2O5	21.47	27.35	5
LOI	5.39	6.94	5

Trace Elements	P(mean)	Std	N
Pb	25	43.3	4
Cu	25	11.94	4
Zn	10.99	18.21	4
Mo	21.21	27.27	4
F	7.4	3.62	4

$$P = \frac{(V1-V2)\times 100}{V1,2}$$

(Carter, Swinden, 1988)

V1= larger value of element pair, V2= smaller value of element pair
V1,2= mean of V1 and V2, P(mean)= mean of all sample pairs analysed

Table A2.1 Duplicate pairs for major and selected trace element analyses.

Major Elements	SCO-1	REC	QLO-1	REC	STM-1	REC	RGM-1	REC
SiO2	63.35	62.78	65.5	65.55	59.35	59.64	72.9	73.45
TiO2	0.58	0.63	0.61	0.62	0.14	0.14	0.27	0 27
Al2O3	13.85	13.67	16.48	16.18	18.63	18.39	13.94	13 72
FeO*	4.69	4.67	3.91	3.89	4.65	4.67	1.62	1.72
MnO	0.06	0.05	0.09	0.09	0.22	0.22	0.04	0.04
MgO	2.8	2. 2	1	1.04	0.1	0.1	0.28	0.28
CaO	2.54	2.62	3.17	3.24	1.09	1.09	1.16	1.15
Na2O	0.97	0.9	4.2	4.23	9.22	8.94	4.21	4.07
K2O	2.87	2.77	3.6	3.63	4.49	4.28	4.62	4.3
P2O5	0.17	0.21	0.25	0.26	0.13	0.16	0.04	0.05

Trace Elements	SY-2	REC	MRG-1	REC	SY-2	REC
Pb	79	85	1	10	81	85
Cu	4	5	119	134	4	5
Zn	258	248	184	191	258	248
Mo	2	2	3	1	3	2

	GS-1	RH-1	AND-1
F	263	121	418

Accuracy of trace element analyses, Memorial University

Trace Elements	G-2	X	Std	N	W-1	X	Std	N
V	36	38	2	4	257	257	4	7
Rb	170	174	7	4	21	20	2	7
Ba	1882	1890	16	4	162	202	5	7
Sr	478	464	3	4	186	186	2	7
Zr	309	303	4	4	99	95	1	7
Nb	12	11	1	4	10	9	1	7
Y	11	18	2	4	26	21	1	7

Trace Elements	GSP-1	X	Std	N
V	53	57	3	3
Rb	254	244	3	3
Ba				
Sr	234	232	1	3
Zr	530	511	5	3
Nb	28	24	1	3
Y	26	39	1	3

REC= recommended value (Govindaraju, 1989)
X= mean, Std= standard deviation, N= number of analyse

Table A2.2 Accuracy of major and trace element analyses, Department of Mines and Energy laboratory. Trace element analyses were conducted at Memorial University.

Accuracy of Th and rare-earth-element analyses
Memorial University Laboratory ICP-MS

Elements	W-2	REC	SY-2	REC
Th	2.3	2.2	382.13	379
La	10.7	11.4	67.47	75
Ce	23.9	24	163.77	175
Pr	3	5.9	19.7	18.8
Nd	13	14	74.03	73
Sm	3.2	3.2	15.4	16.1
Eu	1.1	1.1	2.4	2.42
Gd	3.8	3.8	15.59	17
Tb	0.6	0.63	2.76	2.5
Dy	3.9	3.8	19.54	18
Ho	0.8	0.76	4.38	3.8
Er	2.3	2.5	14.66	12.4
Tm	0.3	0.38	2.39	2.1
Yb	2	2.05	17.41c	17
Lu	0.3	0.33	2.87	2.7

REC= recommended value (Govindaraju, 1989)

Normalization factors (Taylor and McLennan, 198

La	0.367
Ce	0.957
Pr	0.137
Nd	0.711
Sm	0.231
Eu	0.087
Gd	0.306
Tb	0.052
Dy	0.381
Ho	0.0851
Er	0.249
Tm	0.0356
Yb	0.248
Lu	0.0381

Table A2.3 Accuracy of Th and REE analyses, Memorial University of Newfoundland.

A2.2 SAMPLE LOCATIONS

SAMPLE	GRID REFERENCE	SAMPLE	DDH	METERS
86-111B	45+00W 38+31N	86-215	GP-21	22 m
86-114B	45+00W 38+50N	86-216	GP-21	30 m
86-115B	45+00W 38+52N	86-219	GP-19	15 m
86-117D	45+00W 38+56N	86-220	GP-19	47 m
86-119F	45+00W 38+60N	86-221	GP-19	39 m
86-120E	45+00W 38+65N	87-12	GP-23	39 m
86-123A	44+36W 38+62N	87-13	GP-23	73 m
86-129B	45+15W 39+67N	87-18	GP-23	116 m
86-142C	42+00W 39+22N	87-21	GP-23	164 m
86-146B	46+00W 38+08N	87-27	GP-21	88 m
86-149D	47+00W 38+23N	87-39	GP-19	38 m
86-152C	48+73W 38+07N	87-41	GP-19	92 m
86-154B	49+00W 36+78N	87-48	GP-22	28 m
86-184C	41+00W 39+61N	87-49	GP-22	38 m
86-187C	41+00W 39+83N	87-60	GP-26	63 m
86-189B	41+00W 39+87N			
86-196D	40+00W 39+92N			
86-198	40+00W 40+13N			

Table A2.4 Sample locations for those geochemical samples not plotted on the large geology map.

A2.3 TULKS HILL FELSIC VOLCANIC ELEMENTAL AVERAGES

Element	Ave Felsic (wt. percent)	SD
SiO_2	75.80	3.05
TiO_2	0.23	0.14
Al_2O_3	13.14	1.44
FeO	2.80	1.77
Mno	.09	0.05
Mgo	1.78	1.37
CaO	1.25	1.14
Na_2O	3.23	2.10
K_2O	1.65	1.26
P_2O_5	0.05	0.05
LOI	3.11	1.24
Zr	139 ppm	69

Table A2.5 Average element data for the felsic volcanic rocks of the Tulks Hill volcanics (SD - standard deviation) (source Department of Mines and Energy, unpublished data).

APPENDIX 3

ANALYTICAL PROCEDURE ISOTOPIC ANALYSES

A3.1 Pb ISOTOPIC ANALYSES

Pb isotopic analyses were performed by Geospec Consultants, Edmonton, Alberta, using a Micromass MM-30 mass spectrometer. The resultant isotopic ratios were normalized to approximately absolute values based on the U.S. National Bureau of Standards reference lead NBS-981. For a detailed account of the analytical procedure the reader is referred to Thorpe et al. (1984).

ISOTOPIC RATIO	ANALYTICAL UNCERTAINTY
$^{206}Pb/^{204}Pb$	+/-0.064%
$^{207}Pb/^{204}Pb$	+/-0.068%
$^{208}Pb/^{204}Pb$	+/-0.075%

Table A3.1 Analytical uncertainty, lead isotopic ratios (source Swinden, 1987).

A3.2 SULPHUR ISOTOPIC ANALYSES

Sulphur isotopic analyses were performed on pyrite separates at the Geological Survey of Canada Stable Isotopic Facility located at the Ottawa-Carleton Geoscience Centre.

A3.3 CARBON AND OXYGEN ISOTOPIC ANALYSES

Carbon and oxygen isotopic analyses were performed on carbonate separates at Memorial University of Newfoundland using the procedure outlined by McCrea (1950). Carbonate samples were placed in double arm reaction vessels, immersed in a water bath and reacted with 2 ml of 100 % phosphoric acid under vacuum conditions. Evolved CO_2, was then purified using a vacuum line and series of methanol liquid nitrogen traps. Isotopic determinations were made using a PRISM mass spectrometer.

APPENDIX 4

SCANNING ELECTRON MICROANALYSER TECHNIQUE

A4.1 Scanning Electron Microprobe Technique

An Hitachi S570 scanning electron microscope with an accelerating voltage of 15 kv, located at the Department of Geography, Memorial University, was used to examine carbon-coated polished thin sections. A GW Electronics Type 113 solid state backscattered electron detector was used to obtain backscattered electron imaging. Images were recorded using Polaroid Type 665 positive/negative film. A Tracor Northern 5500 energy dispersive X-ray analyzer combined with a Microtrace silicon X-ray spectrometer (Model 70152) performed X-ray analyses.

APPENDIX 5

GEOLOGY MAP

GEOLOGY OF THE MIDAS POND AREA

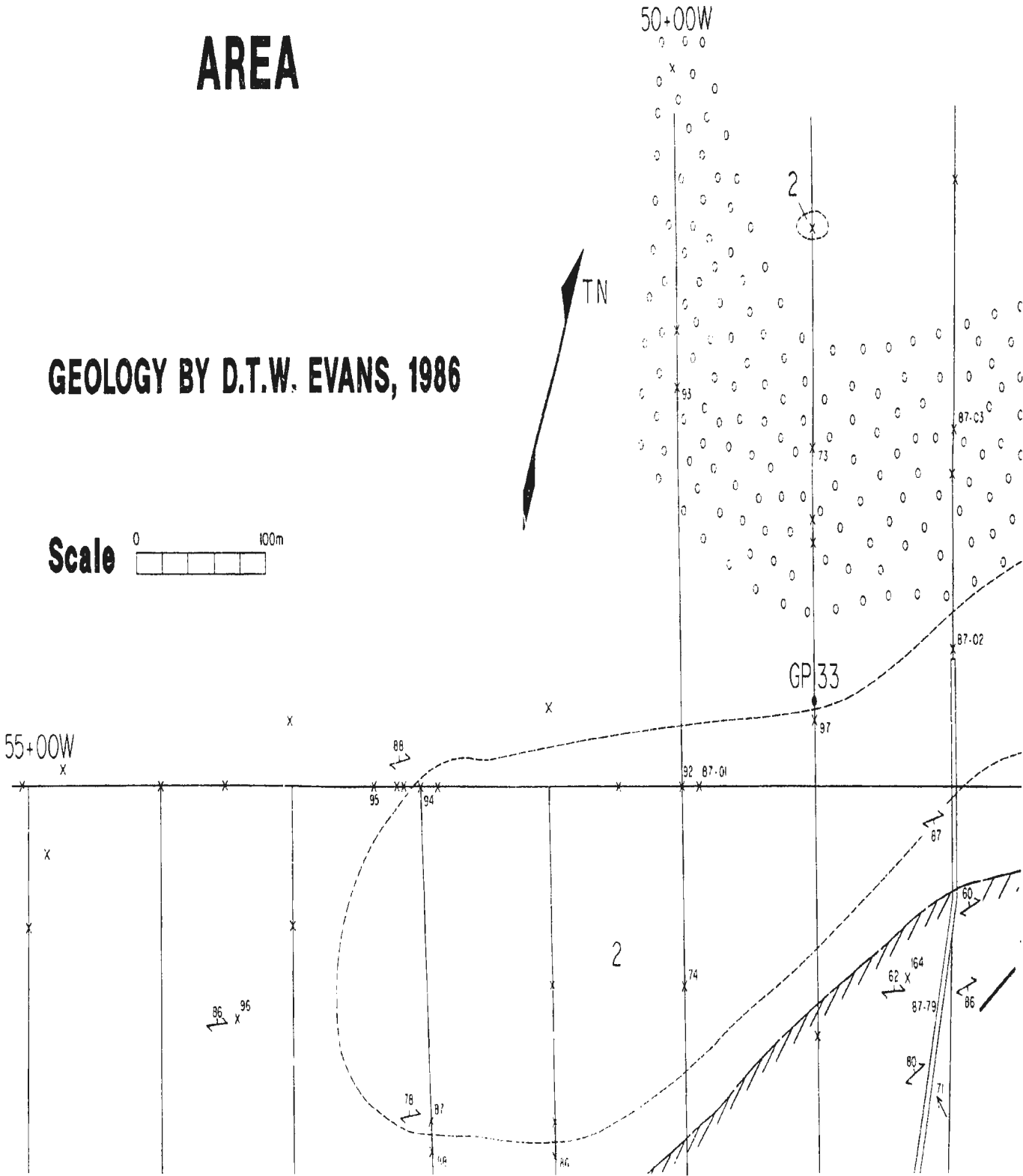

GEOLOGY BY D.T.W. EVANS, 1986

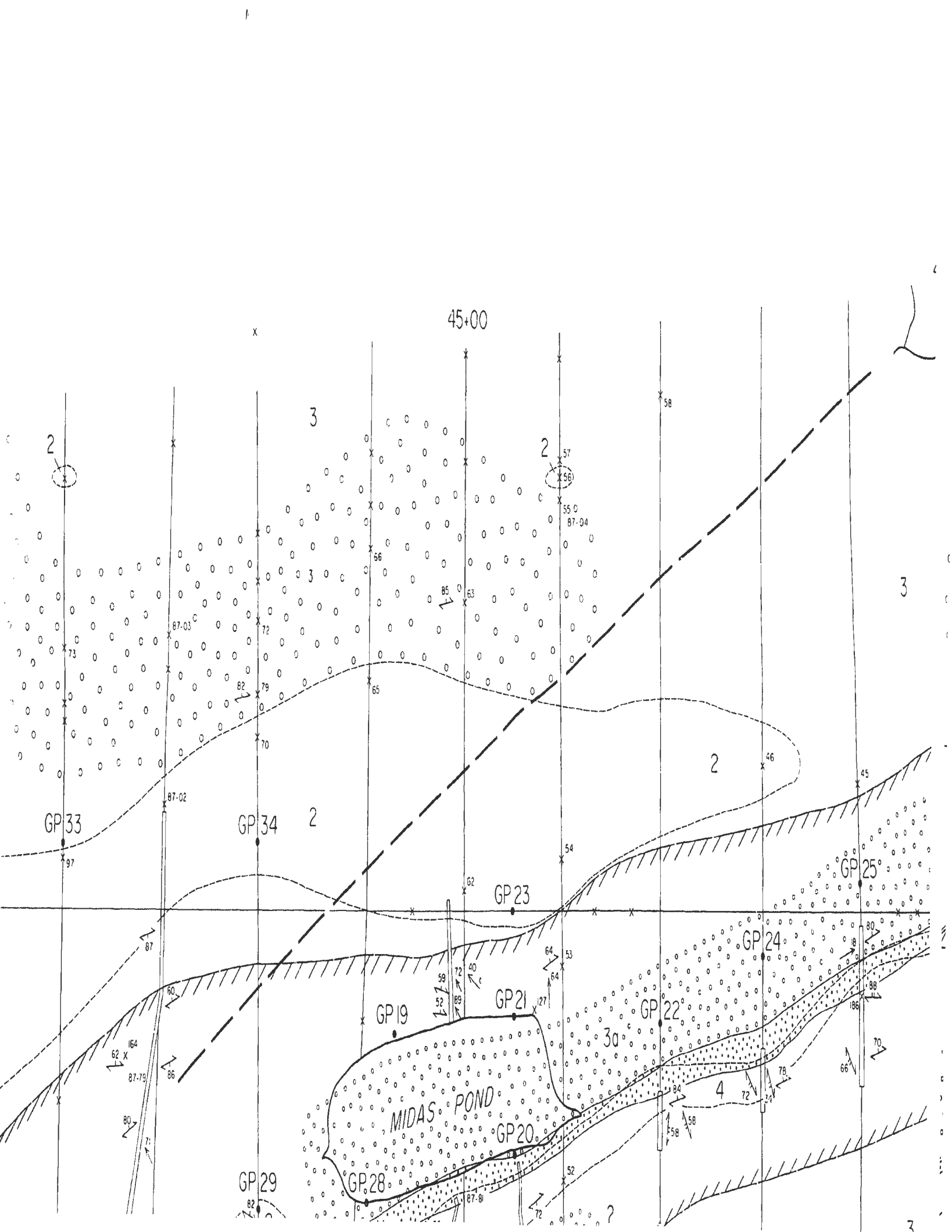
45+00
GP 33
GP 34
GP 23
GP 25
GP 24
GP 22
GP 21
GP 19
GP 20
GP 28
GP 29
MIDAS POND
87-02
87-03
87-04
87-79
87-81
2
3
3a
4

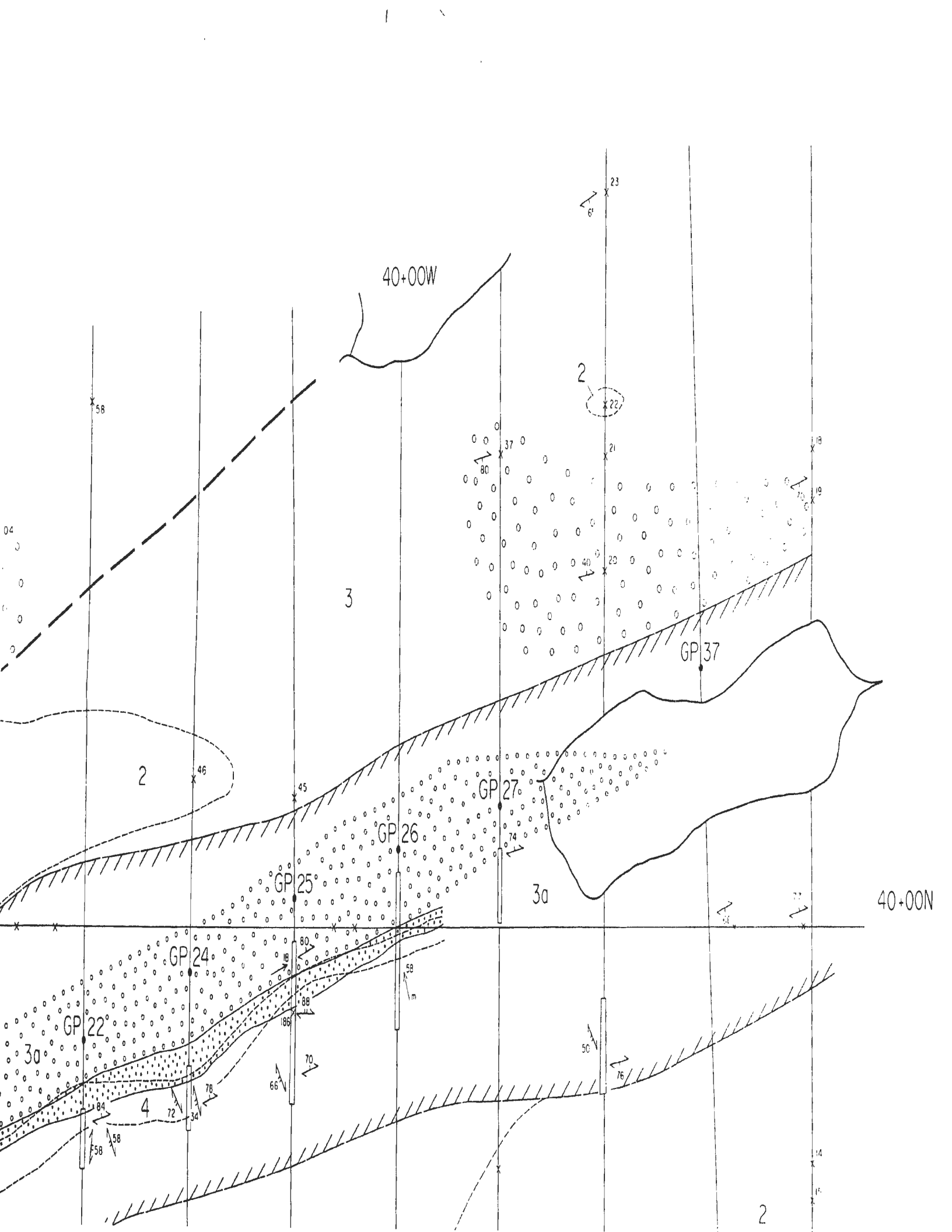
40+00W
40+00N
GP 22
GP 24
GP 25
GP 26
GP 27
GP 37
2
3
3a
4
2
3a
2

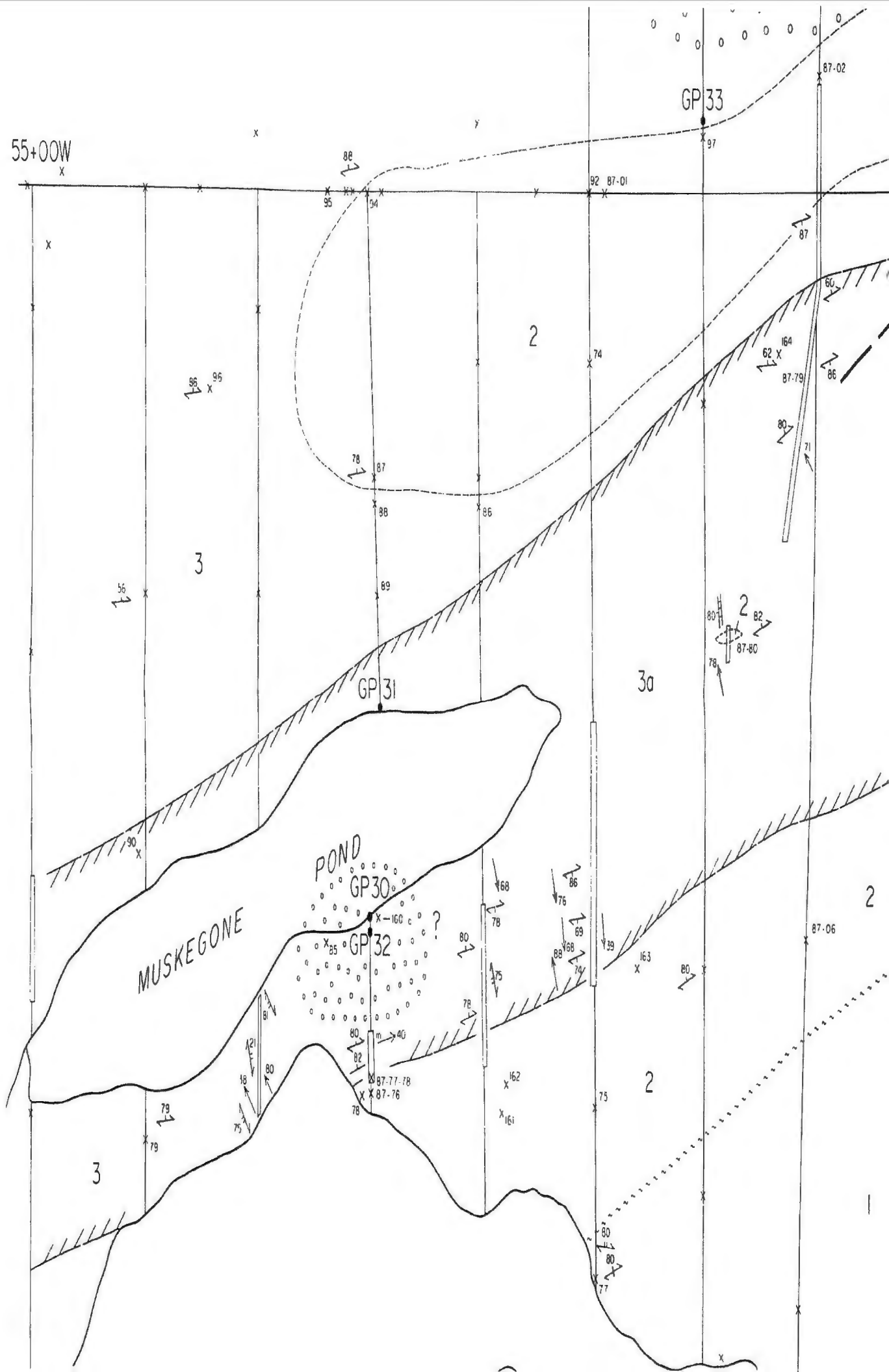
55+00W
GP33
87-02
97
92 87-01
95
94
86
87
60
2
74
62
164
87-79
86
80
71
78
87
88
86
3
56
89
2
82
80
87-80
78
GP31
3a
90
POND
GP30
MUSKEGONE
GP32
?
160
85
68
78
86
76
69
88
68
74
39
163
80
75
78
87-06
2
81
121
18
80
82
87-77-78
87-76
78
162
161
75
2
79
79
3
75
80
80
77
1

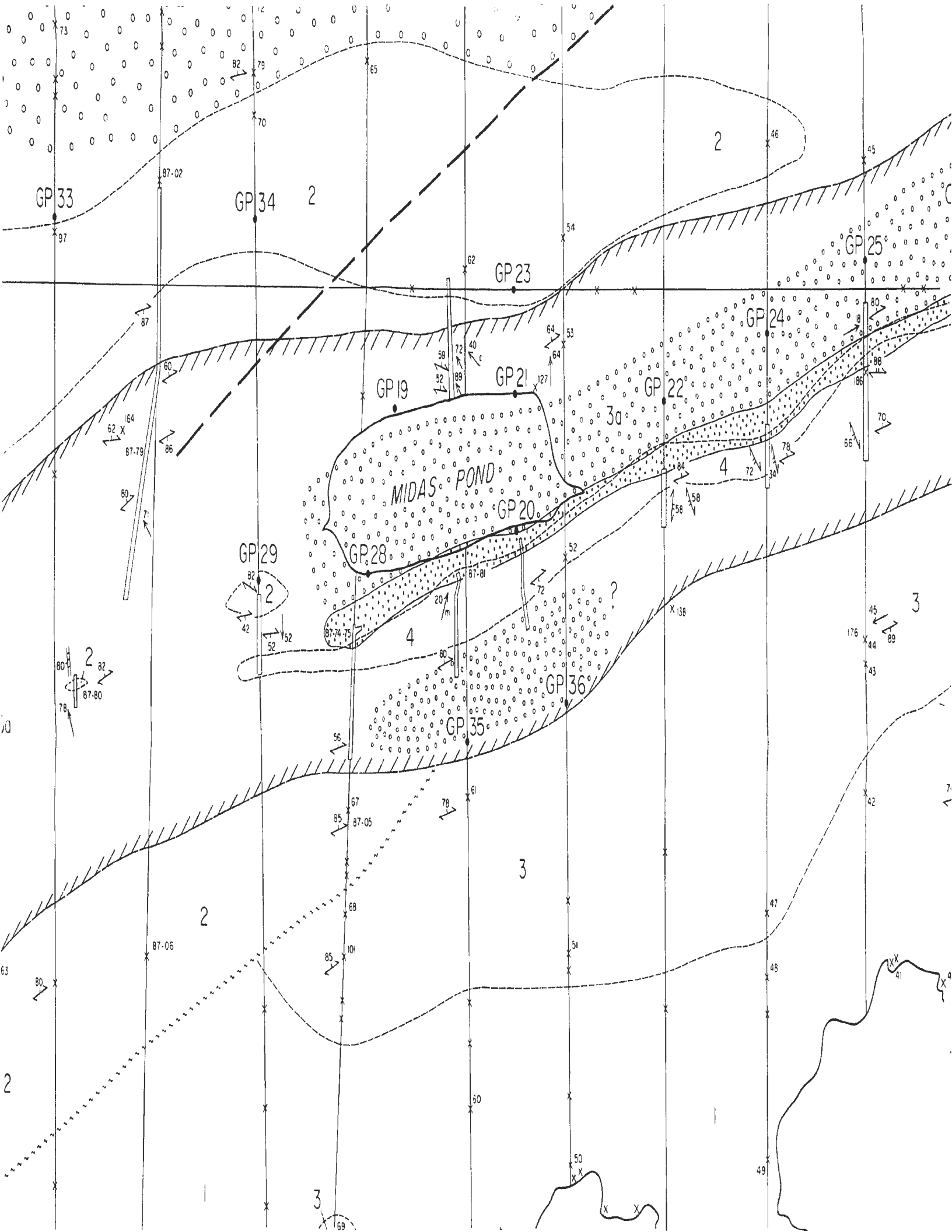
GP 33
GP 34
GP 23
GP 25
GP 24
GP 21
GP 19
GP 22
GP 20
GP 28
GP 29
GP 36
GP 35
MIDAS POND
87-02
87-79
87-81
87-74-75
87-80
87-05
87-06
2
3a
4
3
1
?

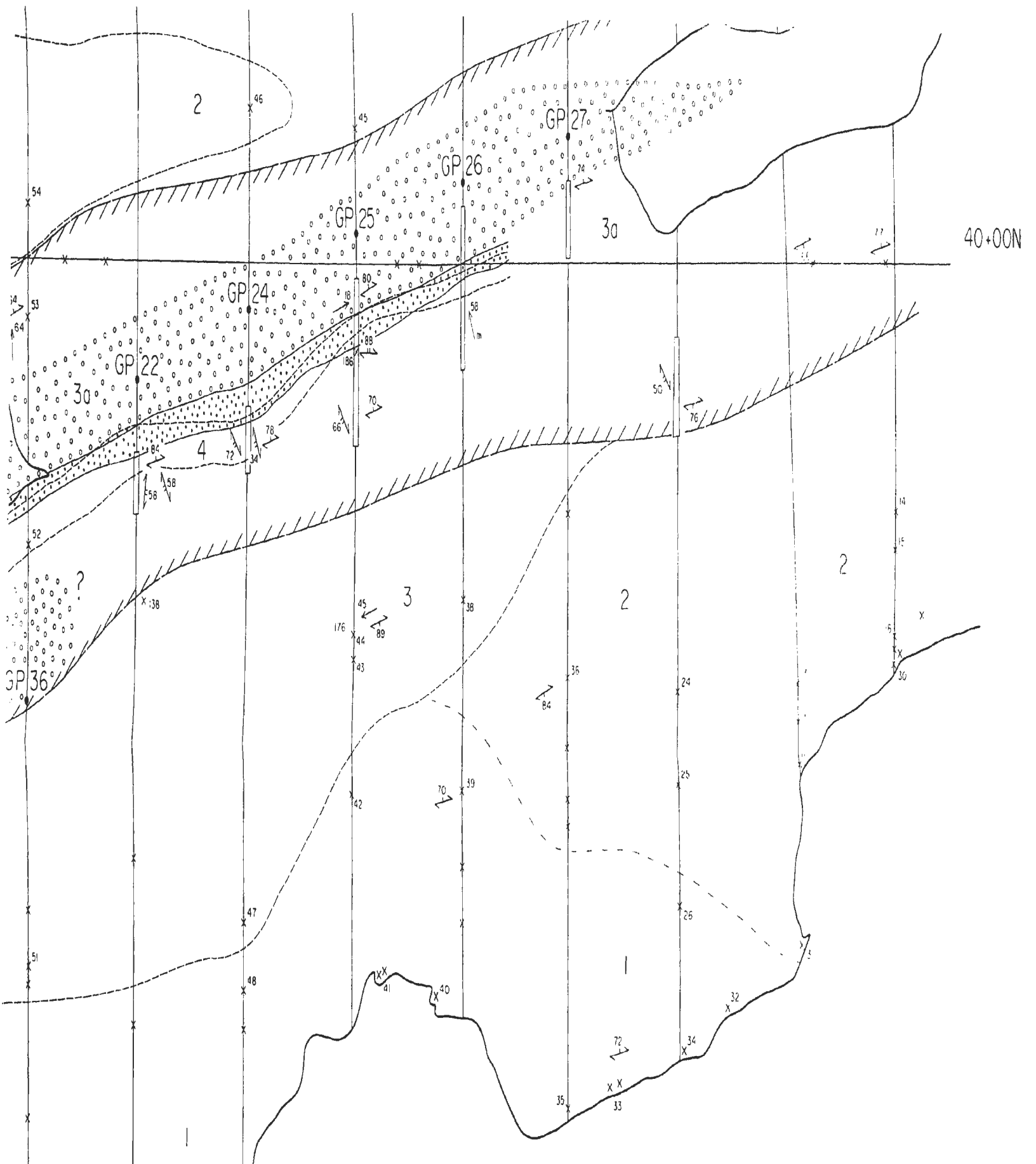

LEGEND

SYMBOLS

LOWER TO MIDDLE ORDOVICIAN

Banded mafic breccia. Highly deformed breccia, locally feldsparphyric,

fault (assumed)

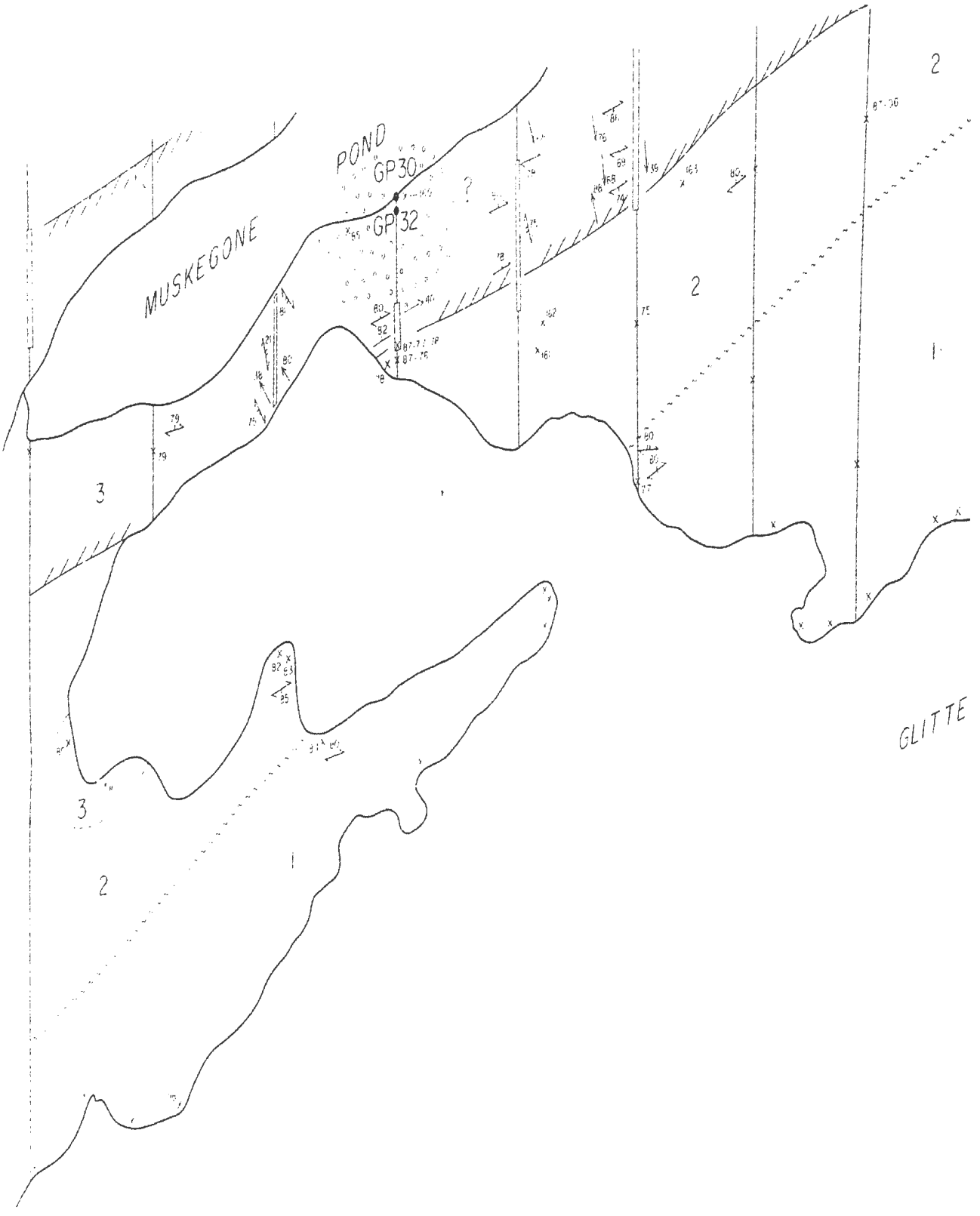
POND
GP30
GP32
MUSKEGONE
GLITTE
1
2
3

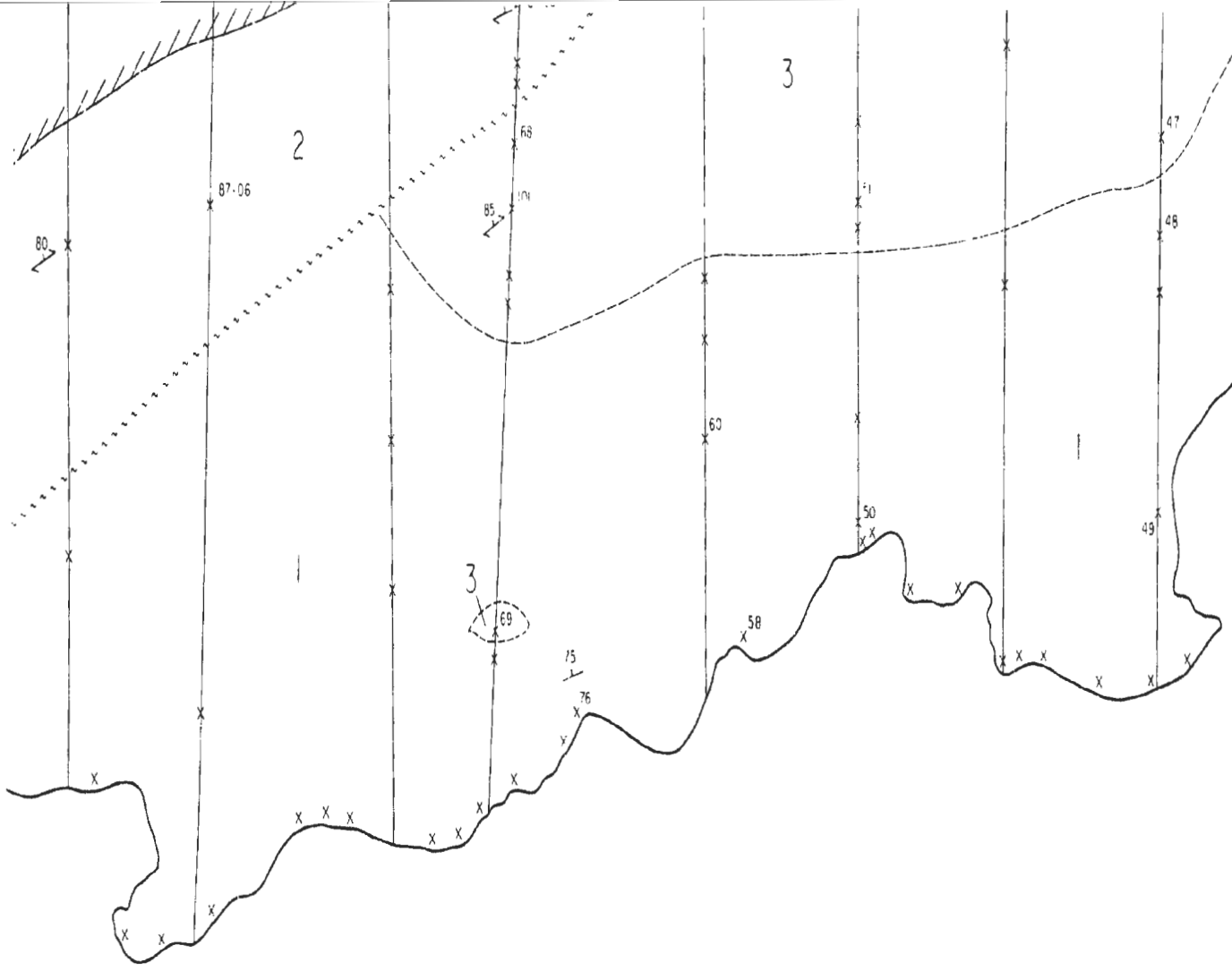

LOWER TO MIDDLE ORDOVICIAN

4 Banded mafic brecc-
comprised of fine-g
textured, locally limo

3 Cream-to buff-weat
crystal tuff, lapilli tu
silicified and sericitic

2 Dark-green, fine-gr
and minor breccia

1 Coarse, angular, loc
in a matrix of fine-g
sparphyric tuff

Zone of relative gol

Zones of extensive

Zones of extensive

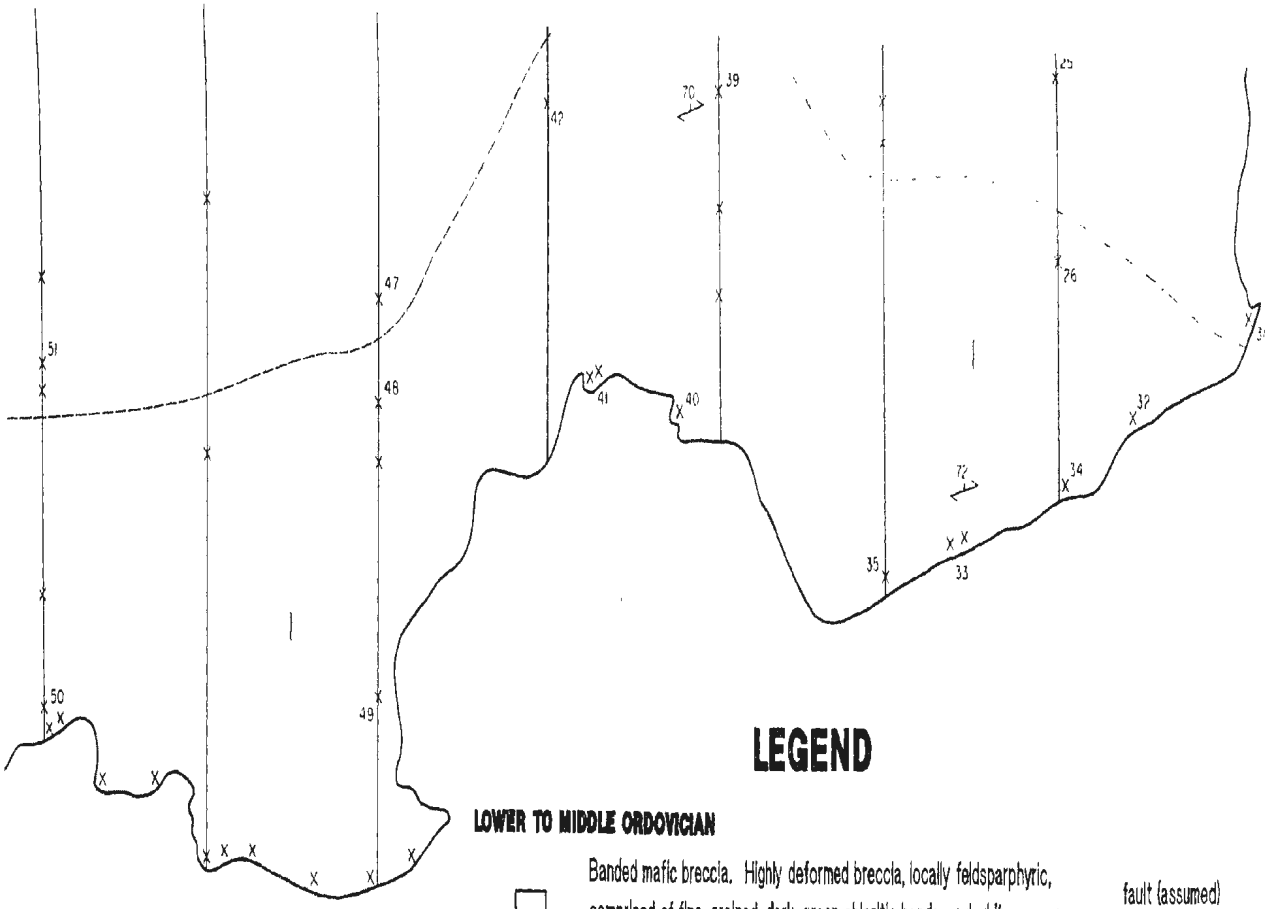

LEGEND

LOWER TO MIDDLE ORDOVICIAN

4 — Banded mafic breccia. Highly deformed breccia, locally feldsparphyric, comprised of fine-grained, dark-green chloritic bands, and white, sugary-textured, locally limonitic, felsic bands

3 — Cream-to buff-weathering, light green-gray, locally sericitic, felsic, crystal tuff, lapilli tuff and minor breccia. 3a. Variably deformed, locally silicified and sericitic felsic tuff and minor mafic tuff

2 — Dark-green, fine-grained, intermediate to mafic, feldspar crystal tuff and minor breccia

1 — Coarse, angular, locally flattened breccia comprised of felsic blocks in a matrix of fine-grained, green, intermediate to mafic, locally feldsparphyric tuff

Zone of relative gold (>10ppb) enrichment and quartz veining

Zones of extensive silicification and minor pyritization

Zones of extensive pyrophyllitization, kaolinitization and silicification

SYMBOLS

fault (assumed)

geological contact (defined, approximate, gradational)

air-photo lineament

shear zone

bedding tops known (inclined)

cleavage (inclined) S_1, S_2

quartz vein (inclined)

outcrop

diamond drill hole • GP

axis of minor fold

crenulation

mineral lineation

trench

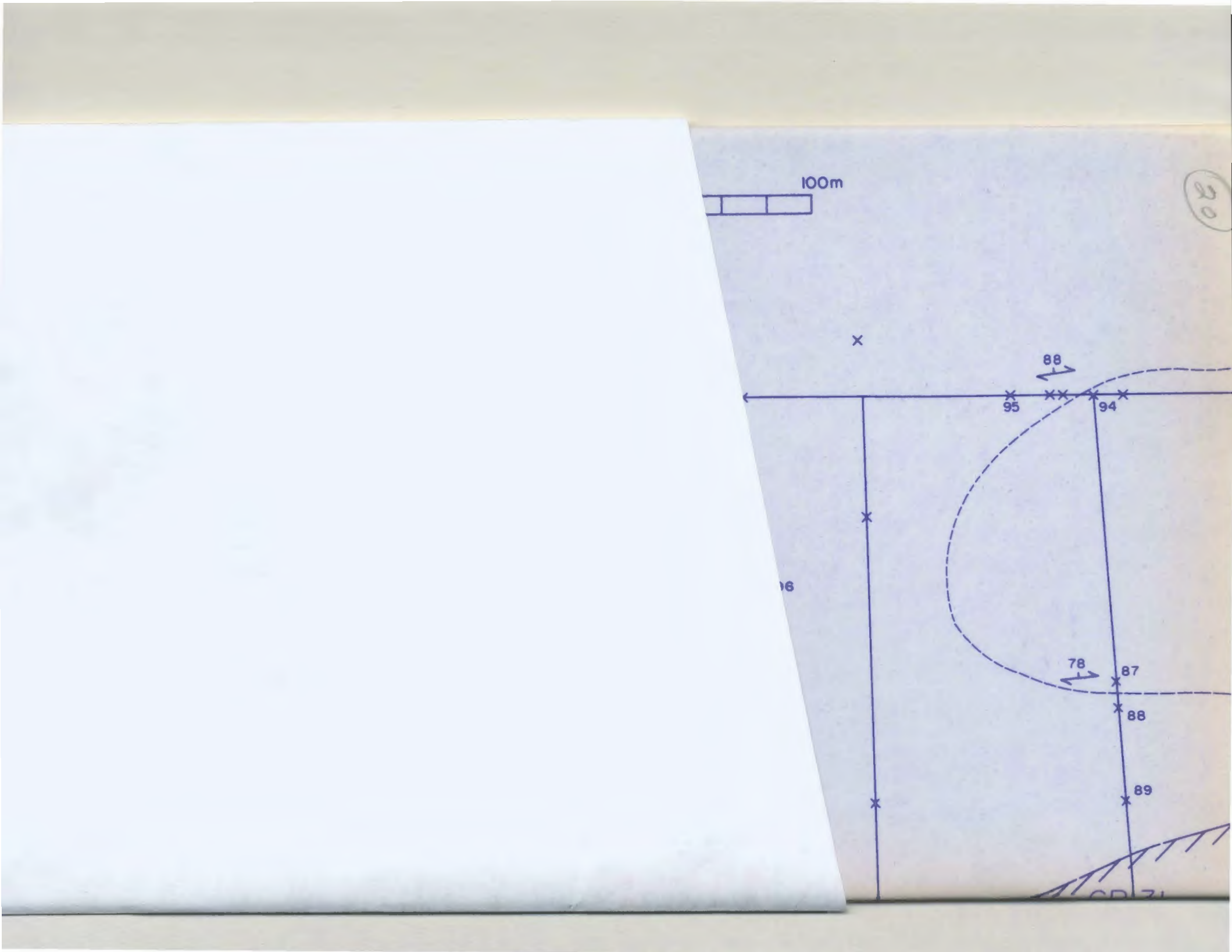
100m
88
95
94
78
87
88
89